

Unravelling industrial sector water use

Developing a conceptual model to quantify global
thermoelectric and manufacturing water uses

Bryan Marinelli

6671349

b.p.p.marinelli@students.uu.nl

Supervisors:

Dr. Rens van Beek

Dr. Michelle van Vliet

Edward Jones

Universiteit Utrecht

30 ECTS

Abstract

PCR-GLOBWB is a gridded global model which simulates water resource availability and sectoral water use. One of the sectors, industrial, is comprised of the manufacturing and thermoelectric sub-sectors. The model initially used lumped input industrial water demand data, but this study altered the spatiotemporal precision of the model by separately calculating the sub-sectoral industrial contributions. Manufacturing water is mainly used to manufacture products, while thermoelectric water is used to cool thermoelectric power plants. Through the development of a conceptual model to estimate national manufacturing water withdrawals, and the integration of a global thermoelectric power plant dataset, the input parameters were adjusted. The conceptual model was created by calculating manufacturing water withdrawals using three equations for a reference year, and then forecasting and backcasting these values using annual technological changes. The national gross manufacturing water demand values were then downscaled by population density and coupled with an existing dataset of industrial return flows to estimate net manufacturing water demand. The manufacturing water demand was then further coupled with the gross and net thermoelectric water demand dataset. By aggregating the gross and net demands, an updated industrial water demand dataset was created. This dataset accounts for the gross and net water demands for the industrial sector at a 5 arc minute spatial resolution, and is theoretically more spatially precise than previous datasets because it incorporates the thermoelectric water demand at exact locations. Initially, PCR-GLOBWB used a downscaled industrial sector, but now that technique is only used for the manufacturing sub-sector. The newly created industrial water demand file was then integrated into PCR-GLOBWB, and the model was simulated between 1980 and 2014. Using the model results, several analyses were performed on the output to assess the effect of the updated industrial water demand dataset. Comparisons were made between the initial and updated industrial demand input files, the supply and demand of industrial water, and the PCR-GLOBWB output for abstractions and discharge. These analyses showed that adjusting the spatial precision of the input data did influence the calculated local and national industrial water scarcity, as well as the industrial water abstractions and discharge. The updated industrial gross demand input file did not greatly affect the total national demand from the initial input file, but did affect temporal trends due to the influence of the technological changes in the conceptual model. In the United States, an analysis of the national data showed that the updated model improved the temporal simulations due to the technological changes. At more local scales, however, the updated model was not as effective at estimating industrial water use. Upon further analysis, it was found that this was due to discrepancies between the input thermoelectric water demand, and the observed thermoelectric water withdrawals. Although the national scale values are improved, more research will need to be done to improve the spatial precision of the model locally.

Keywords: Industrial water demand, manufacturing sub-sector, thermoelectric sub-sector, water use intensity, abstractions, discharge, spatial downscaling.

Table of Contents

1 Introduction	1
1.1 Background information	1
1.2 Problem description and knowledge gap	3
1.3 Aim and research questions	4
2 Theory	5
2.1 Literature review	5
3 Methods	12
3.1 Data collection	14
3.2 Developing the conceptual water demand model	15
3.3 Integration into PCR-GLOBWB	18
3.4 Data analyses	19
3.4.1 <i>Analysis of gross industrial water demand</i>	20
3.4.2 <i>Analysis of modelled industrial water supply and demand</i>	20
3.4.3 <i>Analysis of modelled industrial water abstractions</i>	20
3.4.4 <i>Analysis of modelled global discharge</i>	21
4 Results	21
4.1 Conceptual model output	21
4.2 PCR-GLOBWB modelling	23
4.3 Analysis of results	27
4.3.1 <i>Gross industrial water demand</i>	27
4.3.2 <i>Industrial water supply and demand</i>	33
4.3.3 <i>Industrial water abstractions</i>	36
4.3.4 <i>Modelled discharge</i>	42
5 Discussion	48
5.1 Limitations	48
5.2 Statistical analyses and data validation	49
5.3 Assumptions	57
5.4 Future research	58
6 Conclusion	59
References	iii
Appendix	viii

1 Introduction

1.1 Background information

Global datasets of sectoral water use have been developed for the main water use sectors, including industry, irrigation, livestock, domestic, mining, manufacturing, and energy among others (Flörke et al., 2013; Huang et al., 2018b; Sutanudjaja et al., 2018; Wada et al., 2014). Industrial water use is typically comprised of energy (mainly thermoelectric) water use and manufacturing water use (water used for mining activities may also be included in the industrial sector, however this study is not taking such water use into account). Moreover, within the energy sub-sector, thermoelectric and hydropower contributed 98% of global electricity generation in 2010, and thermoelectric alone contributed 81% (van Vliet et al., 2016). These values emphasize the importance of quantifying the effects of industrial activities on natural water systems.

As the industrial sector accounts for approximately 16.5% of total water withdrawals worldwide, and approximately 48.5% of total water withdrawals in northern North America and Europe (more than the irrigation and domestic use for these regions), a greater understanding of the dynamics of each sub-sector is vital for both environmental and socio-economic practices (FAO AQUASTAT, 2021; Rübberke & Vögele, 2011). Over the two decades from 1980 to 2000, industrial water intake doubled globally, and its contribution to total water use is expected to further increase relative to other sectors (Dupont & Renzetti, 2001; van Vliet et al., 2012). While the significance of industrial water use is very clear, less is known about its specific sub-sectoral contributions. Hydrological models typically lump these sub-sectoral contributions into a poorly defined industrial sector, so a separation of its components proves useful to gain insight into how usage trends have changed in the past decades, as well as for scenario building to theorize how these trends affect future water use in the industrial sector. Water use dynamics within the energy production and manufacturing sub-sectors are constantly changing, whether due to anthropogenic climate change or socio-economic developments, consequently making it important to have an effective model to predict possible scenarios relating to water demand. A greater understanding of the drivers affecting these changes allows for improved modelling of their effects on various types of water uses within the industrial sector.

Sectoral water use is further sub-divided into the water withdrawals (gross water demand), consumption (net water demand), and associated return flows restored to the system (difference between gross and net water demands). The industrial sector withdraws surface water and groundwater for the cooling of thermoelectric power plants and for the manufacturing of goods (e.g., production of textiles). According to the USGS, water withdrawals can be defined as water “diverted from a water source,” and water consumption can be defined as the “portion of water evaporated or incorporated into crops or products, and thus no longer available for downstream use” (Luo et al., 2018, p. 2). For this study, industrial water use is comprised of: “thermoelectric power water withdrawals, thermoelectric power water consumption, manufacturing water withdrawals, and manufacturing water consumption” (Vassolo & Döll, 2005, p. 2). Note that the

water withdrawn for but not consumed by industrial activity is restored to the natural system as return flows. These flows, however, may be affected by industrial processes. Changes to the quality and quantity of water in natural systems are directly linked to abstractions and return flows. Withdrawals, for instance, can be very useful for assessing the dependency of a power plant or manufacturing site on available surface water, while consumption rates and techniques can affect the downstream environmental impacts after flows are restored (Luo et al., 2018). Abstracting too much water at a time will deplete the natural streamflow, rendering a body unusable over time. Further, the temperature of return flows plays a massive role in the health of the downstream ecosystem, as it can affect the habitats of populations as well as increase the risk of contamination.

Much of the withdrawn water for the thermoelectric sub-sector is restored as return flows to its original natural system, albeit often causing thermal pollution (Flörke et al., 2013). While this is often the case for once-through and pond cooling systems, for some cooling technologies, such as dry and tower, recycling ratios (the fraction of water withdrawals which are consumed) can be quite small (Lohrmann et al., 2019). In addition to thermoelectric and hydropower, energy water use has contributions from biofuel, concentrated solar power, and fossil fuel exploration components, although the water use from these components may also be attributed to other sectors (e.g., biofuel consumption may be included in irrigation water use). Note that the energy components identified may also be used to power thermoelectric power plants. Further, as water use in the energy sub-sector is mainly withdrawn and consumed for the cooling of thermoelectric power plants, the energy sub-sector will be referred to as the thermoelectric sub-sector for the purposes of this study. By analyzing data from global power plants, it is possible to gain insight into the current state of water quantity dynamics through analyses of abstraction rates and return flows dependent on cooling technologies and fuel types. This includes, for instance, assessments of the relationships between combinations of cooling technologies and fuel types, similar to the research done by Lohrmann et al. (2019).

Manufacturing water use is “for such purposes as fabricating, processing, washing, cooling, or transporting a product; incorporating water into a product; or for sanitation needs within the manufacturing facility” (Huang et al., 2018b, p. 2119). It covers components such as paper, chemicals, machinery, and food, “which are to a varying degree water-use intensive” (Flörke et al., 2013, p. 148). Withdrawals for this sub-sector can be monitored on the national scale (and subsequently on more local scales provided there is adequate data available), and then be used in conjunction with return flows to estimate water consumption. Although there are aspects of water quantity and water quality affected by the manufacturing sub-sector, this research emphasizes the quantitative issues.

1.2 Problem description and knowledge gap

PCR-GLOBWB is a gridded global model developed by Utrecht University which simulates water resources availability and sectoral water use (Sutanudjaja et al., 2018; van Beek et al., 2011). The model includes industrial, irrigation, livestock, and domestic sectors, and accounts for surface water at specific locations and time steps while running simulations to dynamically estimate withdrawals, consumption, and return flows, among other parameters, for each sector (Sutanudjaja et al. 2018; van Beek et al., 2011). Although the industrial sector is comprised of thermoelectric and manufacturing water uses, PCR-GLOBWB does not distinguish between the sub-sectors (Wada et al., 2014). Instead, the specific contributions from each sub-sector are aggregated, rather than being presented separately. With separate inputs from each sub-sector, there will also be improved spatial distinctions.

While there is ample data regarding the water use for thermoelectric power, less is known about the manufacturing sub-sector. For instance, Lohrmann et al. (2019) found relationships between various cooling technologies and fuel types utilized at power plants, which show that current return flows for particular combinations can be massive. This may change, however, as energy production shifts towards renewable sources. Further, this detailed information can be input into PCR-GLOBWB to differentiate between the thermoelectric and manufacturing sub-sectoral recycling ratios.

This leads to the less-refined data within the manufacturing sub-sector. A greater understanding of manufacturing water use is important from both water quantity and water quality perspectives. Removal of water from natural systems directly influences water availability, while the quality of the return flows can cause downstream pollution that poses risks to human and environmental health. It is therefore scientifically important to improve the understanding of the water use contributions from the thermoelectric and manufacturing sub-sectors to the industrial sector on the whole. This also could allow for more realistic scenario building for future projections as the drivers affecting water use trends is the sub-sectors change.

With this knowledge gap present, it is important to quantify the withdrawals, consumption, and, by extension, the return flows of surface water due to the thermoelectric and manufacturing sub-sectors to help differentiate between process water and water being fully removed from the system. This distinction is necessary to better estimate return flows, which affect future projections (particularly as energy technologies change), and to understand the relationship between return flows and water quality (due to thermal pollution or contamination). As these methods are dependent on water availability and temperature (which are further dependent on the effects of anthropogenic climate change), adaptations are necessary for sustainable security of water use in the coming decades (van Vliet et al., 2016). The effects on water scarcity caused by the industrial sector are related to both water quantity (amount of return flows) and water quality (temperature of return flows), as water scarcity is not just caused by a lack of water, but a lack of usable water.

Water supply and demand interact with water quantity and quality (in addition to desalination and treated wastewater reuse) to affect water scarcity (van Vliet et al., 2021). Regarding manufacturing water use, total withdrawals and wastewater have increased considerably in the 21st century, further contributing to regional water scarcity (Flörke et al., 2013). For scenario building and future projections to best account for these forthcoming changes, more precise inputs are necessary for PCR-GLOBWB to realistically simulate global water demand and usage.

Further, the data in the model only has recycling ratios at the national scale. In PCR-GLOBWB, these return flows are determined using regional and economical classifications, that statistically calculate the percentage of water reentering the surface water system through return flows, although realistically these ratios are unique to each system. It is therefore important to understand how recycling ratios can be applied at a more precise spatial resolution. Currently, thermoelectric data shows that return flows increase proportionally with economic classifications, while also varying regionally. Within the national scale, it is evident that return flows from power plants can differ greatly. Understanding these dynamics at the power plant scale is vital for improving the accuracy of localized simulations. Further, when looking at the sites with the largest and smallest recycling ratios, there are several countries which have sites at both ends of the spectrum. This emphasizes the need to improve the precision of the recycling ratio data, because a national value, while effective, is not the best approach to model current and future water use trends.

1.3 Aim and research questions

This study aims to improve the understanding of the drivers affecting thermoelectric and manufacturing water use by developing a conceptual model to provide spatially explicit water use estimates of both sub-sectors globally. This was done by adjusting the input parameters of the PCR-GLOBWB model to more precisely simulate water withdrawals and localized return flows given current water quantity dynamics. Ultimately, this adjusted the ability of the model to simulate thermoelectric and manufacturing water uses globally.

This information leads into the main research question of this project:

How do the thermoelectric and manufacturing sub-sectors of water use respectively contribute to industrial sector water use?

This research question can be further divided into four research sub-questions as follows:

1. *What are the drivers affecting thermoelectric and manufacturing water uses?*
2. *How can a conceptual model quantify thermoelectric and manufacturing water uses?*
3. *What are the regional contributions of thermoelectric and manufacturing water uses to the industrial sector globally?*
4. *How can a conceptual model be implemented into PCR-GLOBWB to estimate thermoelectric and manufacturing water uses?*

2 Theory

Methods from previous studies were analyzed and, if necessary, further developed to result in a reliable conceptual model to properly assess water use in the industrial sector. By analyzing the strengths and weaknesses of prior work, it was possible to create a conceptual model to simulate the specific contributions from the thermoelectric and manufacturing sub-sectors. The framework set up by Vassolo & Döll (2005) to calculate thermoelectric water withdrawals proved effective, correlating 76% with observed values (with approximately a 50% correlation between calculated and observed values of thermoelectric water consumption). The same study found significantly less success modelling manufacturing withdrawals and consumption. It was therefore particularly important for this research to improve estimation techniques for manufacturing water use.

Regarding thermoelectric water use, a global dataset of power plants developed by Lohrmann et al. (2019), coupled with global power plant datasets from Global Energy Observatory and WRI (2018) to account for construction years, was used. This file contains information regarding the spatial coordinates, region, economic classification, capacity, fuel type, cooling systems present, and water source. Further, it includes values and estimates for water consumption and withdrawals between 2015 and 2050 in intervals of five years. This dataset accounts for an estimated 80-90% of total global thermoelectric water usage and is the most comprehensive dataset available. The data can also be used to estimate return flows. By aggregating the data to the PCR-GLOBWB grid, thermoelectric water usage during the present and past decades was spatiotemporally assessed.

As for manufacturing water use, national data was used and appropriately downscaled to the PCR-GLOBWB grid. There is no localized data for this sub-sector, but national industrial data is available, and it is possible to aggregate power plant data to the national scale (for the purposes of estimating manufacturing water use). Taking the difference between these values results in residual values for the industrial sector, which can ultimately be used to estimate manufacturing water use.

2.1 Literature review

Prior efforts to separate industrial sector water uses have been successful in calculating thermoelectric withdrawals and consumption, but have been less able to get significant estimates for manufacturing withdrawals and consumption; for example, the work by Vassolo & Döll (2005). Their study calculated manufacturing water use by estimating national water withdrawals, and then localizing the data as a function of city nighttime lights. Population density or pollution are also viable metrics to downscale national manufacturing water usage (Bernhard et al., 2018; Vassolo & Döll, 2005). Further, population density and urbanization have proved to be useful indicators to measure total industrial water demand, although GDP is the main driver (Lips, 2020). The study by Lips (2020) also found that using industrial land cover and population would yield similar results. Lips (2020) further recommended a comparison between calculated water demand and an observed dataset, as presented by Bernhard et al. (2018).

The following equations were used to calculate thermoelectric and manufacturing water withdrawals by Vassolo & Döll (2005):

$$TWW = \sum_{i=1}^n EP_i * WI_i(CS_i)$$

TWW is total annual thermoelectric water withdrawal [m³/y], *EP_i* is the annual electricity produced by power plant *i* [MWh/y], *WI_i* is power plant-specific water withdrawal intensity [m³/MWh], *CS_i* is the cooling system of the power plant, and *n* is the total number of power plants in the system.

$$MWW = f * \sum_{i=1}^8 VP_i * WP_i$$

MWW is the nation-specific total manufacturing water withdrawals [m³/y], *f* is an adjustment factor to correct to the most plausible values if there is a lack of literature in data-poor countries, *VP_i* is the annual production volume of each of the eight manufacturing sectors [ton/y], and *WP_i* is the sector-specific water intensity [m³/ton].

The following equations were used to calculate thermoelectric and manufacturing water withdrawals by Flörke et al. (2013):

$$TPWW = \sum_{i=1}^n EP_i * WWI_i(CS_i, PT_i) * Tch_{TP}$$

$$TPWC = \sum_{i=1}^n EP_i * WCI_i(CS_i, PT_i) * Tch_{TP}$$

TPWW is the annual thermoelectric water withdrawals [m³/y], *TPWC* is the annual thermoelectric water consumption, *n* is the number of power plants in the system, *EP_i* is the annual thermoelectric energy production of each power plant [MWh/y], *WWI_i* is the power plant-specific water withdrawal intensity [per unit of electricity production], *WCI_i* is the power plant-specific water consumption intensity [per unit of electricity production], *Tch_{TP}* accounts for technological changes which can reduce such intensities, *CS_i* is the cooling system, and *PT_i* is the plant type.

$$MWW = MWC + MRTF = MWC + MCW + MWAW$$

$$= MWC + MCW + MWAW * \alpha_t + MWAW * (1 - \alpha_t)$$

MWW is manufacturing water withdrawal [m³/y], *MWC* is manufacturing water consumption [m³/y], *MRTF* is manufacturing return flows [m³/y], *MCW* is manufacturing cooling water [m³/y], *MWAW* is manufacturing wastewater [m³/y], α_t is the share of treated wastewater, and $(1 - \alpha_t)$ is the share of untreated wastewater. Note that all variables are on the national scale.

$$MWW_t = MSWI_{2005} * GVA_t * TC_t$$

MWW_t is the manufacturing water withdrawal per nation [m^3/y], $MSWI_{2005}$ is the manufacturing structural water intensity based on 2005 per nation [$m^3/\text{monetary value}$], GVA_t is the gross value added per nation [$\text{monetary value}/y$], TC_t is the rate of technological change for the manufacturing sector, and t is the year.

The equations listed above were adapted as the basis for the manufacturing water withdrawal calculations in this study.

Further, Huang et al. (2018a, 2018b) created a reconstructed global database with gridded spatial resolution of 0.5° . The data is partially reported and partially modelled. Using historical estimates, it considers the sectors present in PCR-GLOBWB, including a disaggregation of the industrial sector into thermoelectric, manufacturing, and mining sub-sectors. The thermoelectric and manufacturing sub-sectors were spatially downscaled using population density, and withdrawals were simulated using the Global Change Assessment Model (Huang et al., 2018b; Edmonds et al., 1997; Kim et al., 2006). The global water withdrawal reconstruction yielded the following results for the industrial sector: 11% of global water use has been for the thermoelectric sub-sector, and 7% has been for the manufacturing sub-sector (Huang et al., 2018b). When considering historical datasets for trend analyses, this study found thermoelectric water withdrawals to be decreasing in the United States and parts of Europe (assumed due to technologies shifting towards less water intensive means of electricity generation). Huang et al. (2018b) estimated less thermoelectric water withdrawal over the period from 1970-2010 than Flörke et al. (2013), but both studies had similar manufacturing water withdrawal estimates. Seasonal variations in the simulated results were determined by temporal downscaling of air temperature (Huang et al., 2018b). Their study also found that thermoelectric and manufacturing water withdrawals tended to be greater in urban or densely populated areas. Furthermore, thermoelectric water withdrawals “showed a winter peak in high-latitude regions and a summer peak in low-latitude regions” (Huang et al., 2018b, p. 2130). This dataset proved helpful to identify drivers of industrial water use as a basis for the conceptual model.

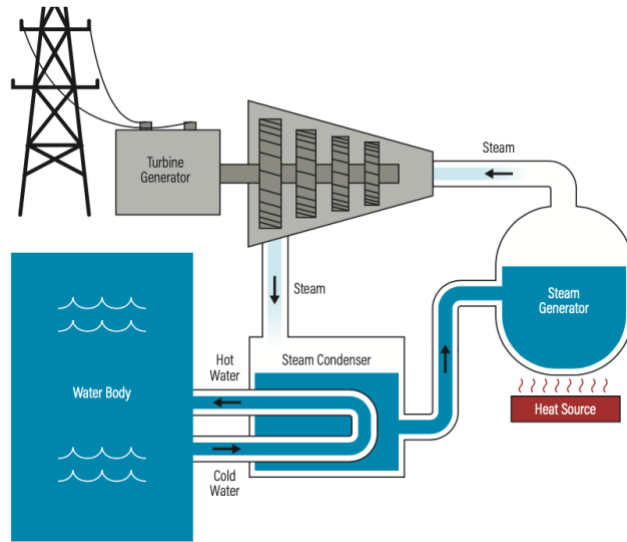
The basis for the thermoelectric data used by this study was a power plant dataset developed by Lohrmann et al. (2019) that accounts for several factors, including the effects of cooling technologies and fuel sources on return flows. Nuclear fuel sources, for example, account for significantly more total water withdrawals and return flows than coal, gas, and oil fuel sources in the Danube River (Lohrmann et al., 2019). When only considering freshwater, however, this research concludes that coal fuel sources currently account for more withdrawals and consumption than the other fuel sources in both the Lifetime Scenario and the Best Policies Scenario. Their study also focuses on the effects of various cooling technologies on water use, such as “wet cooling towers (which include natural-draft towers and mechanical-draft towers), dry cooling systems (known also as air-cooled condensers), inlet cooling systems of gas power plants and the so-called

surface-water cooling systems, which have two subcategories – once-through cooling systems and recirculating cooling-pond systems” (Lohrmann et al., 2019, p. 1045). Water Use Intensity (WUI) factors were used to assess the effect on water use from the combination of cooling technologies and fuel source (Lohrmann et al., 2019).

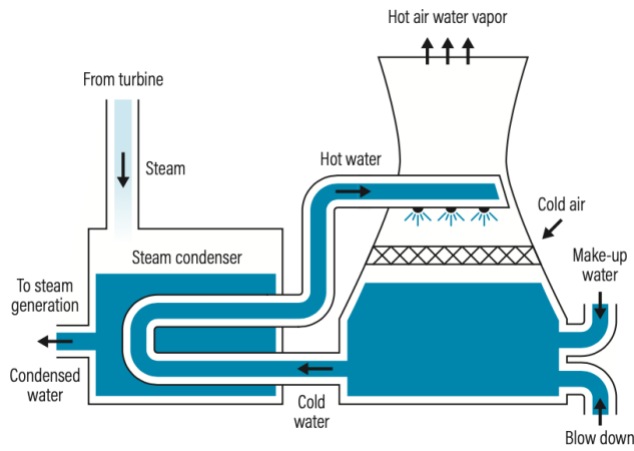
The World Resources Institute (WRI) developed a methodology to create a global power sector water use dataset using satellite imagery. The satellite imagery methodology has 69% precision in water demand estimation, when tested against 200 power plants in the United States (Luo et al., 2018). Table 1 details the cooling technologies identified in the WRI methodology, and diagrams depicting the cooling technologies can be seen in Figure 1. The fuel types identified are as follows: coal, biomass, natural gas and oil, nuclear, geothermal, and concentrated solar power. When using these cooling technologies and fuel types in conjunction, a factor for each power plant can be generated. Luo et al. (2018) did this and presented their findings for each permutation, giving maximum, minimum, and median values for withdrawals and consumption. It should be noted that this technique has not been implemented globally.

Table 1 Descriptions of the cooling technologies identified by the WRI (Luo et al., 2018).

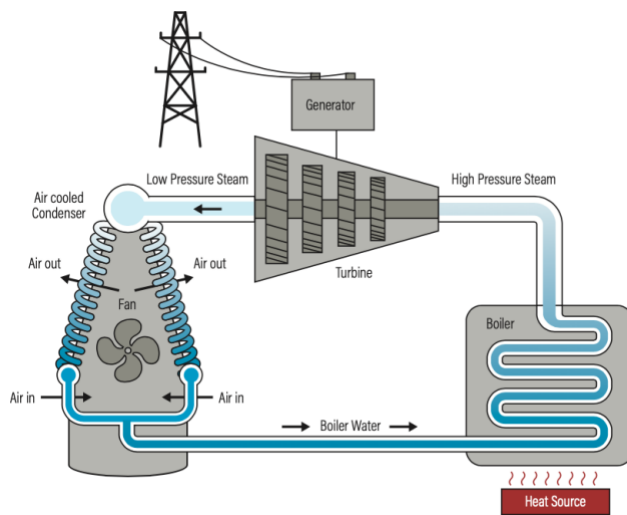
Cooling technology	Description
Once-through	Water is withdrawn, run through the condenser, and returned to the source.
Recirculating tower	Water is used to cool and condense steam, and heat is then dissipated from the cooling water.
Recirculating pond	Similar to recirculating towers, except pools of water are used instead of a vertical structure.
Dry cooling	Air is used as the major heat sink instead of cooling water.



a



b



c

Figure 1 Diagram of once-through (a), recirculating (b), and dry (c) cooling systems (Luo et al., 2018).

Several data-filling techniques could be used for missing values from the national industrial water use data collected from the FAO AQUASTAT (2021) database, including “inverse distance weighing, nearest neighbor, and linear interpolation/extrapolation based on associated variables” (Liu et al., 2016, p. S2). These techniques are further based on the number and values of available data over five-year intervals during the study period. Other methods of estimating industrial sector water use include the following. In a study of the Canadian industrial sector, manufacturing water use was estimated economically using input, treatment, recirculation, and output, to calculate the total amount of water used by specific subsets of the sub-sector (Renzetti, 1992). This method also proved to be imprecise, due to a lack of reliable data, when comparing the ranges of the datasets and standard deviations. Renzetti (1992) further emphasizes the negligence that has been shown towards industrial water use statistics. Dupont & Renzetti (2001) then found that there is a proportional relationship between the percentage of total water withdrawals from the industrial sector and income per capita (nationally). This has an application if there is a dearth of data regarding a nation’s total industrial water use. Finally, Frost & Hua (2019) estimated manufacturing water withdrawals using technology and electricity data from the SEMI database. SEMI includes production, capacity, geospatial, and temporal data for specific plants, which was used in the estimations for national (and regional in the case of the United States and China) water withdrawals (Frost & Hua, 2019).

Flörke et al. (2013) identified the following drivers for industrial sector water use. Electricity production is the main driver for the water requirements of the thermoelectric sub-sector. Further, for the manufacturing sub-sector, gross value added (GVA), technological change (with set values for nations and regions), and urban population distribution (also used for downscaling) are the main drivers.

Shang et al. (2017) found that as gross domestic product (GDP) increased in Tianjin, China, between 2002-2010, industrial water use initially increased as well, then plateaued, and finally decreased. This is because the initial focus was on high output, but then, as output increased, the focus shifted towards efficiency. For member nations of the Organisation for Economic Co-operation and Development (OECD), a Kuznets curve can be assumed for the relationship between GDP and industrial water use (Jia et al., 2006). The decrease in industrial water use as GDP increases beyond a certain (inflection) point can be explained by an increase in environmental sustainability associated with large-scale industrial development (Bao & Fang, 2012; Munasinghe, 1999). The improvement of water management systems and economic control measures, as well as reasonable industrial structure, high water efficiency, and water saving technologies can drive the reduction of industrial water use (Reynaud, 2003; Tate, 1986; Shang et al., 2017). Further, adjustments to the structure of industrial water supply may lead to reductions in freshwater use, as well as improving the reuse of water (Yu et al., 2014). Shang et al. (2017) further identified industrial scale expansion, water-saving technologies, and industrial structural adjustment as drivers of industrial water use.

Shang et al. (2017) used a refined Laspeyres model to assess the effects of the identified drivers on industrial water use. This model accounts for n factors affecting result A . The main drivers used for this analysis were: “industrial output, water use per unit of output, and the relative size of various industrial sectors” (Shang et al., 2017, p. 6). These main drivers can be simplified to *output*, *technology*, and *structure*.

Output, which is driven by the industrial output, shows a three-stage correlation with water use (Shang et al., 2017). As industrial output initially increases, there is rapid development leading to a positive correlation and a corresponding increase in industrial water use. Then, while industrial output continues to increase, industrial water use decreases due to improved efficiency, which can be associated with industrial expansion. Finally, as industrial output increases further, and there is no scope for further water conservation techniques, industrial water use again increases (Shang et al., 2017). In all, it was found that a larger industrial scale will lead to a stronger demand for industrial water, and further determined that the “industrial scale is uncontrollable and is expected to increase with social development and progress” (Shang et al., 2017, p. 6). Shang et al. (2017) concluded that increasing *output* will lead to an increase in industrial water use for all sub-sectors.

Technology is driven by production processes and the water efficiency of the industrial sector, which varies between sub-sectors (Shang et al., 2017). This study also concluded that larger water use per unit of output leads to a stronger demand for industrial water. Further, “water efficiency is controllable and can be improved by upgrading production technologies and strengthening water management” (Shang et al., 2017, p. 6). Shang et al. (2017) concluded that improving *technology* generally reduces water use, although this varies by sub-sector, as some may have already reached maximum water efficiency.

Structure is driven by the relative size of various industrial sub-sectors (Shang et al., 2017). The proportion of sub-sectoral sizes to each other directly affects this driver, and therefore, as water use efficiency varies, industrial water use will as well. Finally, “industrial structure is controllable, and the shutdown or rectification of water-intensive industries and encouragement to low water-use industries will be conducive to saving water” (Shang et al., 2017, p. 6). Shang et al. (2017) concluded that changes to *structure* may have varying results depending on the reapportionment of sub-sectoral sizes.

3 Methods

The main steps of this study were as follows:

1. **Literature analyses** to assess the drivers of present and historical thermoelectric and manufacturing water uses.
2. **Development of a conceptual model for manufacturing water use**, as there are already good approaches for thermoelectric water use. This resulted in the creation of a global dataset of industrial sector water use.
3. **Quantification of thermoelectric and manufacturing water use** to determine the separate contributions of each sub-sector to total industrial water use over the past decades.
4. **Validation of and manufacturing water use estimations** from conceptual model (at the national scale) by comparison with observational datasets.
5. **Implementation in PCR-GLOBWB** using Python.
6. **Analysis of the effects of the industrial sector on the hydrologic cycle** by assessing if water abstractions are meeting water demands, as well as the long-term effects on discharge.

The main focus of the project was on parameterization, both for the creation of the conceptual model and for the implementation in PCR-GLOBWB. Through an updated literature review to identify historical drivers influencing thermoelectric and manufacturing demand, and pressures of water use changes in these two sub-sectors from data rich regions, it was possible to understand production changes, leading to model improvement in data poor regions. This information was useful to provide a greater understanding of the specific changes to which these sub-sectors respond. After this, PCR-GLOBWB was simulated with its initial dataset, and the results were used as reference values. This control data was used to both evaluate the model initially, as well as for comparison with updated results.

A detailed framework of the methodology can be seen in Figure 2.

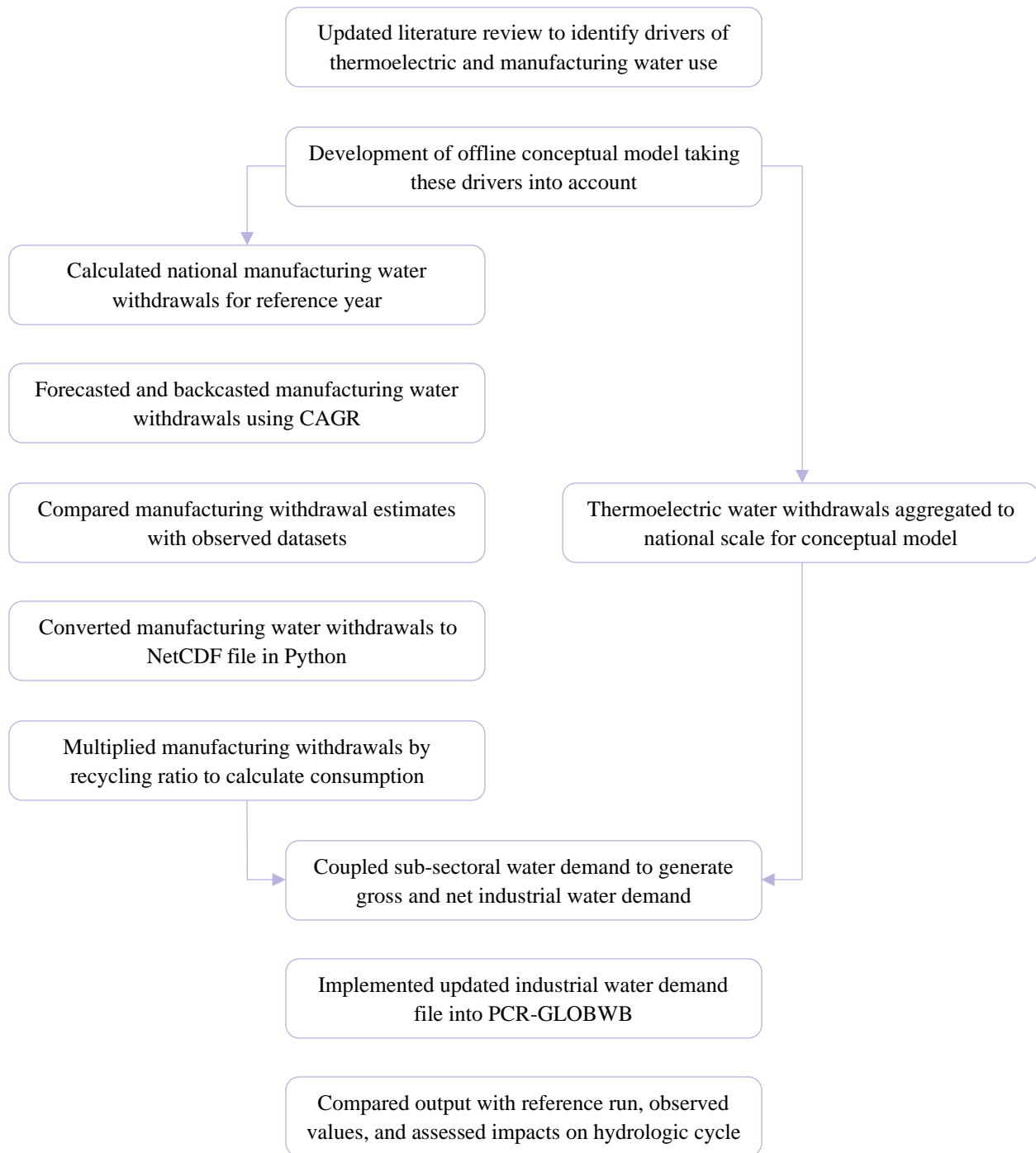


Figure 2 Framework of the methodology.

3.1 Data collection

Table 2 details the datasets used by this study, as well as characteristics and a description of each. Links to available datasets are provided, although some of the datasets used by this study may be licensed, and therefore not further distributed.

Table 2 Overview of datasets used, including characteristics and descriptions.

Source	Date of data	Spatial resolution	Description
Australian Bureau of Statistics (2020)	2014-2019	National and provincial	Manufacturing water supply and use for manufacturing components at the national scale, and total manufacturing at the provincial scale.
Eurostat (2021)	2007-2018	National	Annual manufacturing water abstractions, including specific data for paper and metal components.
FAO AQUASTAT (2021)	2017	National	Global industrial and total water withdrawals.
Lohrmann et al. (2019)	2015	Coordinates, national, PCR-GLOBWB gridcell ID	Global power plants with thermoelectric withdrawals and consumption for 2015-2050, including ‘Best Policies’ and ‘Lifetime’ Scenarios, cooling technologies, fuel types, regional economic classification, construction year, capacity, and water source.
StatCan (2014)	2011	Province and territory (Canada)	Manufacturing water intake, recirculation, gross use, discharge, and consumption for each province and territory.
USGS (2018a, 2018c)	1985-2015	County (United States)	Industrial and thermoelectric withdrawals and consumption by source, salinity, and/or cooling technology.
WRI (2018)	2018	Coordinates, national	Global power plants with thermoelectric generation, fuel type, capacity, and construction year.
World Bank (2021)	1960-2019	National	Annual gross domestic product and manufacturing gross value added at the national scale for several decades, as well as geographic and economic regional classifications.

National industrial water withdrawal data from FAO AQUASTAT (2021), power plant scale thermoelectric water use data from Lohrmann et al. (2019), and national values of GDP, manufacturing gross value added (MVA), and regional classifications from The World Bank (2021c, 2021g, 2021k) to develop the conceptual model and calculate national manufacturing water withdrawals. National and sub-national manufacturing water withdrawals and consumption from the Australian Bureau of Statistics (2020), Eurostat (2021), StatCan (2014), and USGS (2018a) were used as validation datasets. In the case that there was missing data from a nation, values were estimated through regional analyses. If these methods were not possible or unreliable, data from that nation was not included in the analysis. Furthermore, in the case of missing data, the inclusion of additional datasets proved useful to fill in missing values, either due to poor spatial resolution or a lack of reporting.

For the United States, USGS data for county-level water use was collected. This dataset accounts for sectoral water use, including different data for the thermoelectric power and industrial sectors (Dieter et al., 2018a; Dieter et al., 2018b). As there is also a sector in this dataset accounting for mining, the industrial sectors from Dieter et al. (2018a and Dieter et al. (2018b) were used as manufacturing sub-sectoral data for the purposes of this study. For Australia and Canada, total manufacturing water use was presented provincially for each nation, and specific components of manufacturing water use was present for each nation overall (Australian Bureau of Statistics, 2020; StatCan, 2014). In Europe, public and self-supplied manufacturing water use was available for several nations between 2009 and 2018.

The thermoelectric data (Lohrmann et al., 2019) was initially evaluated by taking aggregated values based on characteristics of each power plant. This was done for the consumption, withdrawals, and recycling ratios for each classification. The analyses were performed by assigning code values to each variable within each classification, and then aggregating the total consumption and withdrawals for each variable. The recycling ratios were then calculated by dividing the return flows (difference between withdrawals and consumption) by the withdrawals. The groupings used include the following: nation (Table A1), region (Table A2), economic classification (Table A3), primary fuel type (Table A4), technology (Table A5), cooling system (Table A6), and whether or not seawater is used (Table A7). All data used was from 2015.

3.2 Developing the conceptual water demand model

The offline conceptual model was created using three possible equations for calculating manufacturing water withdrawals. The first, using the definition of industrial water use, took the difference between the industrial water withdrawals and the thermoelectric water withdrawals. This method was used for nations which had observed industrial water withdrawals that were greater than their thermoelectric water withdrawals. The second applied specific manufacturing attributes, by multiplying a nation's gross manufacturing value added (MVA) by the average regional manufacturing water use intensity. This method was used for nations which did not have

manufacturing water withdrawal estimates using Equation 1, but did have observed MVA values. The third method used the same average regional manufacturing water use intensity, and multiplied this value by a regional correlation between MVA and GDP. This third method was used for nations that did not have manufacturing water withdrawal estimates using Equation 1, and also did not have observed MVA values. The first method was given priority, followed by the second, and finally the third. The resulting dataset included the preferred manufacturing water withdrawal estimate for each nation in the reference year 2015. These equations were adapted from the equations used by Flörke et al. (2013) and Vassolo & Döll (2005).

The three equations are as follows:

$$MWW = IWW - TWW \quad (1)$$

Where MWW is the manufacturing water withdrawals [m^3], IWW is the industrial water withdrawals [m^3], and TWW is the thermoelectric water withdrawals [m^3].

$$MWW = MVA * rIntensity \quad (2)$$

Where MVA is the manufacturing gross value added [US\$ 2010] and $rIntensity$ is the average regional manufacturing water use intensity [$\text{m}^3/\text{US\$ 2010}$].

$$MWW = r \left(\frac{MVA}{GDP} \right) * GDP * rIntensity \quad (3)$$

Where $r^{(MVA/GDP)}$ is the average regional correlation between MVA and GDP [unitless].

Raw data used for these three equations can be seen in Table A8. Any nation or autonomous region included in one or more of these datasets was added to the offline model. The first step was to make a list of these nations. For MVA and GDP, data was collected in units of US dollars at their constant 2010 value. This eliminates the effect of inflation and currency fluctuation, allowing each nation to have standardized values. Additionally, regional classifications were assigned according to The World Bank (2021k) and the UNSD (2021), as seen in Table A9. This was done both geographically and economically; to maintain statistically significant sample sizes, the nations were divided into their geographic regions while also being assigned a ‘high’ or ‘low’ economic classification, rather than using the four economic classifications utilized by The World Bank (2021k). The economic classifications were determined by the gross national income (GNI) per capita.

To begin the analyses, each nation’s industrial water withdrawals were collected from FAO AQUASTAT (2021) and assigned. The 2015 data from FAO AQUASTAT (2021) was provided directly by the institution, as it is not readily available from the online directory. FAO AQUASTAT collects its water withdrawal data from government agencies, but also uses other data sources (such as Eurostat, OECD, or other UN agencies) for data filling, in addition to water balance models and regression analyses (FAO AQUASTAT, 2021).

Aggregated national values of thermoelectric water withdrawals, calculated from the dataset created by Lohrmann et al. (2019), were then assigned to each nation. In this dataset, water withdrawals for the cooling of thermoelectric power plants are identified for a global database of power plants. This includes site information for 13,506 power plants across 145 nations and autonomous regions. The data was aggregated from the power plant scale to the national scale, accounting for the national thermoelectric water withdrawals in 2015. Any nations not included in the thermoelectric water use dataset were assumed to not have thermoelectric power plants, and therefore assigned values of 0 for their thermoelectric water withdrawals. This assumption is acceptable because it is estimated that the power plants included in the dataset account for 95.8% of global thermal power plant capacity, as well as 80-90% of global thermoelectric water usage. Values for this dataset were collected through analyses of the cooling technologies present at each site, its water footprint including power generation and fuel type, as well as technological changes (Lohrmann et al., 2019). 2015 was used as the reference year for the dataset, and future projections were based off these measured values. For this reason, 2015 was used as the reference year for the conceptual model in this thesis.

With every nation and autonomous region listed, and the raw data available for each variable, the conceptual model was constructed. For each nation in which industrial water withdrawals were present, and greater than the thermoelectric water withdrawals, the manufacturing water withdrawals were estimated by taking the difference of the two. These withdrawals were then divided by each nation's corresponding MVA, if available, to determine the manufacturing water use intensity – a measure of the volume of water necessary to increase the MVA by 1 unit.

The next step was to data fill for nations with missing values. To begin, average intensities were taken for each region. As the intensity does not account for the size of the nation (population or economy based), average values could be applied to missing nations. The coefficient of variation for the average intensity was also calculated to determine the consistency within each region. Application of regional intensities provided each nation with either an observed or estimated value.

After updating the intensity values, data filling was necessary for MVA estimates. For this, the regional classifications were used again. MVA takes the economic size of a nation into account; therefore, regional averages could not be used because the size of any country in a region does not affect the size of other countries in the region. For this reason, the correlation between the MVA and GDP for each region was calculated, giving an indication of the regional contribution of the manufacturing sector to the total economic output of a nation. This was done by taking the slope of the MVA and GDP values, and then calculating the r-squared and correlation of the data points for purposes of statistical significance. For each nation with missing MVA values, the regional slope was used in conjunction with the observed GDP values from The World Bank (2021c). Thus, for every nation with GDP values, the manufacturing water withdrawals could be calculated by multiplying the average regional intensity by the estimated MVA.

With input values for industrial water withdrawals, thermoelectric water withdrawals, manufacturing water use intensity, MVA, MVA-GDP correlation, and GDP, the three equations to estimate manufacturing water withdrawals could be applied. A new dataset was created to apply all three methods and select the most precise value. This was done by first adding the nations and their corresponding regions. Then, the model looked up the input values for each nation. At this point, the model was setup to calculate manufacturing water withdrawals using each of the three equations for each nation. The preferred manufacturing water withdrawals were then added to the observed thermoelectric water withdrawals to recalculate the total industrial water withdrawals. For each nation, the contribution of manufacturing and thermoelectric water use to industrial water use was also calculated.

The 2015 reference values were then forecasted and backcasted to produce a table of manufacturing water withdrawals for each nation from 1970 through 2050. To calculate the annual changes, supplemental data from Bijl et al. (2018) was analyzed. For each region in that study (see Table A9), the compounded annual growth rate (CAGR) was calculated using the historical 2010 data for annual national industrial water withdrawals and their corresponding SSP-2 predictions for 2050. By using the regional CAGR, the annual change in industrial water withdrawals over the full time series was extracted. The CAGR for each nation in the conceptual model was then looked up according to its regional classification used by Bijl et al. (2018), providing each nation with an expected annual change in industrial water withdrawals. These annual changes were then applied to the 2015 manufacturing water withdrawals and extrapolated to 2050. In addition, the CAGR was used to backcast the 2015 data to 1970. Finally, the FID codes used by PCR-GLOBWB were applied to the nations in the conceptual model.

3.3 Integration into PCR-GLOBWB

This data table of annual manufacturing water withdrawals from the conceptual model was then applied to PCR-GLOBWB as a text file and converted into a NetCDF file using a Python script. This spatiotemporal dataset accounted for gross manufacturing water demand and was adjusted for compatibility with PCR-GLOBWB. These adjustments consisted of setting the spatial grid to an existing PCR-GLOBWB map file at 5 arc minute spatial resolution, dividing the volumes of water by cell area to convert them into water slices, downscaling the national values according to a population distribution map used by PCR-GLOBWB, dividing the annual values by days per year as PCR-GLOBWB runs daily (note that this results in uniform values for each location within each year), and finally trimming the data to the time range between 1980 and 2020.

In addition to the gross manufacturing water demand, net manufacturing water demand data, as well as gross and net thermoelectric water demand data, were needed. The net manufacturing water demand was derived from calculated industrial water demand data (Wada et al., 2014). Using the gross and net industrial water demand at 5 arc minute spatial resolution from the Wada et al. (2014) dataset, the ratio of consumption to withdrawals was calculated by dividing the net demand by the

gross demand. These ratios were then multiplied by the gross manufacturing water demand file created by the conceptual model to estimate net manufacturing water demand. Note that the data from Wada et al. (2014) included industrial water estimates through 2014, after which the 2014 values were applied to the manufacturing estimates from 2015 through 2020.

Next, thermoelectric data (Lohrmann et al., 2019), cross-referenced with thermoelectric power plant construction years (WRI, 2018), was collected. In this power plant dataset, the withdrawals and consumption of water used for the cooling of thermoelectric power plants were aggregated to the gridcell level for compatibility with PCR-GLOBWB. With the raw data, similar adjustments were made (as with manufacturing withdrawals) to ensure compatibility. The files were given uniform characteristics, such as setting the spatial grid to the PCR-GLOBWB map file, dividing the volumes of water by the cell area, dividing the annual values by days per year, and trimming the data to 1970 through 2020. As this dataset includes the initial operation year of power plants, it accounts for spatiotemporal variations. With the thermoelectric data inputted at the power plant scale, the spatial precision of the model was immediately adjusted. Initially, PCR-GLOBWB downscaled all industrial sector water use according to population density, but with a more localized dataset of observed values, this was changed. By first inputting the spatial characteristics of the thermoelectric water demand, the parameterization of the model was altered.

At this point, there were NetCDF files for gross and net manufacturing and thermoelectric water demand for the period between 1980 and 2020. The next step was to aggregate the gross and net files for compatibility with PCR-GLOBWB. PCR-GLOBWB runs gross and net industrial water demand, so the gross manufacturing and thermoelectric water demands were aggregated to gross industrial water demand, and the net manufacturing and thermoelectric water demands were aggregated to net industrial water demand. Upon creation of the industrial water demand files, the percentage contributions of manufacturing and thermoelectric were calculated. This was done by dividing the gross and net sub-sectoral datasets by the gross and net sectoral datasets. Ultimately, this produced NetCDF files indicating the percent contributions of gross and net manufacturing and thermoelectric water demand to total gross and net industrial water demand at 5 arc minute spatial resolution from 1980 through 2020. The updated industrial sector water demand file was then integrated into PCR-GLOBWB, and the model was simulated globally from 1980 through 2014.

3.4 Data analyses

Among the data analyses for this thesis were comparisons between the initial industrial demand input data and the updated industrial demand input data; the updated gross industrial water demand and the updated modelled industrial abstractions; the initial supply and demand of industrial water and the updated supply and demand of industrial water; the initial modelled discharge and the updated modelled discharge; and the initial modelled industrial abstractions and the updated modelled industrial abstractions.

3.4.1 Analysis of gross industrial water demand

To analyze the differences between the initial industrial input dataset (Wada et al., 2014) and the updated industrial input dataset, the two were aggregated nationally for 2000 and 2014. These years were selected because 2000 was used as the reference year by Wada et al. (2014) and 2014 was the closest year to the reference year used in the conceptual model (2015). By aggregating the initial dataset annually, and upscaling both datasets to the national level, national estimates of gross industrial water demand were determined for each. These values were then compared for both years to assess how the input files relate to each other. The statistical relationship between the input files was determined by taking the correlation between the two datasets at each identified year (2000 and 2014) for each nation, as well as by taking the total gross industrial water demand globally. These statistical analyses were also done at the regional scale. Additionally, time series were created to show the relationship between the two input datasets for three nations. These plots show how the initial and updated gross industrial water demand vary temporally. The annual time scale was used for this analysis as the updated input data was provided at that time scale. Additionally, plots of the manufacturing and thermoelectric demand were included to show their contributions to the updated gross industrial water demand, as well as their respective trends over time.

3.4.2 Analysis of modelled industrial water supply and demand

Regarding comparisons between industrial demand and abstractions, the abstractions (supply) were divided by the gross demand to assess if the demand for industrial water was being met. This was depicted as the fraction of gross industrial water demand that was supplied. Data for each was reliably available at the annual time scale and the national spatial scale. Further, national and regional abstractions and gross demand values were extracted for 2014 (the closest output year to the conceptual model reference year, 2015). The ratio of industrial water supply to demand was also calculated globally for the initial model run for comparison. Nationally, the data was assessed by plotting an exceedance graph of nations and thresholds of ratios between abstractions and gross demand. Regionally, this information was presented as a table of the total values.

3.4.3 Analysis of modelled industrial water abstractions

The abstractions from the initial and updated model runs were then compared. This was performed in a similar manner to the analysis of the input industrial water demand: the national values for 2000 and 2014 were compared, the regional correlations and total percent changes were calculated, and time series were extracted for three nations to compare the output datasets temporally. The same methodology was used for the abstraction analyses as was used for the input analyses.

3.4.4 Analysis of modelled global discharge

The initial and updated discharge datasets were first averaged temporally (over the entire time range) to yield average discharge values at each location per month. To assess the effects of the updated industrial water demand data on discharge, the difference between the two output datasets was divided by the initial output data to determine the percent change globally. This was done by subtracting the initial values from the updated values to first determine the change in raw values, and then dividing by the initial values to determine the percent change. Further, time series data from three rivers globally were analyzed. This was done by extracting and comparing the average monthly discharge over the full time span of the model for a station on each river from the initial and updated model output. Fixed sites were used for each of the datasets to ensure uniformity. Plots were made to compare the raw difference between the output data, as well as the percent change caused by adjusting the industrial water demand input file.

4 Results

4.1 Conceptual model output

Using national data collected from FAO AQUASTAT (2021) for industrial water use, Lohrmann et al. (2019) for thermoelectric water use, and The World Bank (2021c, 2021g) for economic parameters, a list of 219 nations and autonomous regions was constructed. This list included any nation listed in at least one of the datasets. Industrial water withdrawals were available for 185 nations for 2015 (FAO AQUASTAT, 2021). MVA values were provided for 174 nations (The World Bank, 2021g). GDP values were provided for 217 nations (The World Bank, 2021c; UNSD, 2021). Geographical and economic indicators from The World Bank (2021k) resulted in 14 regional classifications.

Industrial and thermoelectric water withdrawals were collected as annual volumes [m^3] for 2015. Taking the difference between the industrial and thermoelectric water withdrawals (for nations in which the industrial values were greater than the thermoelectric values) yielded manufacturing water withdrawal estimates for 138 nations. Dividing these manufacturing water withdrawal estimates by each nation's MVA, if available, yielded manufacturing water use intensity [$\text{m}^3/\text{US}\$ 2010$] estimates for 119 nations.

Ultimately, after all the input values were applied to a new dataset, and the model was run with the three manufacturing water withdrawal equations, each of the 219 nations and autonomous regions had output values from the conceptual model. These output values can be seen in Table A10, along with the recalculated industrial water withdrawals and the percentage contributions from the manufacturing and thermoelectric sub-sectors.

Using the regional compounded annual growth rate (CAGR) values derived from Bijl et al. (2018), the 2015 reference year manufacturing water withdrawals were forecasted and backcasted to cover the time period between 1970 and 2050. These annual percent values (see Table 3) account for the technological changes in each nation. A positive CAGR implies manufacturing water withdrawals are increasing, while a negative CAGR implies manufacturing water withdrawals are decreasing. After this step, the PCR-GLOBWB FID codes were applied, with only two nations being omitted. The resulting data table included the annual manufacturing water withdrawal estimates, from 1970 through 2050, for 217 nations and autonomous regions.

Table 3 Regional compounded annual growth rate (CAGR) values – computed using the 2010 and 2015 data from Bijl et al. (2018) – used for forecasting and backcasting the 2015 reference year manufacturing water withdrawal output values from the conceptual model.

Region	CAGR	Region	CAGR
Brazil	0.8697%	Oceania	0.0489%
Canada	-2.2430%	Rest of Central America	0.7423%
Central Europe	0.1835%	Rest of Southern Africa	2.4798%
China	0.8105%	Rest of South America	0.7202%
East Africa	3.2823%	Rest of South Asia	2.4133%
India	2.2291%	Russia	-0.2891%
Indonesia	2.0421%	Southeast Asia	1.2570%
Japan	-0.6909%	South Africa	0.6590%
Central Asia	0.4932%	Turkey	1.0685%
Korea Region	0.4422%	Ukraine Region	0.5612%
Mexico	0.8380%	USA	-1.8008%
Middle East	-0.7403%	West Africa	2.1860%
North Africa	1.2696%	West Europe	-0.2480%

4.2 PCR-GLOBWB modelling

The gross manufacturing water demand dataset was created using the output from the conceptual model. The net manufacturing water demand dataset was created using the ratio between industrial water consumption and withdrawals (Wada et al., 2014). In those industrial water demand datasets, the ratio of consumption to withdrawals was estimated at 20%, 30%, or 40%, depending on the development of a nation. The application of these ratios at the 5 arc minute spatial resolution was compatible with the gross manufacturing water demand dataset (see Figure 3), and used to estimate net manufacturing water demand (see Figure 4). When these datasets were coupled with the gross and net thermoelectric water demand datasets (see Figure 5 and Figure 6), the total gross and net industrial water demand for the globe was calculated at 5 arc minute spatial resolution between 1980 and 2020 (see Figure 7 and Figure 8). Further, with the percentage contributions of manufacturing (see Figure A1) and thermoelectric (see Figure A2) water demands to total industrial water demands, the localized influence of each sub-sector was determined. These figures depict the input water demand data spatially for the reference year 2015. It should be noted that where the displayed range is not very visible in the legend, the values increase from dark blue to green to yellow to red.

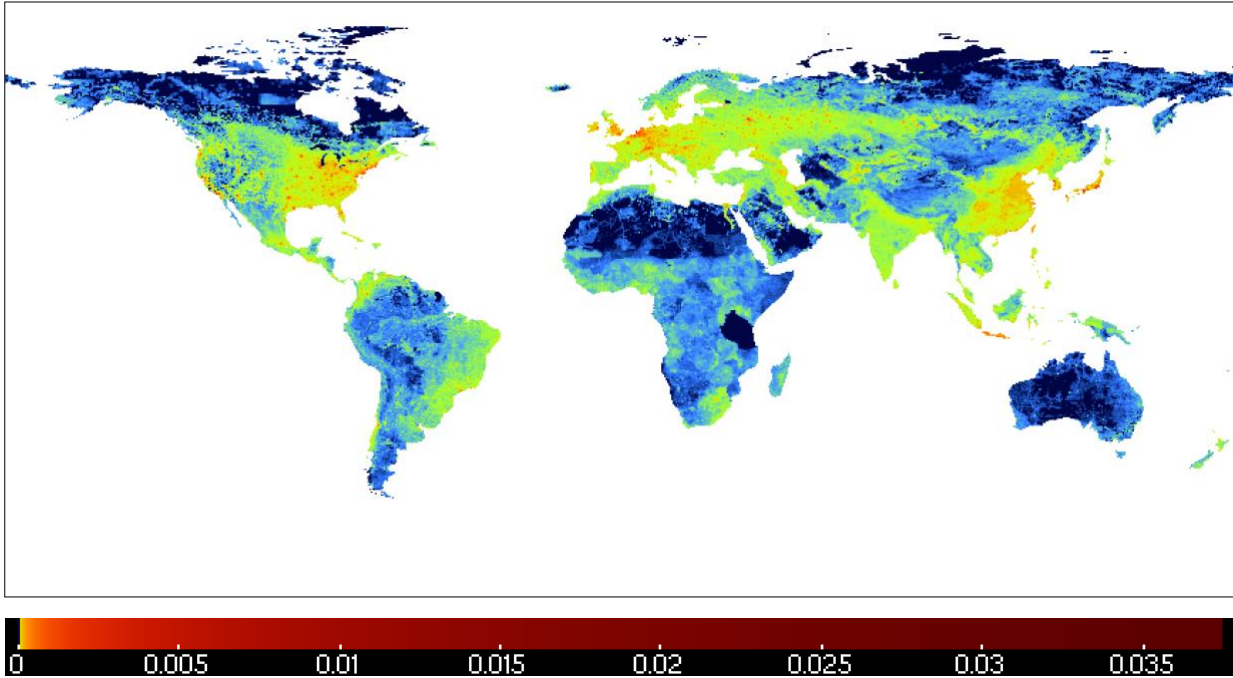


Figure 3 Gross manufacturing water demand in m^3/a for 2015.

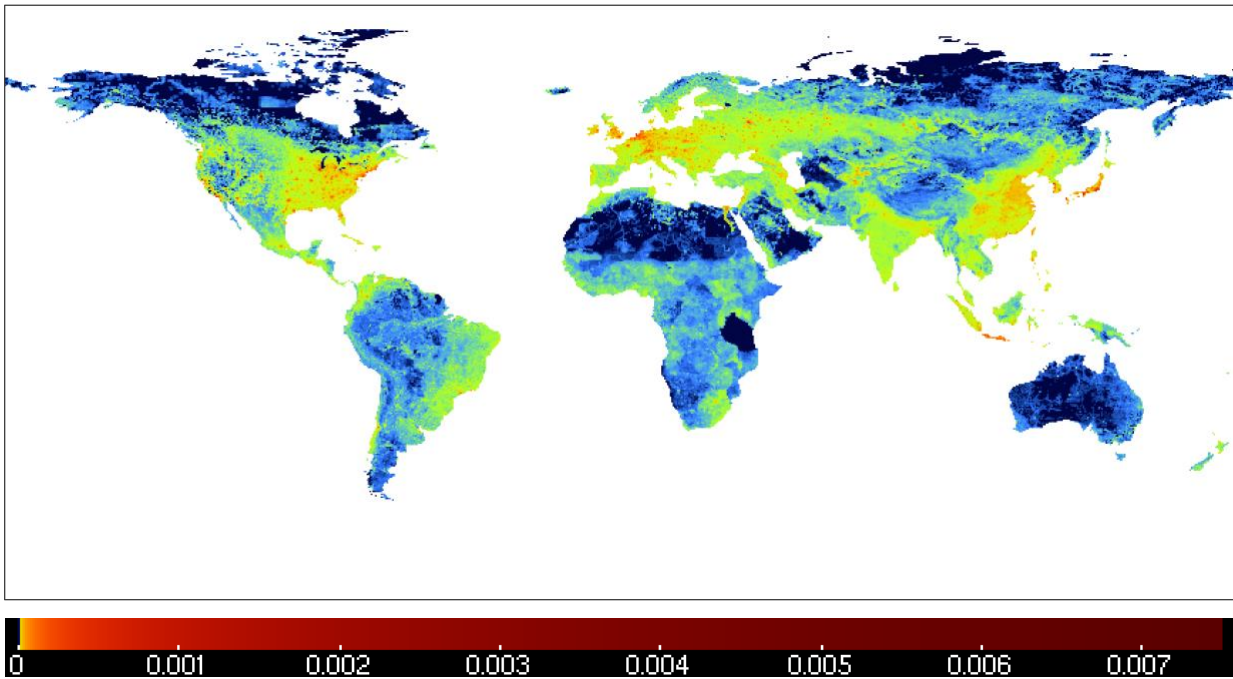


Figure 4 Net manufacturing water demand in m^3/a for 2015.

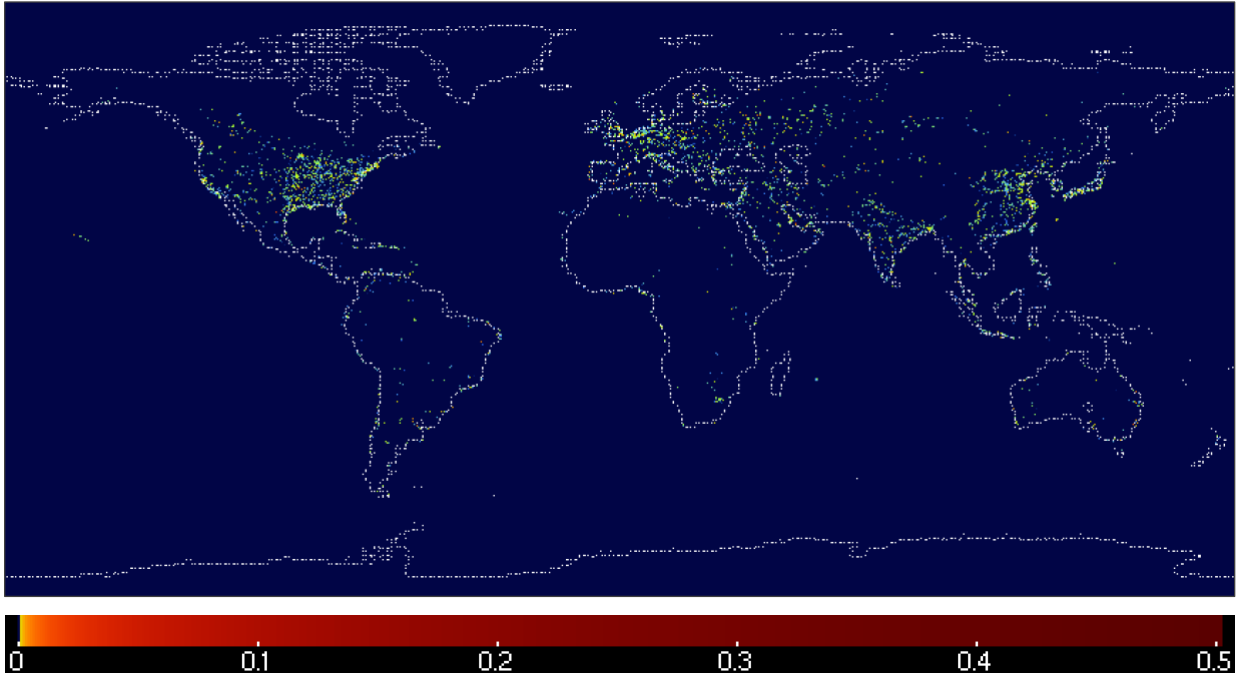


Figure 5 Gross thermoelectric water demand in m^3/d for 2015.

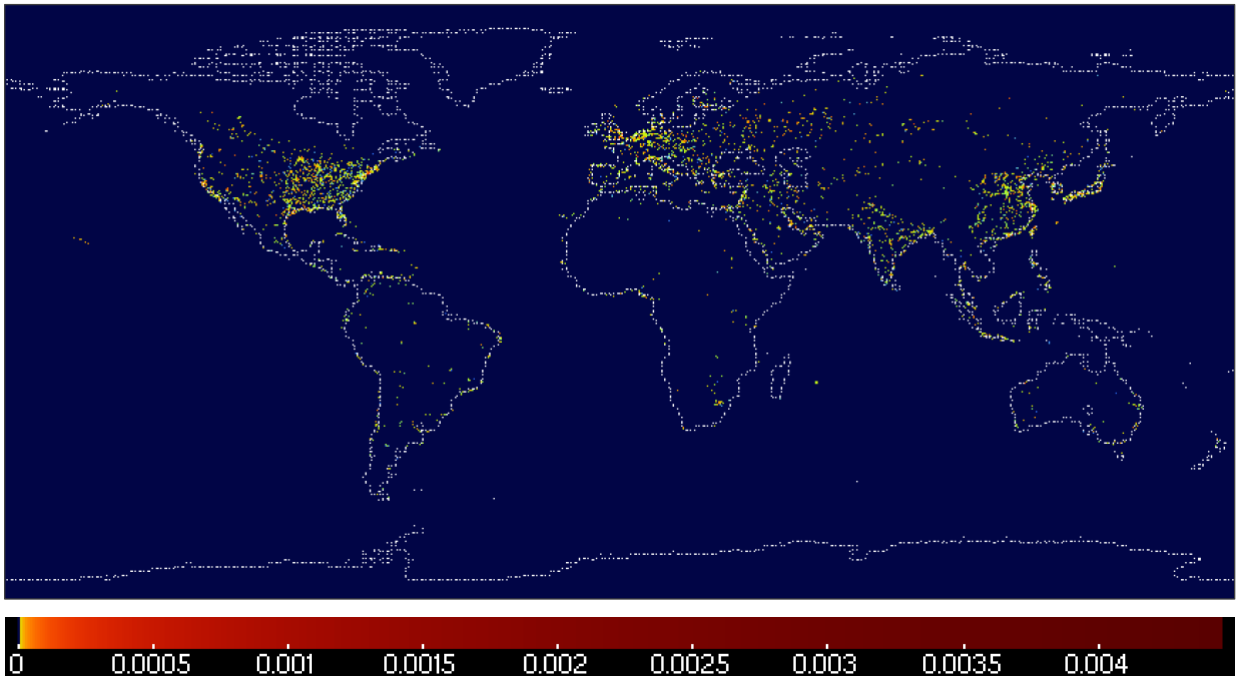


Figure 6 Net thermoelectric water demand in m^3/d for 2015.

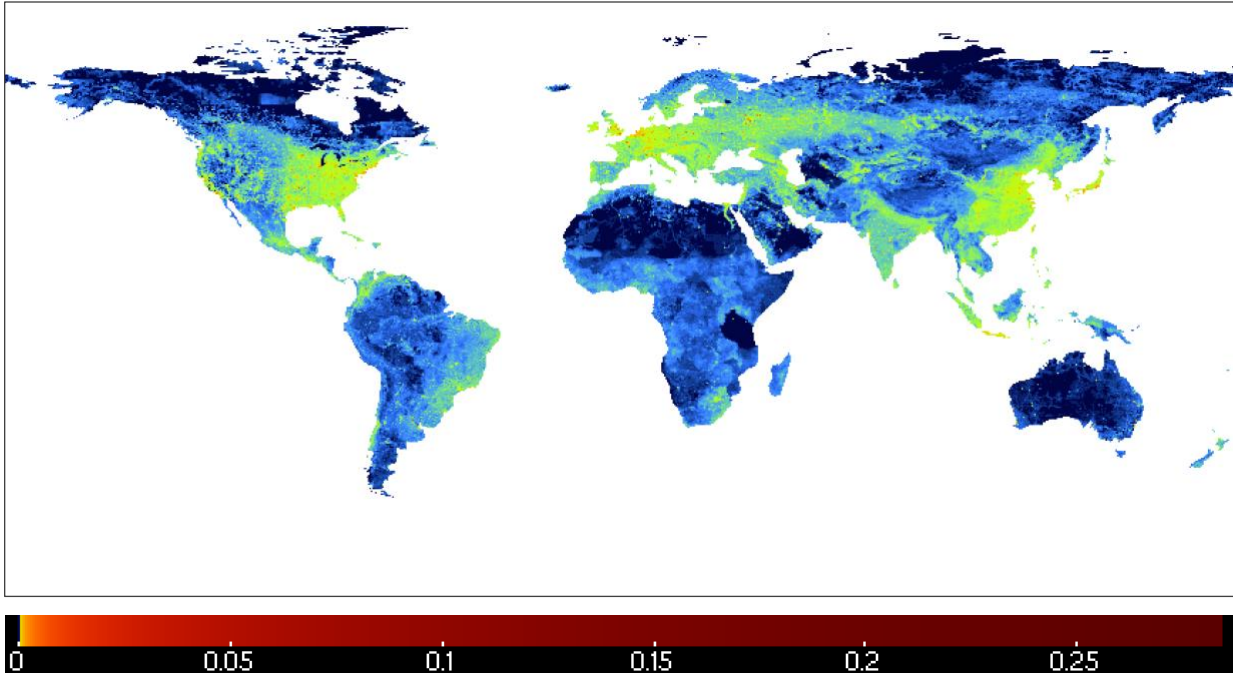


Figure 7 Gross industrial water demand in m^3/d for 2015.

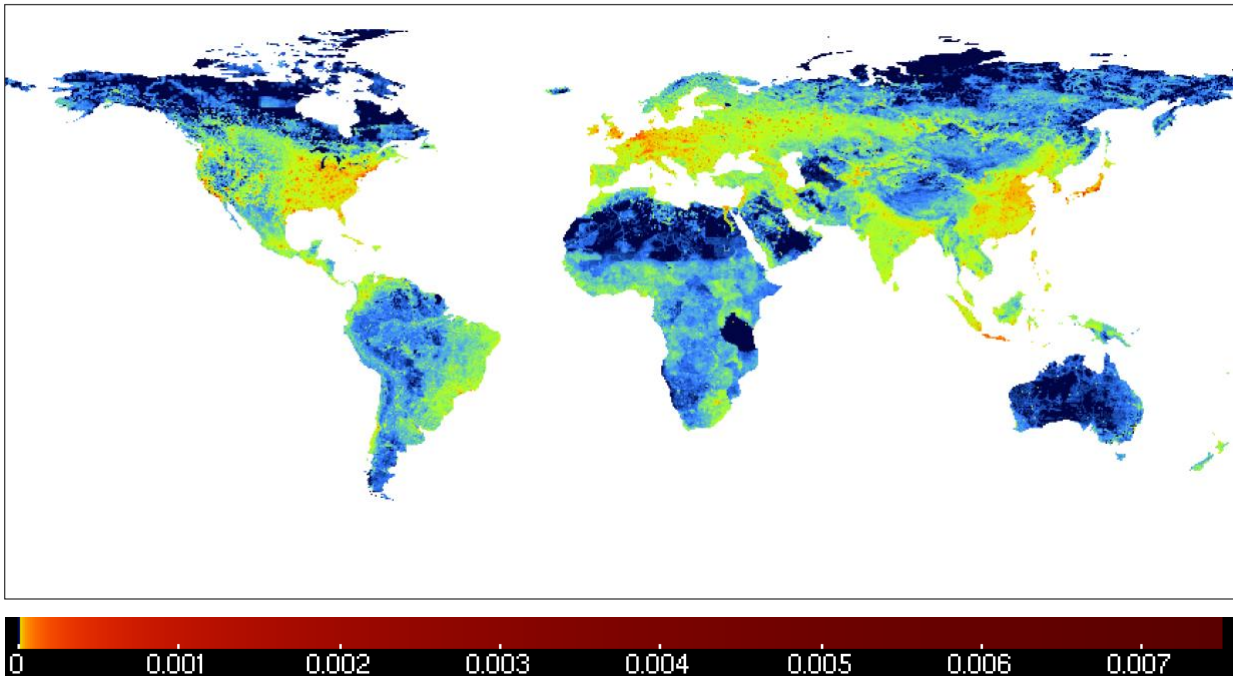
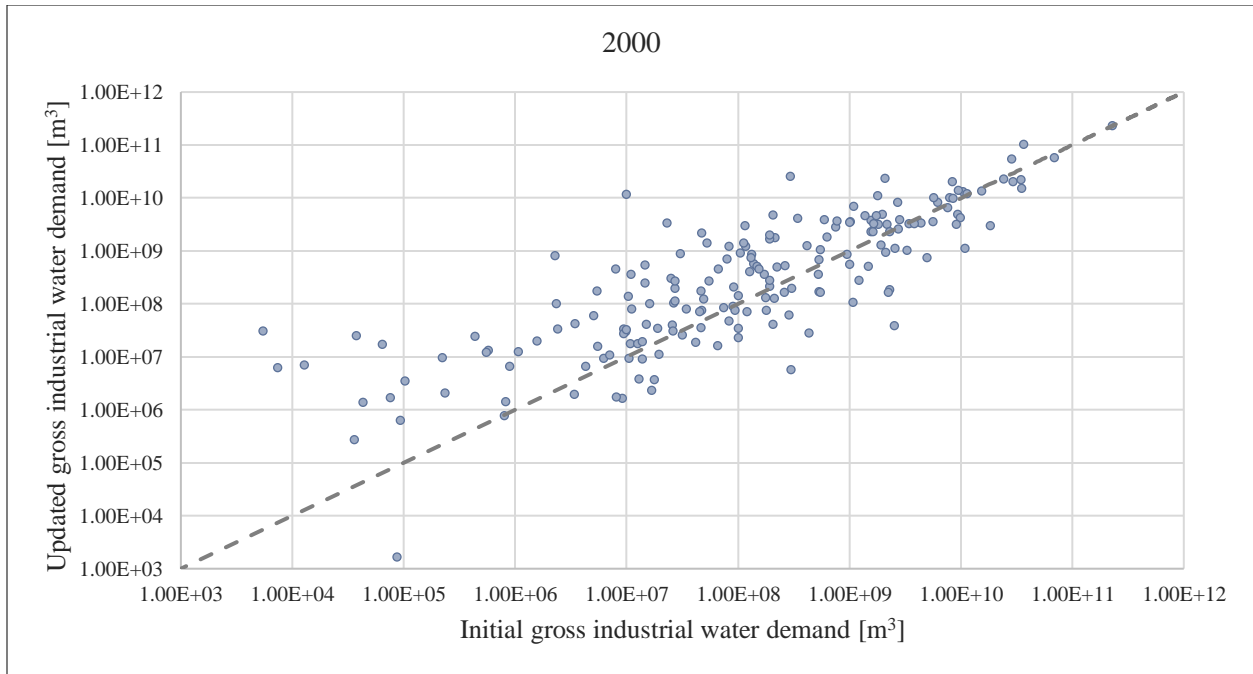


Figure 8 Net industrial water demand in m^3/d for 2015.

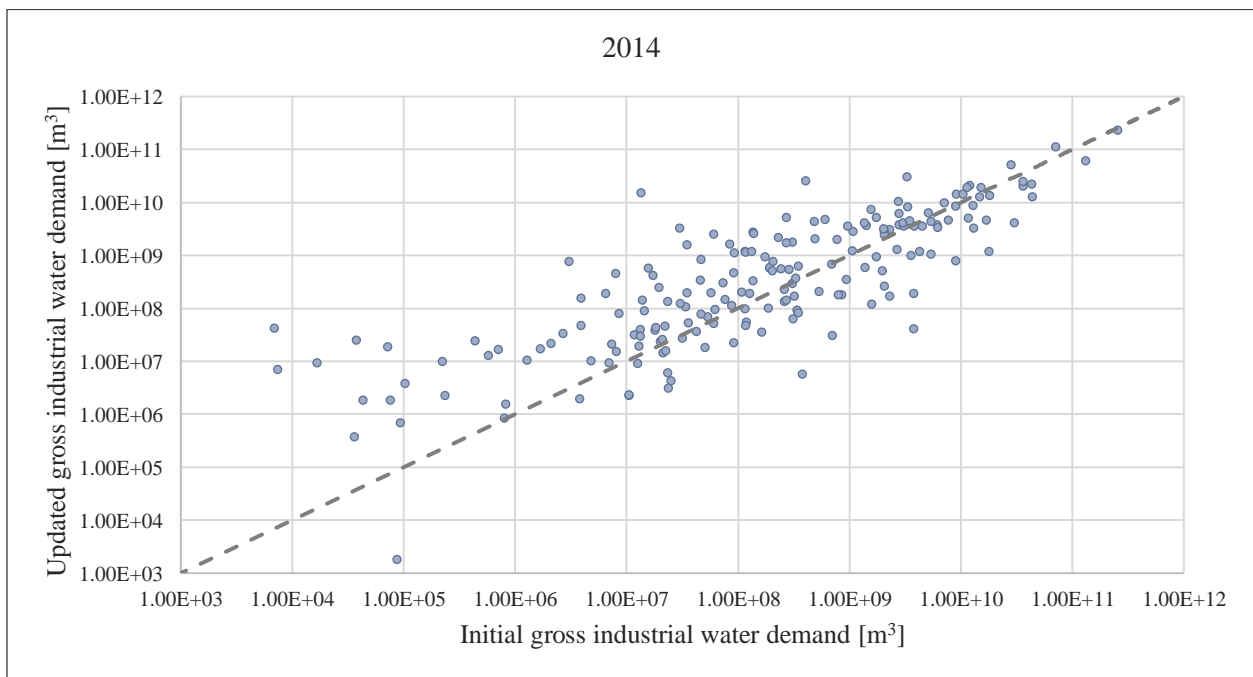
4.3 Analysis of results

4.3.1 Gross industrial water demand

To analyze the input industrial demand files, the initial gross demand was compared with the updated gross demand (see Figure 9). The plots depict a nation's gross industrial water demand according to each dataset, as well as a line delineating a perfect fit. Points close to the fit line indicate both datasets had similar estimates for a nation's gross industrial water demand, while points farther away indicate discrepancies between the two datasets. The updated national data for 2000 overestimated the initial national data by approximately 2%, while the updated national data for 2014 underestimated the initial national data by approximately 16.5%. Further, there is a 94% correlation between the national gross industrial water demand values for 2000, and a 93% correlation for 2014. As for the total global gross industrial water demand, the updated model estimated 21% more global water demand for 2000 than the initial model, and 5% less global water demand for 2014. The high level of fit, and similar global totals, between each of the input industrial water demand files indicates that although the spatial precision of the model was adjusted, the overall national values were not greatly affected. Large discrepancies in the individual data points may be due to differences in available data used by Wada et al. (2014) and in the creation of the conceptual model. The nations in which the conceptual model most overestimated the initial model were Liberia and Qatar, while the nations in which the conceptual model most underestimated the initial model were Bosnia and Herzegovina and Luxembourg.



a



b

Figure 9 Comparison of the initial and updated national gross industrial water demand input data for 2000 (a) and 2014 (b).

Regional breakdowns of the correlation and percent of the initial values which were estimated can be seen in Table 4 for 2000 and Table 5 for 2014. When comparing the gross industrial water demand regionally for 2000, there are two very notable differences. While the datasets correlate quite well in most regions, there are correlations of 35% for low-income nations East Asia & Pacific and 26% for high-income nations in Middle East & North Africa. As seen in the ‘percent change’ column, for both regions the updated gross industrial water demand file overestimated the initial dataset. This difference is much greater for high-income nations Middle East & North Africa, where the updated model estimated total gross industrial water demand volumes 7.5 times greater than the initial model. The relationships between the datasets for 2014 are similar, with a few notable exceptions. The correlation for high-income nations in Middle East & North Africa is only 15%, although the overestimation by the updated model was only 5.6 times greater than the initial model. Further, in several regions, the correlation and total values were quite similar. A plot depicting the initial and updated total regional gross industrial water demand for 2000 and 2014 can be seen in Figure 10. It shows a generally good fit between the two datasets, as well as similar increases from the 2000 values to the 2014 values for each region.

Table 4 Regional correlation between the initial and updated input gross industrial water demand files for 2000, including the percent change from the total initial values to the total updated values.

Region	Correlation	Percent change
East Asia & Pacific High	94%	155%
East Asia & Pacific Low	35%	155%
East Europe & Central Asia High	97%	-19%
East Europe & Central Asia Low	87%	-76%
Latin America & Caribbean High	88%	105%
Latin America & Caribbean Low	63%	44%
Middle East & North Africa High	26%	664%
Middle East & North Africa Low	92%	40%
North America High	100%	-6%
South Asia Low	99%	10%
Sub-Saharan Africa High	100%	50%
Sub-Saharan Africa Low	73%	126%
West Europe High	93%	-1%

Table 5 Regional correlation between the initial and updated input gross industrial water demand files for 2014, including the percent change from the total initial values to the total updated values.

Region	Correlation	Percent change
East Asia & Pacific High	97%	81%
East Asia & Pacific Low	37%	124%
East Europe & Central Asia High	96%	-48%
East Europe & Central Asia Low	94%	-82%
Latin America & Caribbean High	95%	87%
Latin America & Caribbean Low	62%	25%
Middle East & North Africa High	14%	460%
Middle East & North Africa Low	82%	53%
North America High	100%	-19%
South Asia Low	99%	-18%
Sub-Saharan Africa High	100%	30%
Sub-Saharan Africa Low	78%	73%
West Europe High	87%	-12%

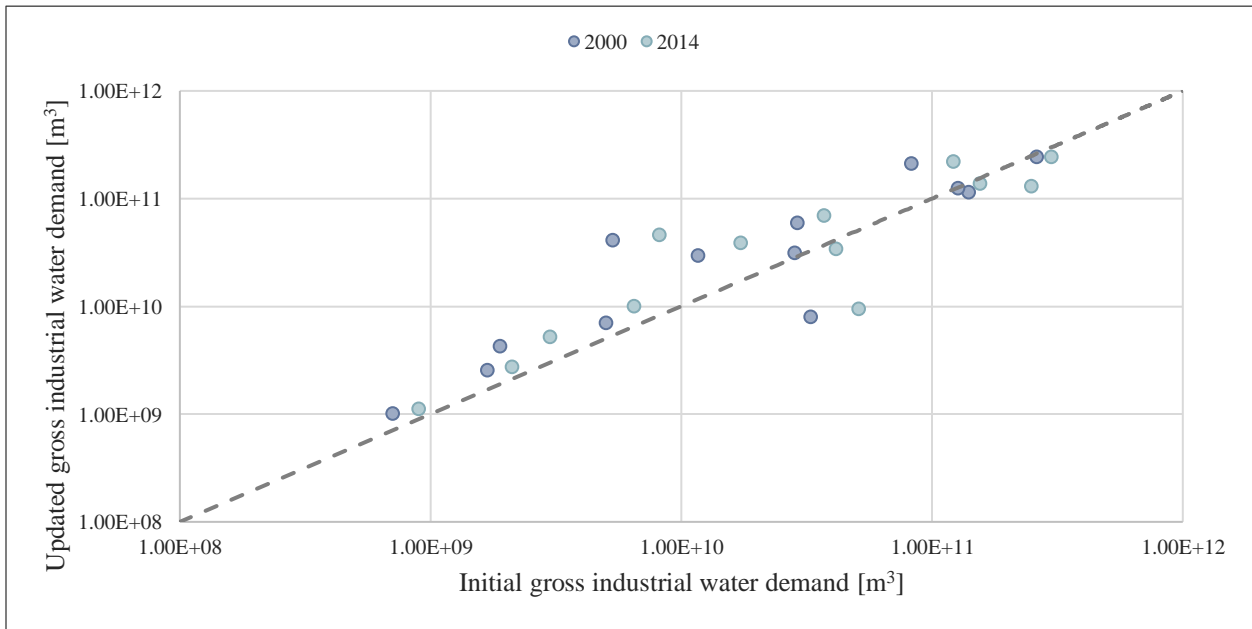
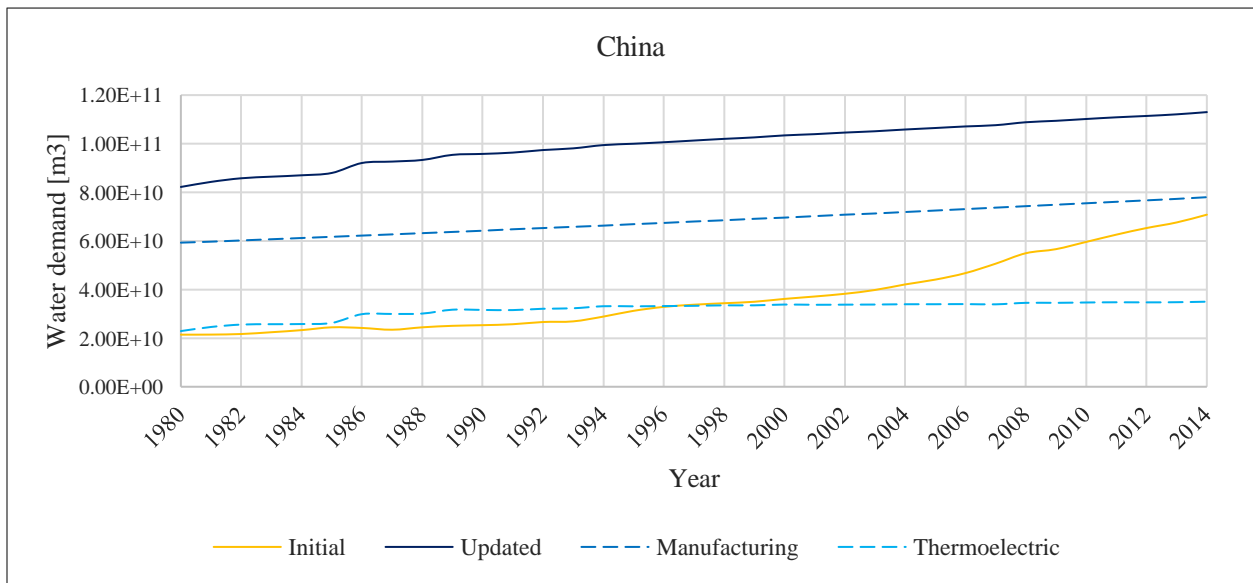
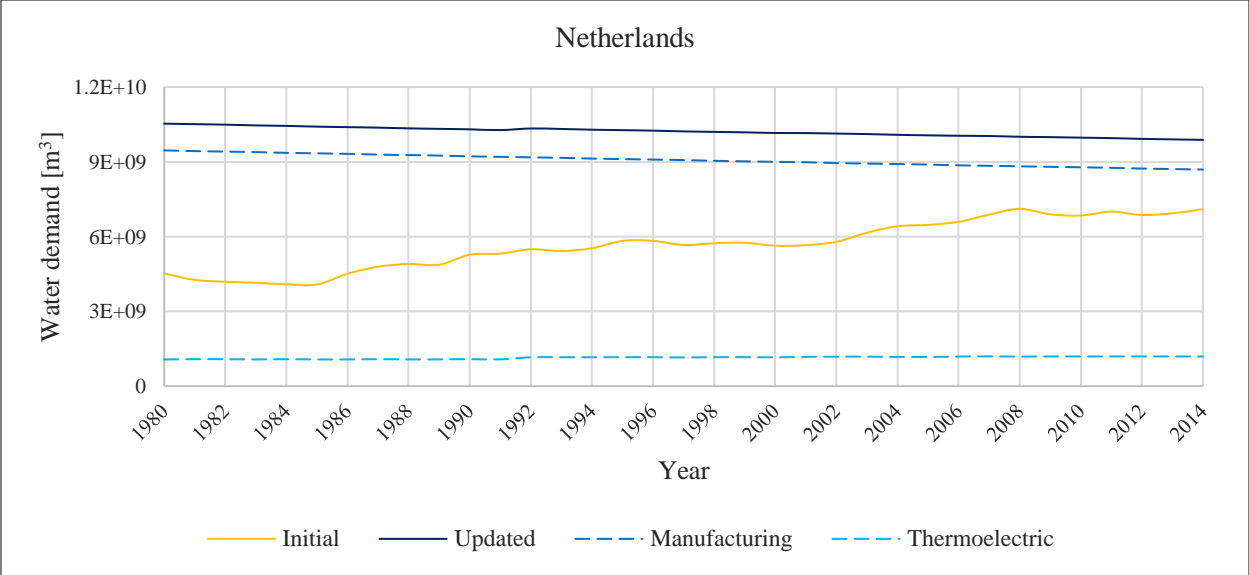


Figure 10 Comparison of the initial and updated regional gross industrial water demand data for 2000 and 2014.

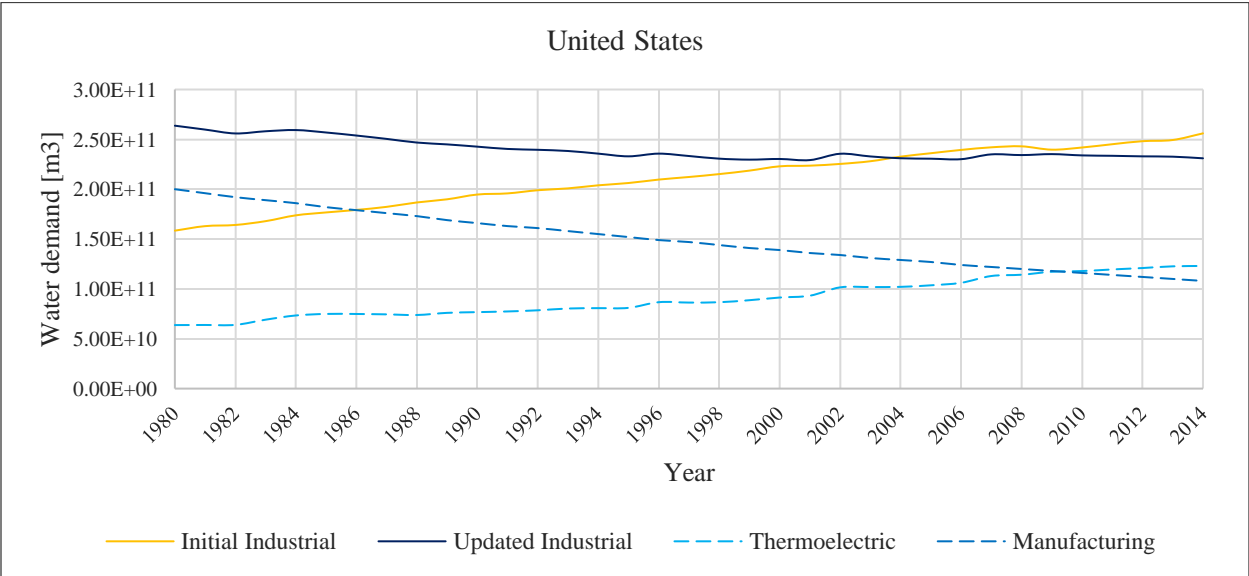
Additionally, time series for three nations, China, the Netherlands, and the United States, were extracted to compare the initial and updated gross industrial water demand input files (see Figure 11). In these plots, the differences between demands can be seen without the effects of downscaling. It is evident that the updated model consistently estimated greater gross industrial water demand in China and the Netherlands, as well as greater gross industrial water demand in the United States at the start of the model run. In the United States, however, the two input datasets predict very similar total volumes water demand towards the end of the model – and more significantly, towards the reference years used by each dataset. Further, the decrease in gross industrial water demand in the Netherlands and the United States over time indicates a shift towards improving water efficiency in industrial processes. Also included in these plots are the trend in gross manufacturing and thermoelectric demand. In China, both sub-sectoral demands at the start of the model run exceed the initial gross industrial demand and have similar increases over time. By the final years, however, the initial gross industrial demand is approximately equal to the updated gross manufacturing demand. The trends of demand in China all show an increase in gross water demand. In the Netherlands, the thermoelectric demand remains relatively constant, while the manufacturing demand decreases slightly. These factors contribute to the slight decrease in updated industrial demand, thereby causing a difference in the trend when compared with the initial industrial demand. In the United States, the thermoelectric demand increases slightly over time, while the manufacturing demand decreases. As the technological changes associated with the decrease in gross manufacturing water demand offset the increases in gross thermoelectric water demand, the updated industrial demand decreases over time. Further, while the manufacturing demand in the United States contributed approximately 75% of industrial water demand in 1980, by 2014 the thermoelectric demand slightly exceeded manufacturing.



a



b



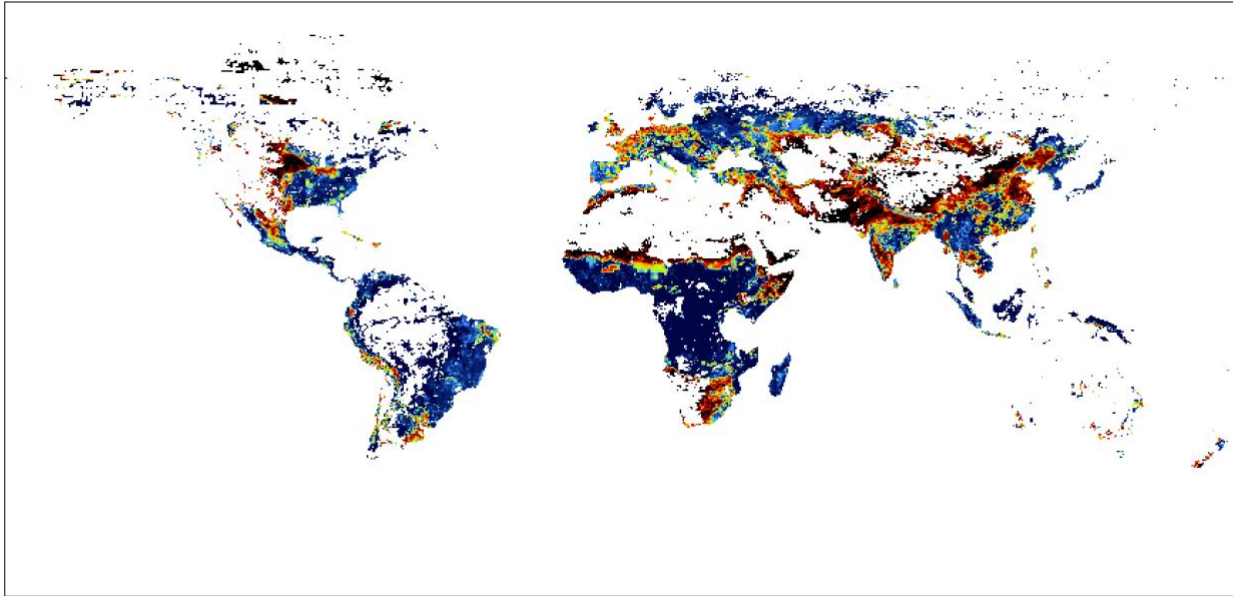
c

Figure 11 Comparison of the initial and updated gross industrial water demand input files used in PCR-GLOBWB, including the specific contributions from the manufacturing and thermoelectric sub-sectors, for China (a), the Netherlands (b), and the United States (c).

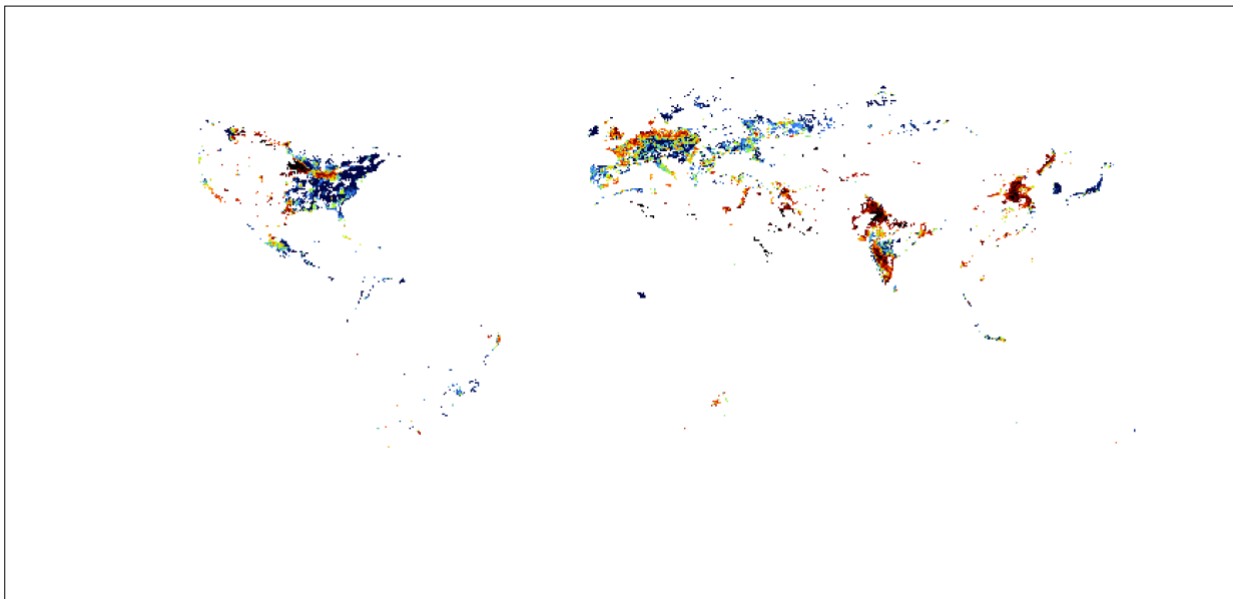
4.3.2 Industrial water supply and demand

To compare the supply and demand of industrial water from the model runs, the abstractions were divided by the gross demand. This was done using the NetCDF files, creating a spatiotemporal dataset of the ratio of gross industrial water demand that was being met. Included is a map (see Figure 12) depicting these ratios globally for the updated model in 2014. It shows the parts of the world in which gross industrial water demand is being met, but also the locations in which there is insufficient water supply to meet these demands. Large parts of Europe and Asia are notably experiencing lower percentages of demand being met, while much of the United States, South America, and Africa have enough available water to meet their industrial demands. For comparison, the percentage of gross industrial water demand which was met by industrial water abstractions for 2014 from the initial model run are also displayed. It shows where the initial model estimated industrial water scarcity (particularly Northern Europe, India, and Eastern China) and sufficient industrial water availability (particularly Eastern United States, Scandinavia, and Japan). White cells indicate missing values, but as the map zooms out, it interpolates average values for the display. When magnified, there are localized values in this output dataset, however many of these values are not visible at the global scale.

It should be noted that the demand data is population-driven, as it was downscaled using population distribution; while the supply data is water availability-driven, as industrial water abstractions require natural water systems. Therefore, local differences between industrial water supply and demand depicted in these figures may not realistically represent industrial water scarcity. That is, the locations with high industrial water demand can be supplied by cells at other locations. To counter this dilemma, national values of industrial water supply and demand must also be considered to assess how nations meet their industrial water demands on the whole.



a



b



Figure 12 Percentage of updated (a) and initial (b) gross industrial water demand which was met by abstractions (supply) for 2014.

Figure 13 depicts the national exceedance of supply-demand threshold values. It shows the total percent of nations included in the analysis which meet certain levels of demand. It can be seen that 19% of nations have industrial water supply that is less than half of their gross demand; 11% of nations fully met their gross industrial water demands; and 43% of nations met at least 90% of their industrial demands. This plot gives a better indication of water scarcity, as the local ratio of abstractions to demand can be inaccurately limited by the local population and water availability. At the national scale, this bias is reduced, although still present because many sub-national cells are capped.

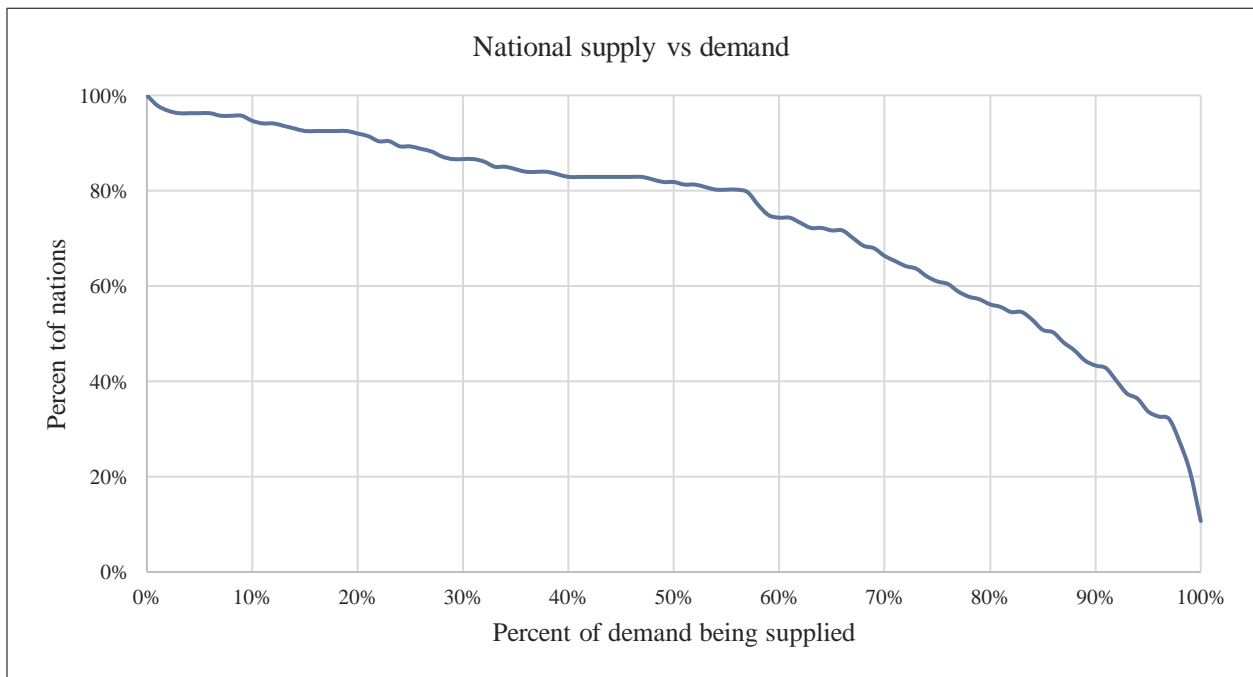


Figure 13 Percent of nations exceeding percentage thresholds of ratio between total industrial water supply (abstractions) and (gross) demand in 2014.

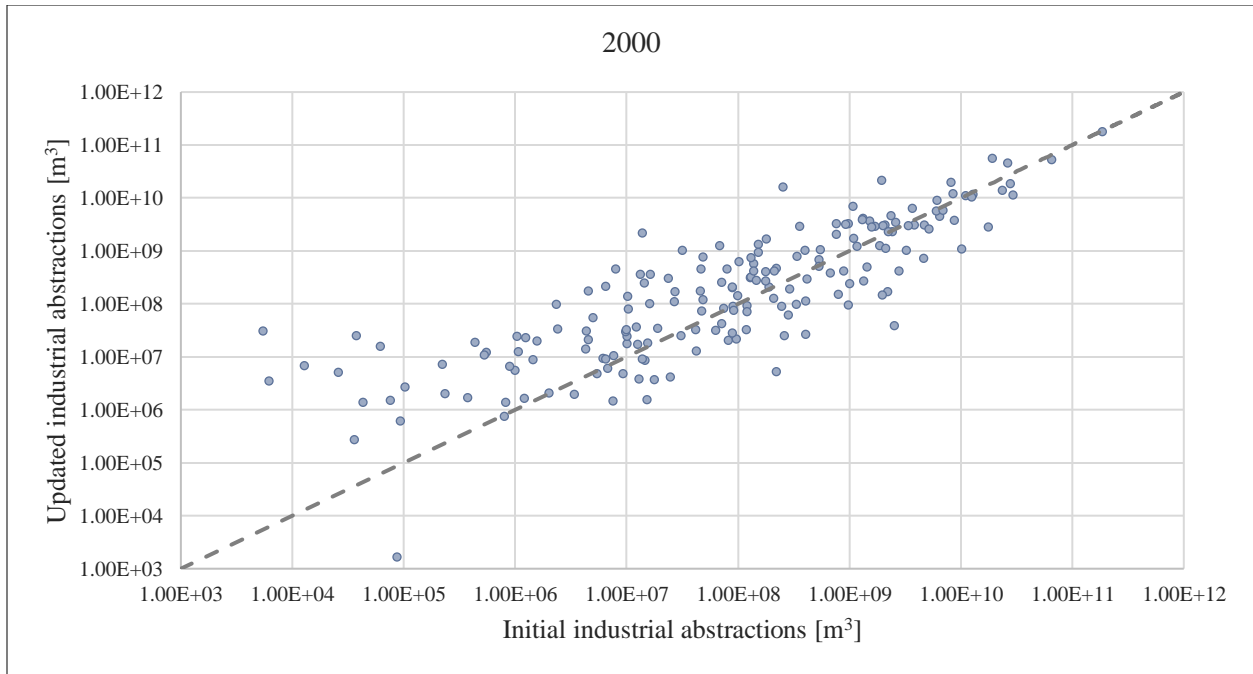
Regionally, Table 6 shows the total industrial water abstractions and gross demands, as well as the percent of demand which is being met. Nations in the Middle East & North Africa and low-income nations in South Asia had the lowest percent of water demand being met. High-income nations in the Middle East & North Africa in particular were not meeting their industrial water demands, with total regional abstractions only 15% of the total regional gross industrial water demands. Conversely, low-income nations in East Asia & Pacific, Latin America & Caribbean, and Sub-Saharan Africa had the highest percent of water demand being met, at 89%. These analyses of global, national, and regional water abstractions and gross demand serve to highlight where industrial water scarcity is most prevalent.

Table 6 Regional total industrial water supply (abstractions) and (gross) demand, including the percent of demand which supplied for 2014.

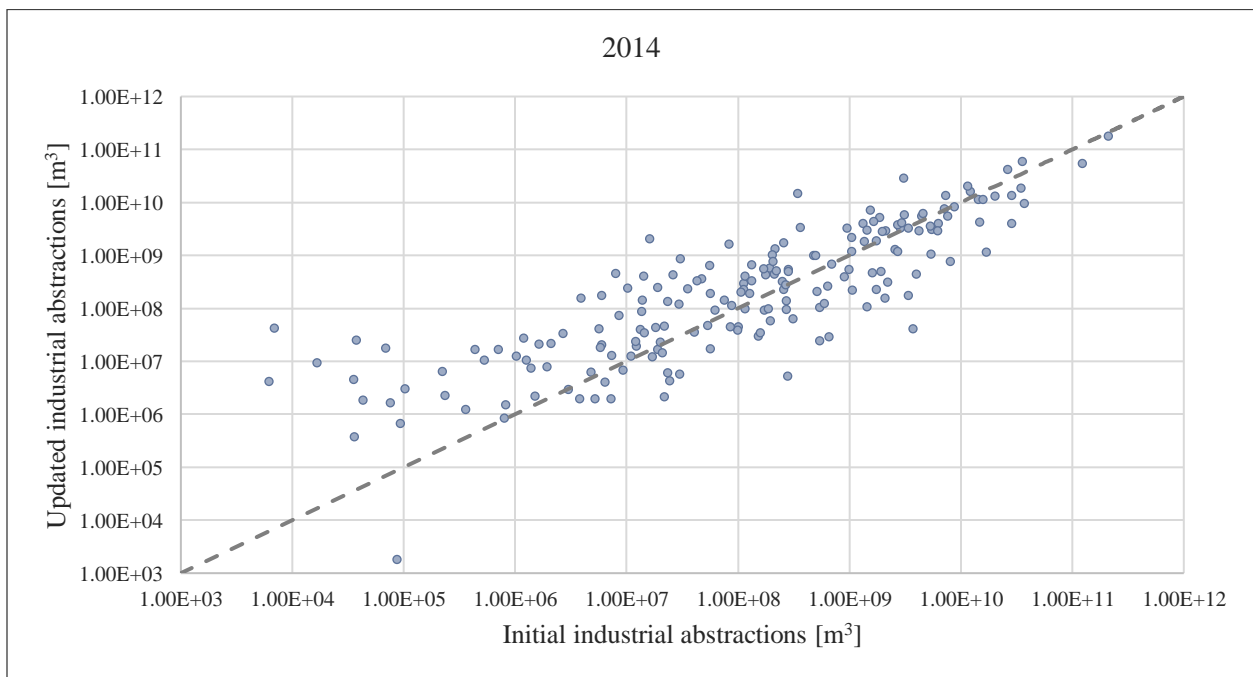
Region	Abstractions [m³]	Demand [m³]	Supply-Demand percent
East Asia & Pacific High	1.43E+11	2.22E+11	65%
East Asia & Pacific Low	3.44E+10	3.87E+10	89%
East Europe & Central Asia High	1.05E+11	1.29E+11	81%
East Europe & Central Asia Low	5.78E+09	9.43E+09	61%
Latin America & Caribbean High	5.24E+10	6.95E+10	75%
Latin America & Caribbean Low	1.00E+09	1.12E+09	89%
Middle East & North Africa High	6.46E+09	4.44E+10	15%
Middle East & North Africa Low	3.95E+09	9.96E+09	40%
North America High	1.89E+11	2.44E+11	78%
South Asia Low	1.54E+10	3.39E+10	45%
Sub-Saharan Africa High	2.05E+09	2.75E+09	75%
Sub-Saharan Africa Low	4.62E+09	5.20E+09	89%
West Europe High	1.02E+11	1.38E+11	74%

4.3.3 Industrial water abstractions

As with the analysis of the industrial demand input files, the analysis of the output abstractions for the updated model were compared with the output from the initial model. Plots and tables of the national total values, regional total values, and time series for three select nations were created to depict the changes between the initial and updated model runs. Figure 14 compares the total national industrial water abstractions from the initial and updated model runs for 2000 and 2014. In these plots, it is evident that the national total values from the updated model did not deviate significantly from the reference run output. The updated model run underestimated the initial model run nationally by 6% for 2000 and by 25% for 2014. Further, there is a 95% correlation between the model outputs for 2000 and a 93% correlation for 2014. Regarding the total global abstractions, the updated model overestimated the initial model by 7% for 2000 and underestimated the 2014 values by 16%. These analyses show that the change in sub-national spatial precision of the updated model, and disaggregation of the manufacturing and thermoelectric sub-sectors, did not greatly affect the total national and global industrial water abstractions. From these data comparisons, Liberia was the nation in which the updated model most overestimated the initial model, while Bosnia and Herzegovina, Saint Vincent and the Grenadines, and Luxembourg were the nations in which the updated model most underestimated the initial model.



a



b

Figure 14 Comparison of the initial and updated modelled industrial water abstractions for 2000 (a) and 2014 (b).

Regionally, Table 7 and Table 8 show the regional correlation between the initial and updated model output, as well as percent changes from the initial model output to the updated model output, for 2000 and 2014 respectively. For low-income nations in East Asia & Pacific and Latin America & Caribbean, as well as all nations in Middle East & North Africa, the two datasets differed the most. For the remaining regions, the correlation was high, and often above 95%. For 2000, total abstractions from the updated model run in low-income nations in East Asia & Pacific and high-income nations in Middle East & North Africa increased the most from the initial run, while total abstractions in low-income nations in East Europe & Central Asia decreased the most. For 2014, the same trends were present except in high-income nations in Middle East & North Africa, where the relative difference in abstractions decreased. Figure 15 plots the total regional industrial water abstractions for 2000 and 2014 from the initial and updated model runs. It shows relatively similar increases in industrial water abstractions for each region between 2000 and 2014 from both the initial and updated results.

Table 7 Regional correlation between the initial and updated industrial water abstractions for 2000, including the percent change from the total initial values to the total updated values.

Region	Correlation	Percent change
East Asia & Pacific High	91%	128%
East Asia & Pacific Low	40%	197%
East Europe & Central Asia High	98%	-24%
East Europe & Central Asia Low	98%	-82%
Latin America & Caribbean High	84%	87%
Latin America & Caribbean Low	54%	31%
Middle East & North Africa High	68%	194%
Middle East & North Africa Low	58%	22%
North America High	100%	-13%
South Asia Low	100%	-3%
Sub-Saharan Africa High	100%	76%
Sub-Saharan Africa Low	78%	117%
West Europe High	95%	-8%

Table 8 Regional correlation between the initial and updated industrial water abstractions for 2014, including the percent change from the total initial values to the total updated values.

Region	Correlation	Percent change
East Asia & Pacific High	96%	72%
East Asia & Pacific Low	45%	168%
East Europe & Central Asia High	96%	-52%
East Europe & Central Asia Low	99%	-85%
Latin America & Caribbean High	91%	61%
Latin America & Caribbean Low	61%	21%
Middle East & North Africa High	66%	77%
Middle East & North Africa Low	47%	20%
North America High	100%	-24%
South Asia Low	100%	-29%
Sub-Saharan Africa High	100%	49%
Sub-Saharan Africa Low	82%	68%
West Europe High	89%	-17%

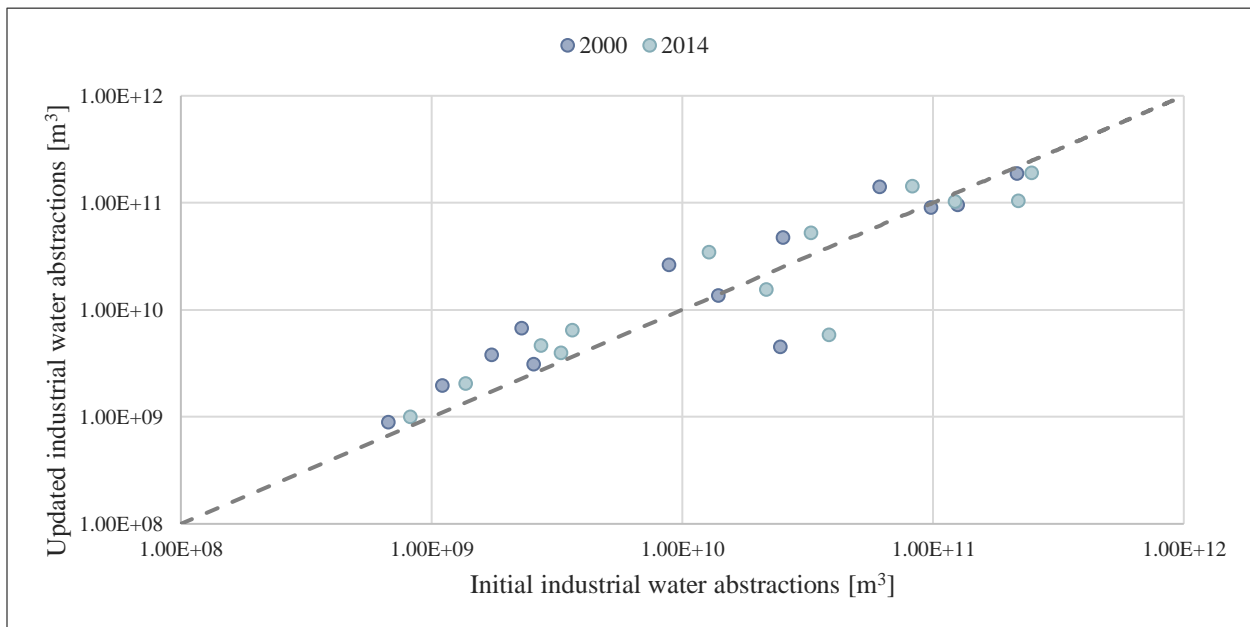
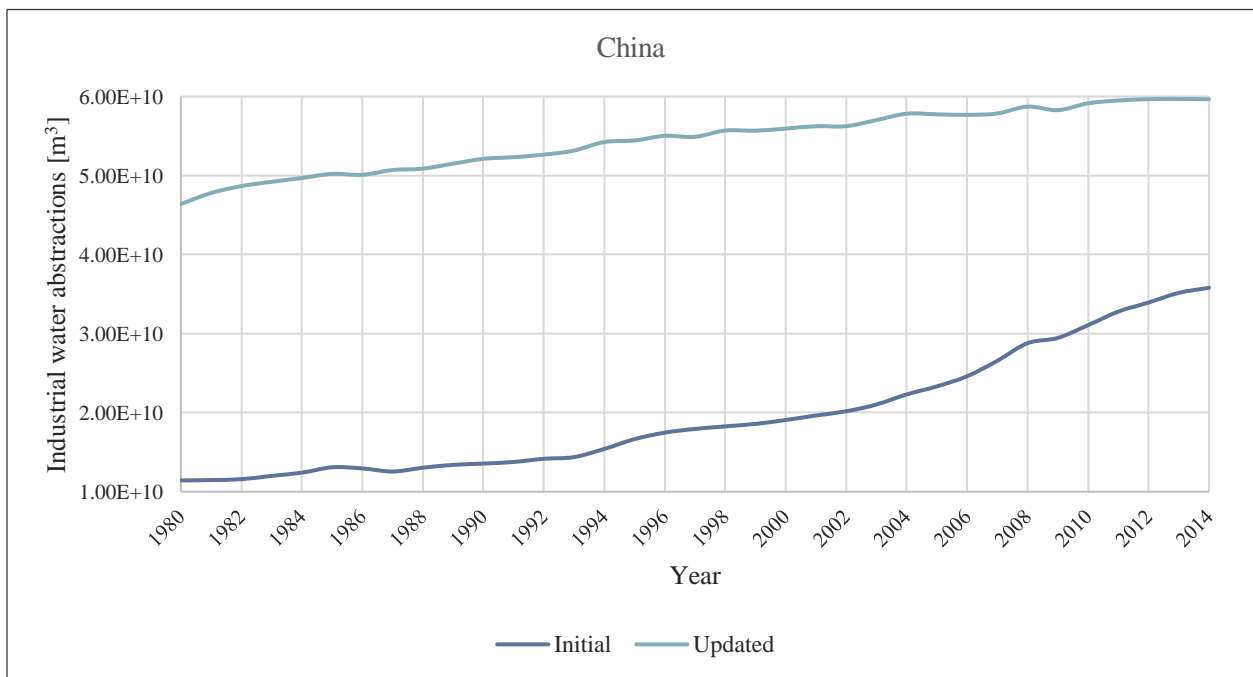
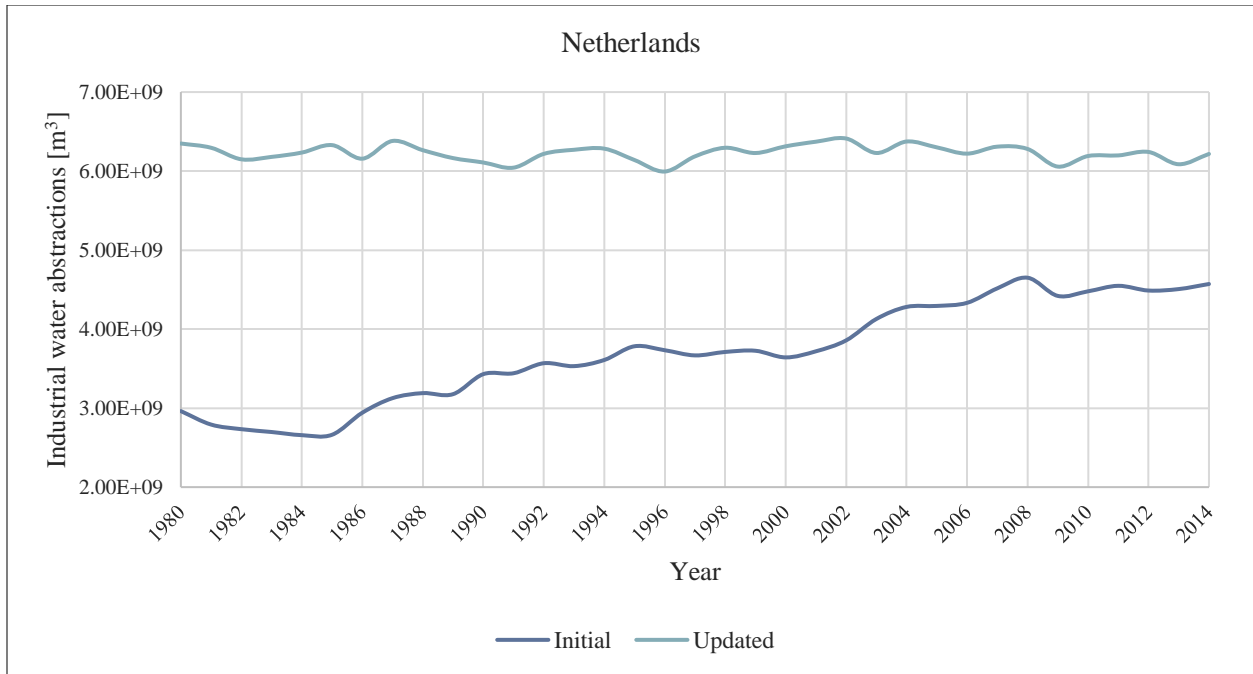


Figure 15 Comparison of the initial and updated regional industrial water abstractions for 2000 and 2014.

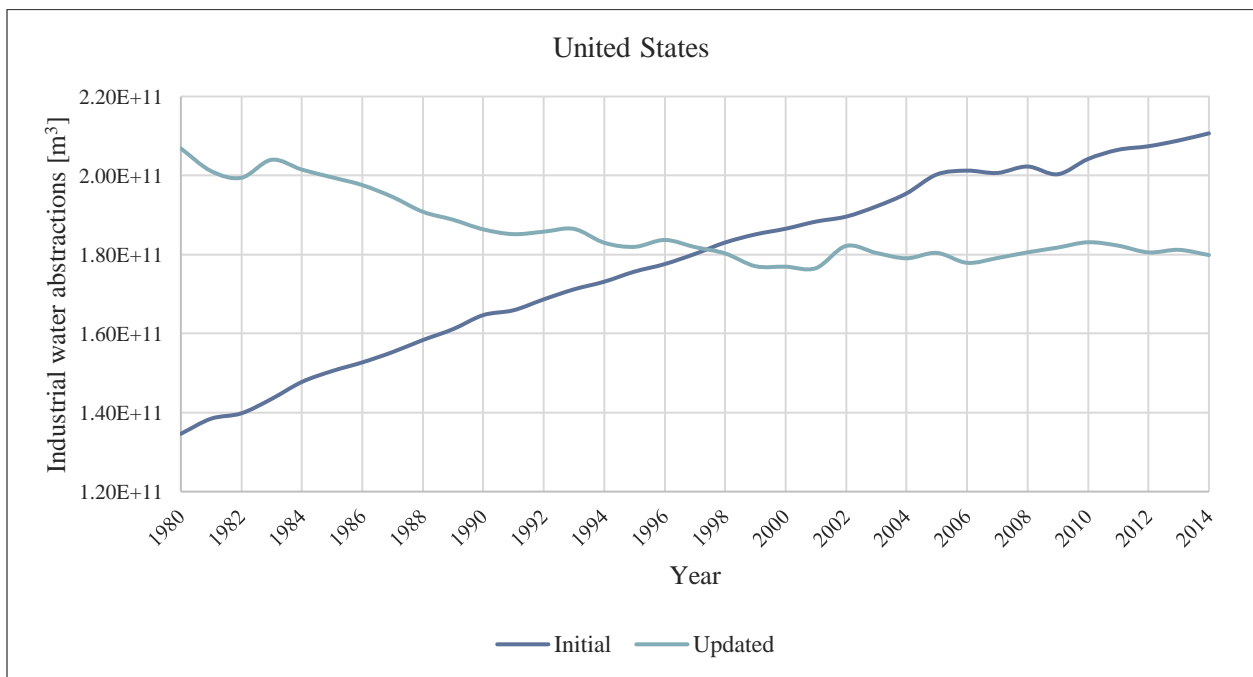
Time series were extracted for annual industrial water abstractions in China, the Netherlands, and the United States (see Figure 16). Similar to the time series of the gross industrial water demand input files, the updated model estimated greater values throughout the simulation in China and the Netherlands, and estimated greater values in the United States at the outset, but again estimated lesser values by the final years. In China, both models estimated similar trends annually. In the Netherlands, the initial model estimated a relatively constant long-term trend of industrial water abstractions, while the initial model estimated a net increase in time. Finally, in the United States, the updated model estimated a decrease in industrial water abstractions over time, while the initial model estimated an increase. This is likely due to the difference in reference years and study years between the creation of the input datasets, as the initial model estimated an increase in both supply and demand for the United States, but the updated model (due to the technological improvements associated with the CAGR values) estimated a decrease in demand. The supply of industrial water, therefore, would decrease as well. It should be noted that the point at which the two model simulations estimate similar industrial water abstractions in the United States occurs approximately seven years before the input files estimate similar industrial water demand.



a



b



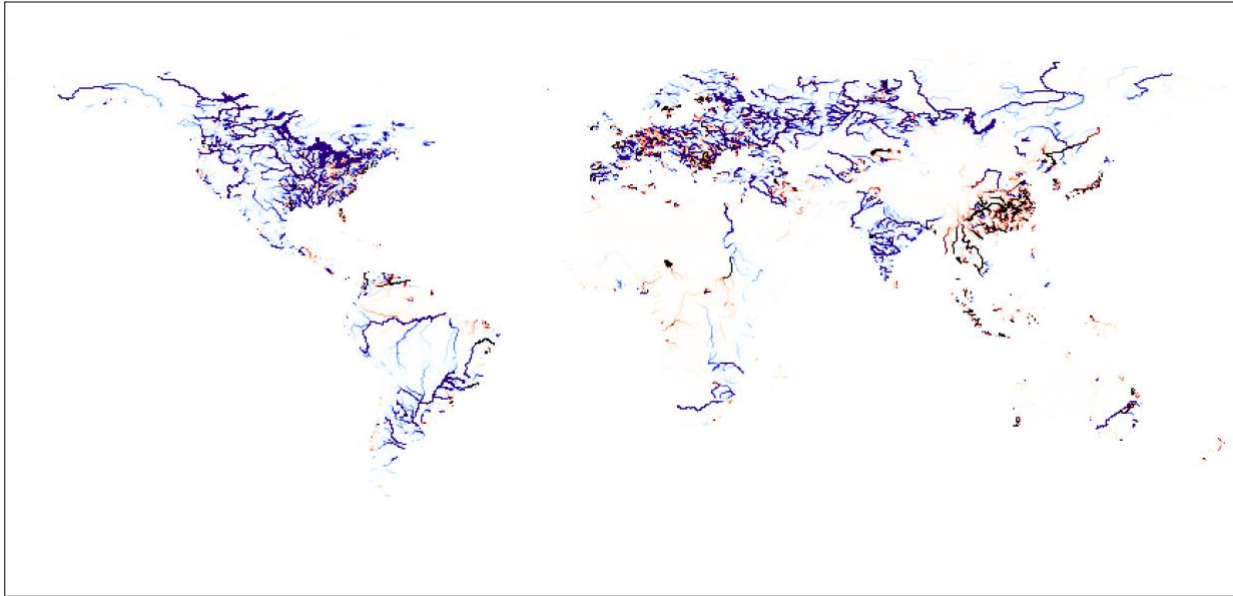
c

Figure 16 Comparison of the initial and updated modelled industrial water abstractions for China (a), the Netherlands (b), and the United States (c).

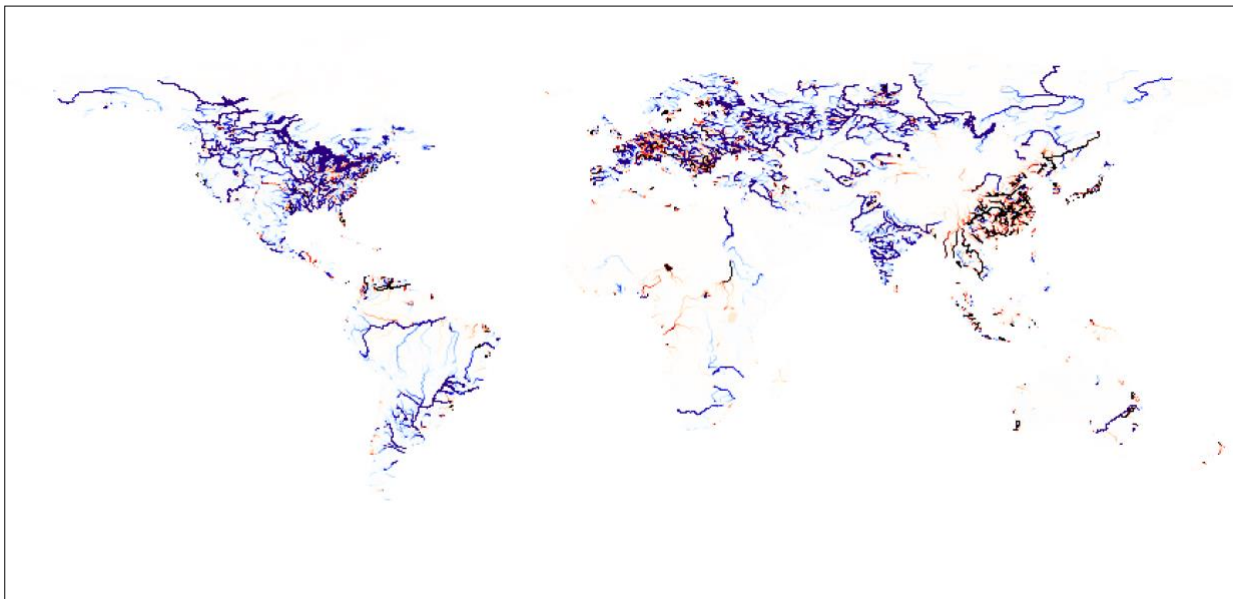
4.3.4 Modelled discharge

The raw difference between the temporally averaged global discharge from the initial and updated PCR-GLOBWB model runs can be seen in Figure 17. In these plots, the initial discharge values were subtracted from the updated discharge values to yield the global change. Blue cells indicate the updated model estimated greater discharge, while red cells indicate the updated model estimated smaller discharge. The data was collected for January and July to depict data during seasons which experience different flow rates. The maps show that in North America, South America, Eastern Europe, and India, the updated model generally estimated greater discharge. In much of Central Europe and Eastern Asia, the updated model estimated smaller discharge. It should be noted that the displayed range was trimmed to highlight smaller differences as well as larger differences.

The raw changes in discharge between the initial and updated model runs were then divided by the initial discharge values to show the percent change. Figure 18 highlights the regions in which the updated model estimated an increase in discharge, while Figure 19 highlights the regions in which the updated model estimated a decrease in discharge – both relative to the initial model. Noticeable differences are in the United States, where the updated model generally estimated an increase in discharge in the Western United States, but a decrease in discharge in the Eastern United States. In South America, the updated model estimated a slight increase in discharge near the Río Colorado. Finally, in parts of Western Europe, parts of Eastern Europe, Central Asia, and Southwestern India, the updated model estimated an increase in discharge. Conversely, in much of Central Europe, parts of Eastern Europe, and East Asia, the updated model estimated less discharge than the initial model. Deviations from the initial model values appear to be more pronounced in January than in July. It should be noted that the displayed range in Figure 18 was trimmed to highlight smaller differences as well as larger differences.



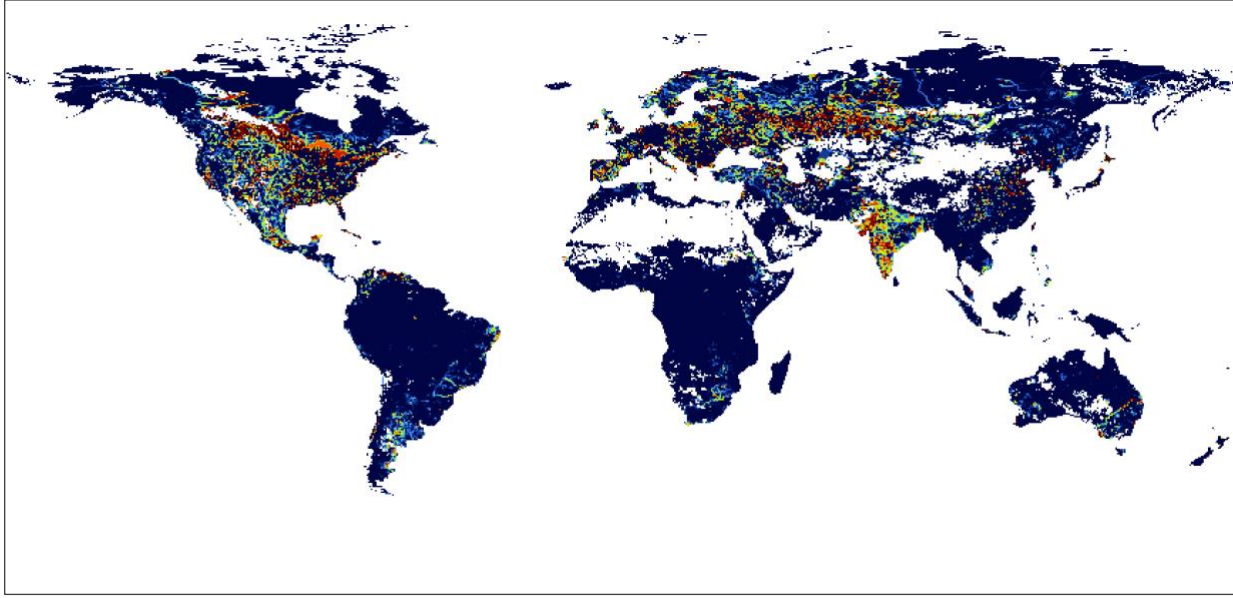
a



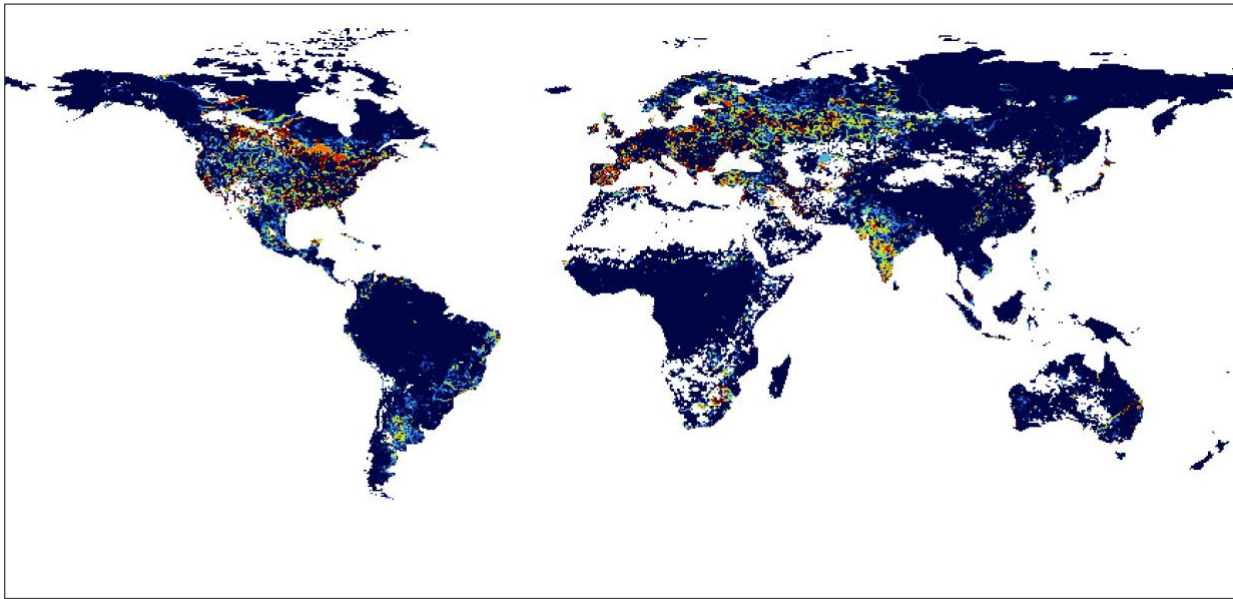
b



Figure 17 Difference between the temporally averaged updated and initial global monthly discharge for January (a) and July (b) in m^3/s .



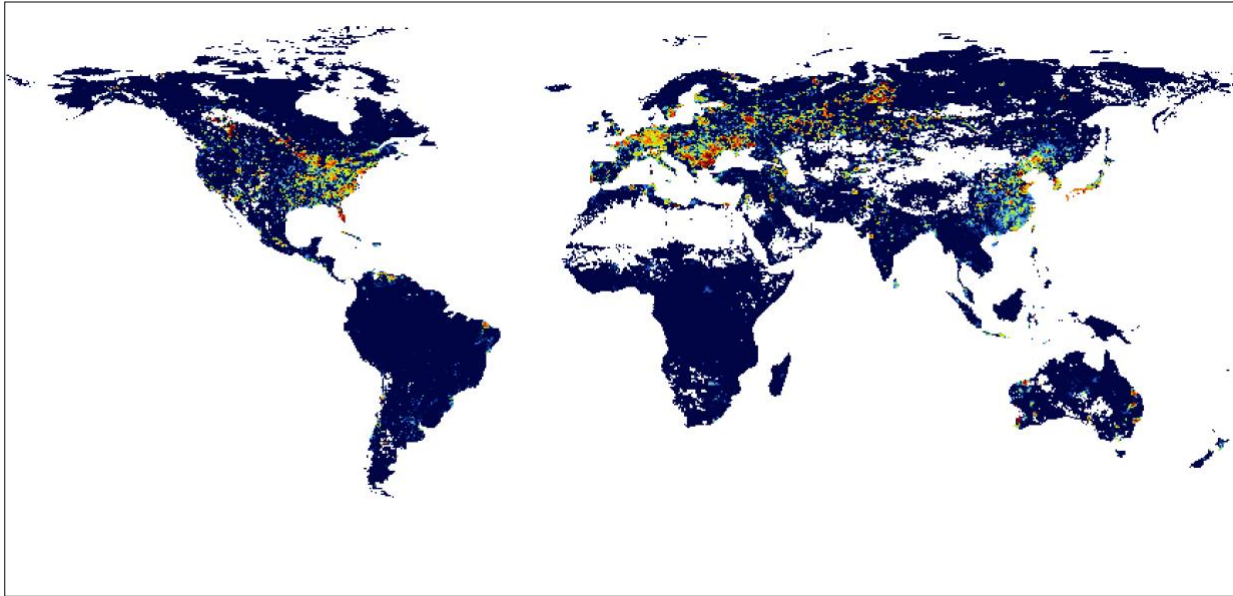
a



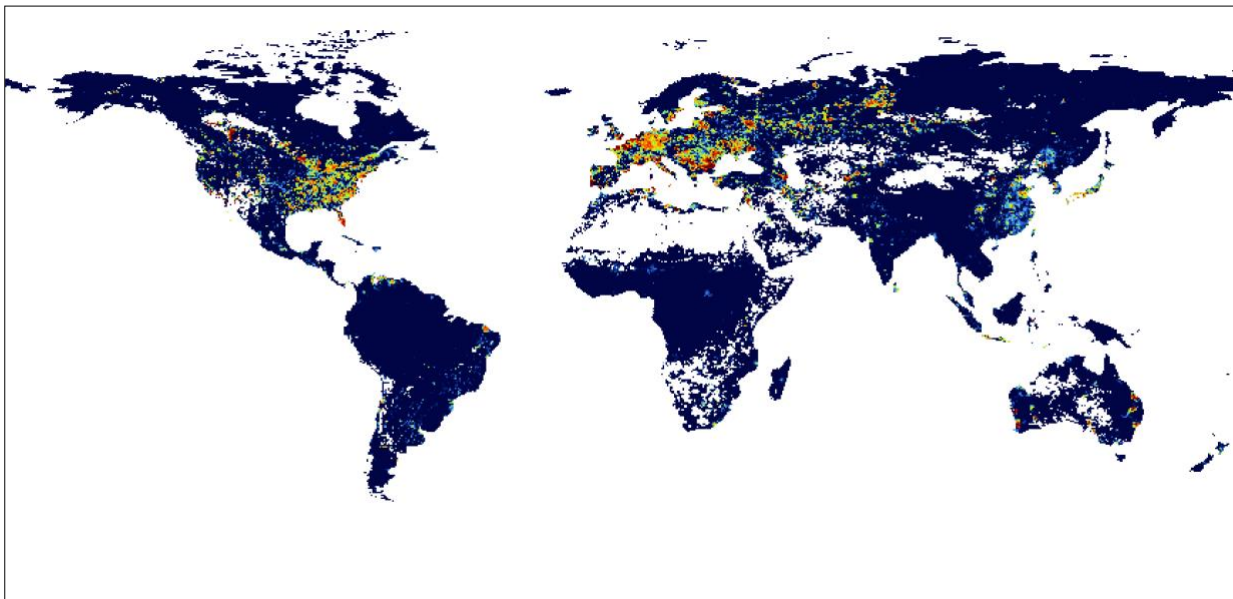
b



Figure 18 Map depicting the temporally averaged percent increases in monthly simulated global streamflow from the updated model run relative to the initial model run for January (a) and July (b).



a

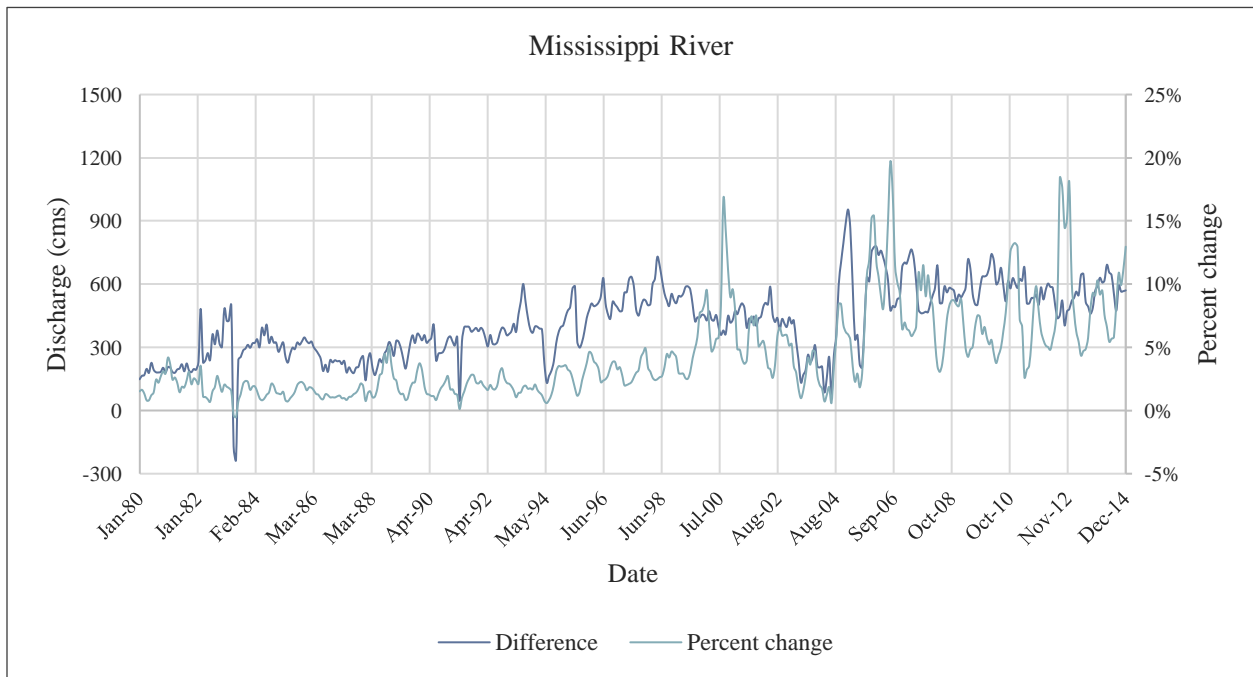


b

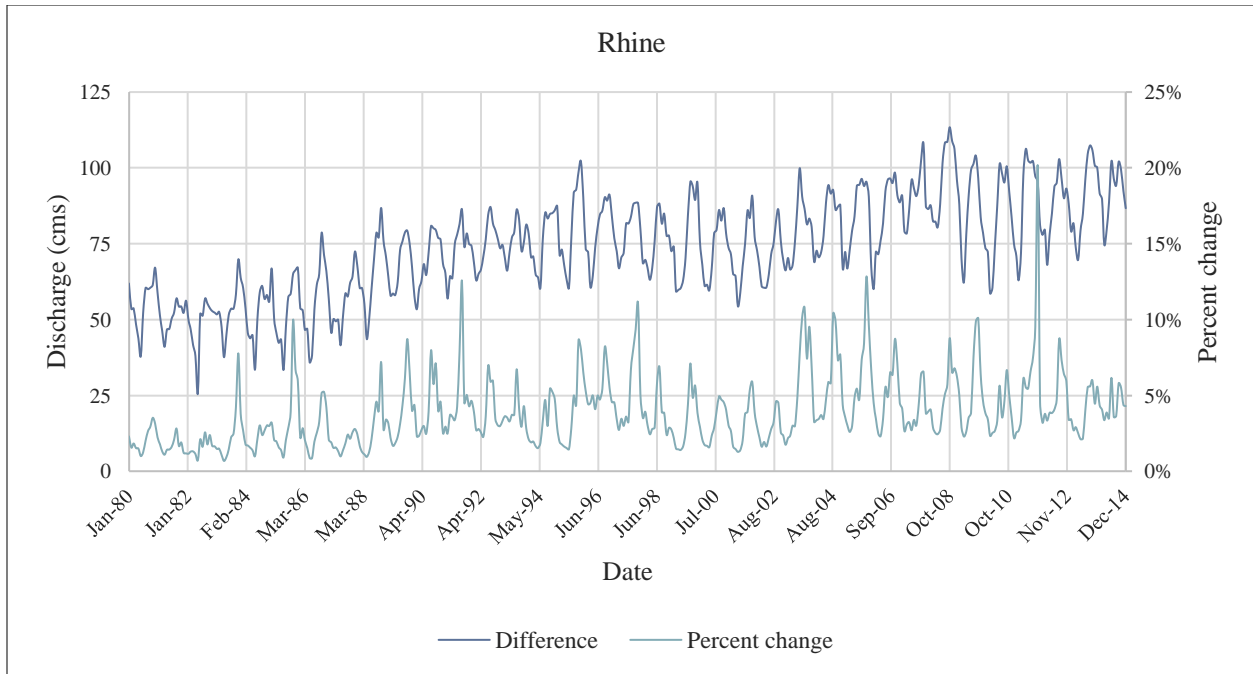


Figure 19 Map depicting the temporally averaged percent decreases in monthly simulated global streamflow from the updated model run relative to the initial model run for January (*a*) and July (*b*).

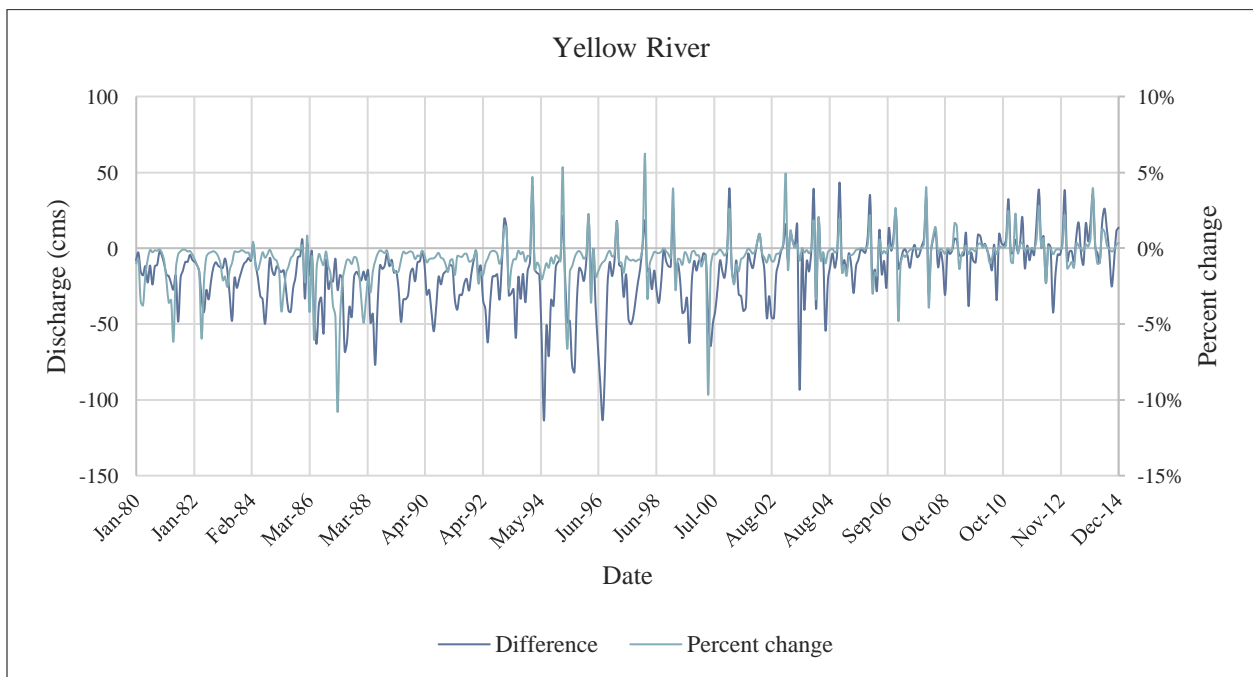
The effect of the updated industrial demand file on discharge can be seen in time series depicting the changes between streamflow given the industrial water demand input file (see Figure 20). The plots at Vicksburg along the Mississippi River, Rees along the Rhine, and Huayuankuo along the Yellow River show the difference in average monthly river discharge in cubic meters per second (by subtracting the initial discharge from the updated discharge), as well as the percent change in discharge (by dividing the difference by the initial discharge). The plots show that the updated model consistently estimates an increase in river discharge along the Mississippi River and the Rhine, with these values appearing to increase towards the end of the time series. Along the Yellow River, however, the updated model generally estimates less river discharge than the initial model, until the end of the time series where the two estimates become more similar. As for total discharge along the Mississippi River, the updated model estimates approximately 418 cubic meters per second more discharge than the initial model per month, and a 3% increase in total river discharge over the time series. Along the Rhine these values are 74 cubic meters per second more and a 3% increase; along the Yellow River they are 16 cubic meters per second less and a 0.4% decrease. It should be noted that the change in average monthly discharge increases for all three stations toward the end of the time series. The alterations in river discharge can be attributed to the different industrial demand input files, and more specifically the change in spatial downscaling of the national values.



a



b



c

Figure 20 Difference and percentage change between the initial and updated model output for river discharge over time along the Mississippi River (a), the Rhine (b), and the Yellow River (c).

5 Discussion

The integration of the updated industrial water demand dataset into PCR-GLOBWB served to reduce uncertainty, as the model now only uses population distribution as a spatial downscaling technique for the manufacturing sub-sector, while the thermoelectric sub-sectoral values are being input at their exact locations. This separation of the industrial sector was expected to improve the precision of the model by reducing the necessary estimation to map global industrial water demand, however its efficacy remains inconclusive. An improvement made by the updated model is that the integration of two separate classes into the industrial sector allows for different return flows between the manufacturing and thermoelectric sub-sectors. By accounting for this ratio at the sub-sectoral scale, PCR-GLOBWB is able to provide a more precise indication of the specific effects of sub-sectoral industrial water use on the hydrologic cycle over time.

The data analyses performed for the input industrial demand, output abstractions, and output discharge serve to display how the updated model compares with the reference run. The global, regional, and national changes are highlighted for the purpose of assessing how PCR-GLOBWB responded to the updated industrial water demand input file. These analyses do not necessarily show improvement, but rather how the model was affected.

5.1 Limitations

There were several difficulties in developing the conceptual model to calculate manufacturing water withdrawals. The main cause was a lack of reliable data, including at the national scale. Ultimately, rather than using observed manufacturing data, thermoelectric data was subtracted from industrial data to calculate manufacturing data where applicable. For many nations, however, the observed thermoelectric values exceeded the observed industrial values. In these cases, the thermoelectric values were considered more accurate, and the industrial values were therefore recalculated. Upon completion of the analysis for the reference year 2015, it was found that 66% of global manufacturing water withdrawals were observed, while 34% were simulated by the conceptual model.

Difficulties in the compatibility of datasets during the development of the conceptual model also included issues with extrapolating regional output values globally. Manufacturing values from data-rich regions, for example, could be found or reliably estimated, however the methods of global estimation could not be applied to data-poor regions. For instance, using the Bernhard et al. (2018) and Eurostat (2021) manufacturing data for Europe, it was possible to identify manufacturing water withdrawal values, as well as the contributions from specific components of manufacturing. This proved very efficient for Europe, but the manufacturing water use intensity values could not be applied to the rest of the world. For this reason, the global FAO AQUASTAT (2021) dataset was used as the basis for initial manufacturing water withdrawal estimates, in conjunction with the power plant dataset from Lohrmann et al. (2019).

As for the integration of the conceptual model data into PCR-GLOBWB, the national and annual values had to be adjusted. Spatially, the national manufacturing withdrawals were downscaled using population density. While this is generally accepted as a reliable method for determining the spatial distribution of national manufacturing water use, it is an imperfect technique. This is mainly due to the assumed clustering of manufacturing demand around population centers, which is not always the reality. Further, abstractions at specific locations are limited by demand at those locations. While this may be effective in theory, it is not fully reliable in the real world. Abstracted water is not solely used at the source location, meaning the water supply for any given location can come from other nearby locations. In that sense, the national comparison of industrial water supply and demand can be more thorough, while still considering the fact that modelled abstractions are limited by the local population-driven demand.

Additionally, national estimates were made for the industrial water demand, after coupling the conceptual model output with manufacturing recycling ratios and thermoelectric water use. These national industrial water demand values were then dispersed evenly throughout each year by dividing the annual values by the days per year. This technique, which was also used in the initial model input because industrial demand does not vary much seasonally (Wada et al., 2014), is not wholly representative of the dynamics of industrial water demand intra-annually.

5.2 Statistical analyses and data validation

When comparing the manufacturing water withdrawal estimates with observed values, the following relationships were identified. Observed values account for 66% of the total observed and simulated values; therefore, 34% of the global manufacturing water withdrawals are being estimated by the model. As for validation of these values, the 2015 manufacturing water withdrawals from the conceptual model estimate 92% of the total observed manufacturing water withdrawals in Australia (Australian Bureau of Statistics, 2020), and 96% of the total observed manufacturing water withdrawals in Canada (StatCan, 2014). For the United States, the conceptual model overestimated the USGS (2018a) by approximately five times the observed manufacturing water withdrawals. When applied in Europe for 2015, the conceptual model overestimated Eurostat (2021) by approximately three times the observed manufacturing water withdrawals. This overestimation was similar when the temporally extrapolated model estimations were compared with the available Eurostat (2021) data from 2009 through 2018. These overestimations can be attributed to discrepancies between the thermoelectric withdrawals used in the conceptual model (Lohrmann et al., 2019) and observed thermoelectric withdrawals. While the total industrial values are similar, the specific sub-sectoral contributions differ. Validation values used for the reference year 2015 from Australia, Canada, the United States, and Europe can be seen in Table 9, while validation values from 2009 through 2018 from Europe can be seen in Table A11.

Table 9 Comparison of the observed and modelled manufacturing water withdrawals for Australia (Australian Bureau of Statistics, 2020), Canada (StatCan, 2014), the United States (USGS, 2018a), and several nations in Europe (Eurostat, 2021).

Nation	Year	Observed MWW [m³]	Modelled MWW [m³]	Percent estimated
Australia	2015	3.17E+08	2.91E+08	92%
Canada	2015	5.48E+09	5.29E+09	97%
United States	2015	1.93E+10	1.06E+11	546%
Belgium	2015	1.09E+09	2.97E+09	274%
Bulgaria	2015	2.18E+08	1.07E+09	490%
Croatia	2015	1.77E+08	1.02E+09	577%
Cyprus	2015	3.16E+06	1.27E+08	4023%
Denmark	2015	6.07E+07	1.47E+09	2413%
Estonia	2015	3.59E+07	1.86E+08	519%
Germany	2015	4.42E+09	1.50E+10	340%
Greece	2015	1.89E+08	6.38E+08	337%
Italy	2015	3.74E+09	4.18E+09	112%
Latvia	2015	1.44E+07	2.92E+07	203%
Lithuania	2015	4.03E+07	1.06E+09	2627%
Luxembourg	2015	1.90E+06	1.99E+06	105%
Malta	2015	3.01E+06	6.68E+07	2219%
Netherlands	2015	3.04E+09	8.67E+09	285%
Poland	2015	6.59E+08	3.92E+09	594%
Serbia	2015	1.21E+08	7.76E+08	641%
Slovenia	2015	5.01E+07	5.86E+08	1169%
Spain	2015	9.42E+08	2.02E+09	214%
Sweden	2015	1.78E+09	2.62E+09	147%

When computing the regional averages for the manufacturing water use intensities, the coefficients of variation were found to determine the dispersion of the data (see Table 10). The regional data tends to be quite dispersed, with the standard deviation often exceeding the mean, signifying improvements to the data-filling techniques can be made to reduce uncertainty. The count indicates the number of nations from each region that had industrial water withdrawal values greater than their thermoelectric water withdrawals, as well as data for their MVA in 2015. The average intensity was then calculated by dividing the estimated manufacturing water withdrawals by the MVA, and subsequently applied to the remaining nations in each region which did not have unique values for manufacturing water use intensity.

Table 10 Average regional manufacturing water use intensities.

Region	Count	Average Intensity [m³/\$]	Coefficient of Variation
East Asia & Pacific High	4	0.0289	96%
East Asia & Pacific Low	7	0.1559	111%
East Europe & Central Asia High	16	0.1296	145%
East Europe & Central Asia Low	3	0.1934	13%
Latin America & Caribbean High	15	0.0747	126%
Latin America & Caribbean Low	6	0.0392	56%
Middle East & North Africa High	5	0.0680	191%
Middle East & North Africa Low	2	0.0417	120%
North America High	3	0.0415	33%
South Asia High	1	0.0039	0%
South Asia Low	6	0.0372	59%
Sub-Saharan Africa High	6	0.0175	89%
Sub-Saharan Africa Low	34	0.1283	195%
West Europe High	11	0.0363	86%

For the average regional relationship between GDP and MVA, the r-squared and correlation for each were calculated as well (see Table 11). The range in regional correlations was between 0.8735 and 0.9999, with 12 of the 14 regions having a correlation above 0.95. These statistics are indicative of a good fit between the GDP and MVA by regional and economic national classifications. The count indicates the number of nations from each region that had GDP and MVA values for 2015. The slope indicates the average relationship between the GDP and MVA in each region, where the GDP is used as the independent variable to predict the MVA. This value indicates the ratio of a nation's GDP that comes from its MVA.

Table 11 Average regional relationship between GDP and MVA.

Regions	Count	Slope	Correlation
East Asia & Pacific High	15	0.2106	98%
East Asia & Pacific Low	11	0.2162	100%
East Europe & Central Asia High	22	0.1447	99%
East Europe & Central Asia Low	5	0.1052	100%
Latin America & Caribbean High	25	0.1178	98%
Latin America & Caribbean Low	6	0.1857	97%
Middle East & North Africa High	12	0.1176	87%
Middle East & North Africa Low	4	0.1530	100%
North America High	3	0.1134	100%
South Asia High	1	0.0223	100%
South Asia Low	7	0.1738	100%
Sub-Saharan Africa High	7	0.1240	100%
Sub-Saharan Africa Low	36	0.0925	99%
West Europe High	19	0.1498	92%

To validate the industrial water withdrawals calculated in the conceptual model, the backcasted data was compared with the observed values from FAO AQUASTAT (2021) dating back to 1982. The FAO AQUASTAT (2021) data is available at five-year averaged time scales, so there were seven years in which the estimated values could be validated. Total national (see Table A12) and regional (see Table 12) estimated volumes of industrial water withdrawals were compared with the observed values to assess the percent changes. The tables show that the estimates were significantly more accurate in the later years of the model run. In 2012, for instance, the total global industrial water withdrawals from the conceptual model underestimated the observed values by 6%, while the average regional percent change was a 6% increase. Although the regional and national values differ, globally the total industrial water withdrawals are quite accurate. The spatial discrepancies can therefore be attributed to the use of regional averages to estimate manufacturing water withdrawals in the conceptual model, since values from data-rich nations directly influence the estimated values in data-poor nations. Temporal discrepancies can be attributed to the backcasting estimation technique (CAGR) in the conceptual model being applied beyond the time period for which it was calculated. Annual industrial water use trends from 2010 through 2050 from Bijl et al. (2018) were used to both forecast and backcast the 2015 reference year data in the conceptual model.

Table 12 Percent changes between the observed (FAO AQUASTAT, 2021) and estimated regional industrial water withdrawals from the conceptual model.

Region	1982	1987	1992	1997	2002	2007	2012
East Asia & Pacific High	72%	71%	16%	-6%	-7%	-18%	-15%
East Asia & Pacific Low	-91%	-78%	186%	90%	12%	-15%	13%
East Europe & Central Asia High	-59%	-38%	-30%	3%	15%	27%	39%
East Europe & Central Asia Low			-79%	-70%	-64%	-56%	-42%
Latin America & Caribbean High	97%	76%	-12%	61%	54%	37%	32%
Latin America & Caribbean Low		-35%	54%	10%	-6%	-12%	-9%
Middle East & North Africa High	382%	95%	-8%	-30%	-38%	-24%	1%
Middle East & North Africa Low	12%	-14%	247%	-41%	-32%	-1%	67%
North America High			-41%	-42%	-42%	-40%	-27%
South Asia Low	-17%	-16%	-23%	-13%	-14%	-20%	-25%
Sub-Saharan Africa High		65%	20%	56%	63%	35%	22%
Sub-Saharan Africa Low	-33%	93%	20%	-7%	-3%	-6%	0%
West Europe High	-17%	-36%	-22%	-23%	-15%	1%	24%

Gross thermoelectric water demand (Lohrmann et al., 2019) was then compared with observed thermoelectric withdrawals (USGS, 2018c) at the county and state scale in the United States (see Table 13). USGS values were available for 1985, 1990, 1995, 2000, 2005, and 2010. The comparisons were done to assess how the thermoelectric data input into PCR-GLOBWB relates to observed values at a downscaled level. The statistical analyses show that, over time, the slopes at both scales improve, but they are still unsatisfactory. A slope of 1 would indicate a perfect fit between the values, but this is not seen. Further, the correlations remain relatively constant over time, indicating that the local values are not showing improvement. The small slopes and low correlations between the thermoelectric demand and withdrawals (while not a perfect comparison) are indicative of a poor fit between the datasets. Further, the percent changes between the withdrawals and demand were taken for each state at each of the six years with available data and show a poor relationship (see Table A13). The withdrawals are generally an order of magnitude greater than the demand, causing the percent changes to generally show large decreases in thermoelectric water use.

Table 13 Slope and correlation between the thermoelectric withdrawals (USGS, 2018c) and gross thermoelectric demand (Lohrmann et al, 2019) at the county and state scale in the United States.

Year	County Slope	County Correlation	State Slope	State Correlation
1985	0.0309	8.50%	0.0647	20.49%
1990	0.0307	7.80%	0.0620	18.63%
1995	0.0272	6.42%	0.0843	25.26%
2000	0.0406	7.75%	0.0960	24.36%
2005	0.0401	6.26%	0.0702	14.78%
2010	0.0551	7.12%	0.1584	26.52%

The total national thermoelectric withdrawals and gross demand were then compared over time for the United States (see Figure 21). This time series shows that demand increases gradually over time, and withdrawals increase similarly from 1985 through 2005, but then decrease sharply in 2010. The values of the demand and withdrawals, however, differ greatly. It is evident in this plot that the gross thermoelectric water demand in the United States (Lohrmann et al., 2019) is significantly smaller than the observed thermoelectric water withdrawals (USGS, 2018c). This comparison shows that the data input into PCR-GLOBWB for the United States differs greatly from the observed values from the USGS.

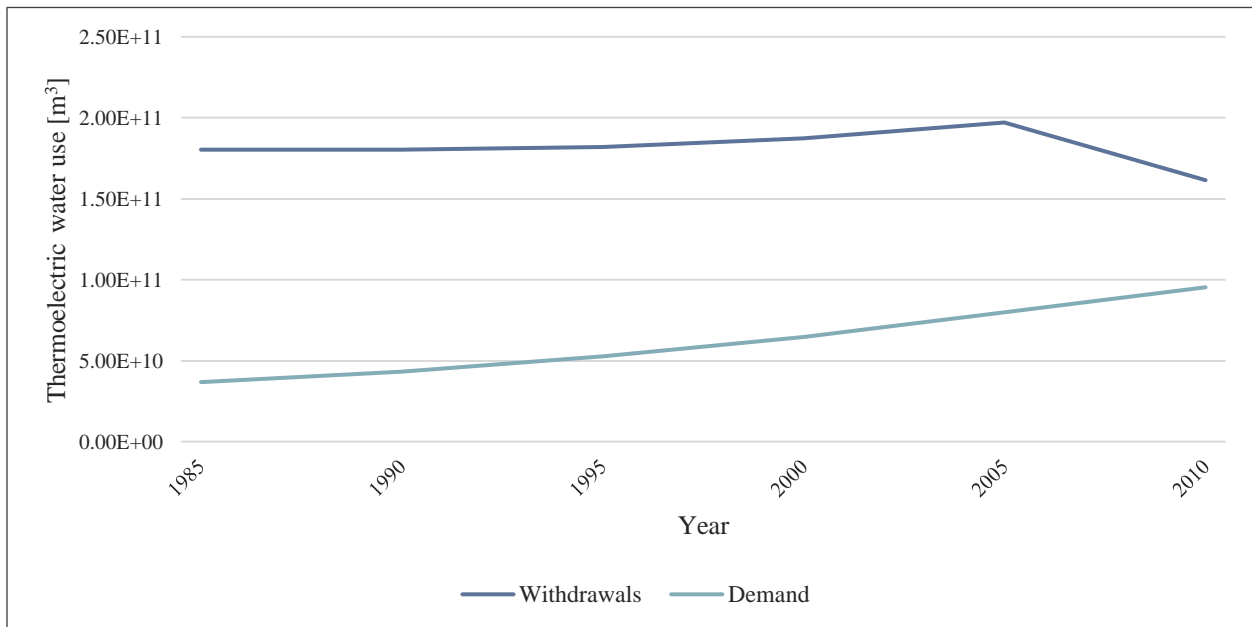


Figure 21 Time series of thermoelectric withdrawals (USGS, 2018c) and gross thermoelectric demand (Lohrmann et al., 2019) for the United States.

To validate the model output for the industrial abstractions, county scale values in the United States were compared to observed data (USGS, 2018c). Comparisons were made between the observed and initial model results, as well as between the observed and updated model results (see Table 14). These statistical analyses show that the initial model run (Wada et al., 2014) had more similar values than the updated model run, when compared with the USGS data. Both runs have poor correlations throughout the years, but they are notably worse from 1985 through 1995. As for the slopes, the initial model has accurate slopes from 2000 through 2010, and while the updated model showed improvement over this time period, there are still discrepancies in the results.

Table 14 Slope and correlation of industrial water withdrawals comparing the initial (Wada et al., 2014) and updated data to observed data (USGS, 2018c) at the county scale in the United States.

Year	Initial Slope	Initial Correlation	Updated Slope	Updated Correlation
1985	6.06	2.58%	55.23	0.71%
1990	7.18	2.68%	346.85	0.12%
1995	9.30	2.53%	-120.56	-0.43%
2000	1.16	21.32%	3.42	15.47%
2005	1.09	22.31%	4.70	13.05%
2010	1.37	20.61%	5.85	12.40%

The same statistical analyses were then performed by aggregating the county values to the state scale in the United States (see Table 15). These results show significant improvement from the county slopes and correlations, but still indicate that the initial model results were more similar to the observed values than were the updated model results.

Table 15 Slope and correlation of industrial water withdrawals comparing the initial (Wada et al., 2014) and updated data to observed data (USGS, 2018c) at the state scale in the United States.

Year	Initial Slope	Initial Correlation	Updated Slope	Updated Correlation
1985	1.35	65%	0.66	49%
1990	1.17	66%	0.71	51%
1995	0.94	66%	0.59	49%
2000	1.29	73%	0.72	44%
2005	1.30	74%	0.61	38%
2010	1.08	74%	0.54	40%

Finally, the total national industrial water abstractions from the initial and updated model were compared with the observed withdrawals from the USGS (2018c). Figure 22 shows that the observed withdrawals in the United States decreased from 1985 through 2010. This trend was captured by the updated model abstractions (due to the negative CAGR value) but not by the initial model abstractions. The negative trend in updated industrial water abstractions over time shows an improvement on the initial model for the United States. While the initial model did not account for the technological improvements in reducing water use intensity, the updated model accurately predicted that trend over time. Further, when looking at the most recent data in this plot, the updated model values only differ from the observed values by 2%.

The validation of the model data through analyses with the USGS (2018c) data show that the national estimates were quite accurate, particularly for the later years in the model, but that the downscaling of the industrial sector to county and state scales was poor in the United States. In the conceptual model, the United States manufacturing water withdrawals were taken as the difference between the industrial and thermoelectric water withdrawals (Lohrmann et al., 2019). These thermoelectric withdrawals were then used as the gross thermoelectric demand in PCR-GLOBWB. While those values are significantly less than the observed thermoelectric withdrawals from the USGS (2018c), the observed industrial water withdrawals from the USGS were quite similar to the observed industrial water withdrawals from FAO AQUASTAT (2021), leading to accurate total industrial withdrawals in the conceptual model. This caused the updated model abstractions to be accurate as well. The backcasting of the data, however, shows that the annual trend in industrial water demand in the United States was much more negative from 1970 through 2010 (USGS, 2018c) than from 2010 through 2015 (Bijl et al., 2018). Overall, the development of the conceptual model, and integration of those values into PCR-GLOBWB, resulted in accurate national scale industrial water use estimates for the United States. The downscaling, however, proved to be ineffective as the county and state scale values differ greatly. This emphasizes the need for either a reliable database of industrial water use, separated sub-sectorally, or an improved downscaling technique to estimate localized industrial water use. The input of the thermoelectric data at the power plant scale theoretically works as a means of improving the spatial precision of the model, however the values differed too greatly from the observed values to improve the spatial precision of the model output.

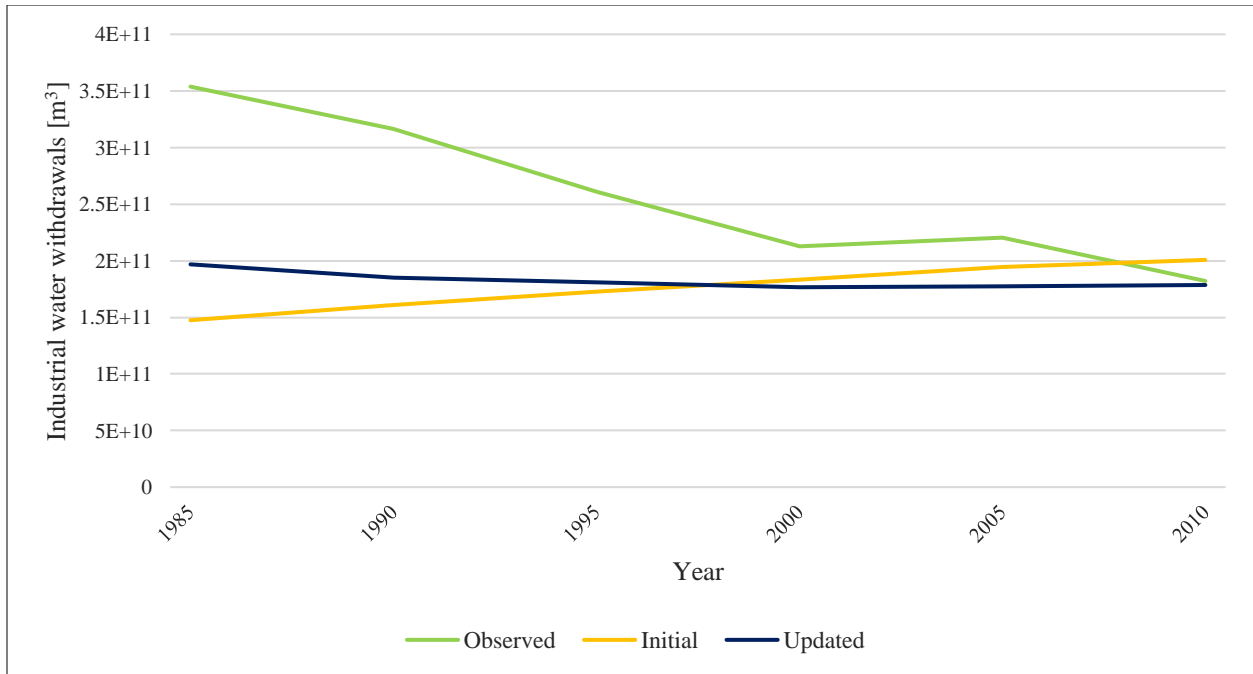


Figure 22 Time series of observed (USGS, 2018c), initial (Wada et al., 2014), and updated industrial water withdrawals for the United States.

5.3 Assumptions

In creating the conceptual model for manufacturing water use, several assumptions were made. First, it was assumed that data from differing sources was compatible, such as the industrial water withdrawal data from FAO AQUASTAT (2021) and the thermoelectric water withdrawal data from Lohrmann et al. (2019). By taking the difference between these two datasets, initial estimates for manufacturing water withdrawals could be made, serving as the basis for the remainder of the conceptual model. When taking these differences, however, several data values had to be excluded when the national thermoelectric water withdrawal values exceeded the national industrial water withdrawal values. The model, therefore, re-estimated the manufacturing (and by extension, industrial) values using regional averages. The threshold was set at 0 for the initial manufacturing water withdrawal estimates to be viable, yet the occurrence of 46 nations (of 184 total) in which the industrial water withdrawal data was deemed insufficient, suggests that improved compatibility of the datasets is vital to produce a more precise model.

Further, the model works under the assumption that nations in the same region, with similar per capita gross national income (GNI), have similarly behaving industrial sectors. The economic classifications from The World Bank (2021k) were also reduced from four groupings to two, so as to maintain larger sample sizes. Using larger sample sizes came with the risk that regional groupings may have been less consistent. To finalize estimations for the reference year, the model then assumed that the computed regional values could be used for purposes of data filling.

When the reference year data was forecasted and backcasted, data from Bijl et al. (2018) was used to determine the annual technological changes. This step took the expected changes between 2010 and 2050 from Bijl et al. (2018) to calculate the compounded annual growth rate (CAGR) for each region identified in their study. As the regions differed from The World Bank (2021k) data used to create the conceptual model, each nation had to be assigned a second regional classification. As with the regional averages computed previously, it was assumed that the CAGR would be consistent throughout the new assigned regions. Further, the data used from Bijl et al. (2018) was for the whole industrial sector, yet the CAGR values were solely applied to the manufacturing sub-sector. Finally, the CAGR values calculated for the period between 2010 and 2050 were applied to the conceptual model data to forecast from 2015 to 2050, as well as to backcast from 2015 to 1970. This works under the assumption that the CAGR for each region between 2010 and 2050 is the same as the CAGR for each region between 1970 and 2050. While the efficacy of this method for the forecasting until 2050 was sound, backcasting worked under the assumption that the same annual trends were present between 1970 and 2015.

5.4 Future research

Regarding the output data from this thesis, it is important that further analyses are performed to assess the model improvements. Analyses of the spatial downscaling in the United States showed that more improvements are necessary to the input parameters. A more precise downscaling method is vital for the model to have reliable local applicability. While the national scale is currently reliable, assessments of water scarcity cannot be conclusively made given the current output. Further, it must be noted that when comparing gross water demand and abstractions, supply is inherently limited by local demand, but this is not indicative of the actual dynamics. Modelled water demand is population-driven, resulting in high demand at population centers, while water abstractions are driven by the presence of natural systems. The model limits the maximum amount of abstracted water at each location to the demand at that location; however, water can be supplied from areas beyond the cell areas defined in the data files, therefore, the ratio of local abstractions to local demand is not a reliable indicator of water scarcity. At the national level, the equivalence is more accurate, but still may not properly account for the water use dynamics in observed datasets. Moving forward, more global analyses assessing the updated model performance at local scales are necessary through comparison with observed industrial water use dynamics.

The need for more thorough datasets of global manufacturing water use is crucial. The thermoelectric data used for this study was very reliable; however, several assumptions had to be made to estimate global manufacturing water use while developing the conceptual model. The latter required datasets from different sources to be used in conjunction, which led to statistical uncertainties. With an improved spatiotemporal manufacturing water use dataset, more precise downscaling of industrial sector water use will be possible in PCR-GLOBWB. This will result in more realistic global simulations to assess current hydrologic dynamics, as well as more accurate scenario building when applying RCPs and their corresponding SSPs. Ultimately, future

projections will be improved and will better account for the effects of anthropogenic climate change, the shift to renewable energy sources, and other factors that will affect global industrial water use. Further, the model may also be able to account for changes in water use strategies and be linked to possible adaptation measures.

Finally, while the separation of the industrial sector into its sub-sectoral components proved effective in calculating specific contributions from each at the national scale, a more temporally explicit input dataset would allow for more accurate modelling of inter-annual hydrologic characteristics. The current industrial water demand dataset was created at the annual scale, and the values were evenly distributed throughout each year. This is not entirely realistic, however, as industrial water demand, and effectively water scarcity, do vary seasonally (van Vliet et al., 2017). A global dataset with monthly trends would clearly be more beneficial as an input source for PCR-GLOBWB, as it would allow for more accurate monthly output files detailing the seasonal effects on water resource availability and sectoral water use.

6 Conclusion

By updating the input parameters of PCR-GLOBWB, the modelled global effects of industrial water use on the hydrologic cycle were altered. With the separation of the manufacturing and thermoelectric sub-sectors, as well as the input of thermoelectric water use at the source, an updated industrial water demand file was used to simulate global water resource availability and sectoral water use. The creation of the conceptual model to estimate manufacturing water withdrawals proved effective at the national scale, and when coupled with recycling ratios from the initial industrial sector input data, the manufacturing water consumption could be calculated. Upon further coupling with the thermoelectric water use dataset, the updated industrial water demand input file was created. Theoretically, this updated dataset is more spatially precise, and therefore more reliable as an input file for PCR-GLOBWB to assess the influence of the industrial sector on the natural water cycle. In practice, however, more validation is necessary to assess the efficacy of the updated model output at estimating sub-national water use. Nationally, the initial and updated industrial demand input datasets had similar global estimations for total industrial water use, as well as similar regional estimations. This study therefore concludes that the disaggregation of the industrial sector into its sub-sectoral components improved the national input to the PCR-GLOBWB simulations by spatially applying the thermoelectric data at the powerplant scale, and only downscaling the manufacturing water demand using population dispersion. Sub-nationally, however, improvements can still be made regarding the integration of the thermoelectric water use data and downscaled manufacturing water use data.

When integrated into PCR-GLOBWB, the updated model results were compared with the initial model results (from a reference run) for abstractions and discharge. The gross demand and abstractions of the updated model run were also compared to assess if the supply of industrial water was meeting its demand. It was found that updated local distribution of industrial water

scarcity, given the input gross demand and output abstractions, was similar to the initial model. This method can be useful for displaying water scarcity, but suffers from limitations to the water abstractions. As abstractions are capped by the gross demand at any location, industrial water supply is being limited by the local demand. This is not realistic, as abstracted water can be supplied to locations beyond their PCR-GLOBWB gridcell IDs. Further, in locations where water is available for abstractions, demand may be limited due to the population density at that site. A better comparison is at the national scale, where total abstractions and gross demand were compared. This analysis found that 19% of nations failed to meet half of their gross industrial water demand, while 11% of nations met all of their industrial water demand (43% met at least 90% of demand, 61% met at least 75%). By aggregating the national supply and demand of industrial water, regional values were calculated. They showed that nations in Middle East & North Africa are meeting the lowest ratio of demand, while low-income nations in East Asia & Pacific, Latin America & Caribbean, and Sub-Saharan Africa are meeting the highest ratio of demand.

As for the change in modelled industrial water abstractions from the initial model to the updated model, there was a 7% increase in global supply in 2000, and a 16% decrease in 2014. These values relate very closely to the gross industrial water demand, and follow similar trends globally, regionally, and nationally. Comparisons of the model output in China, the Netherlands, and the United States highlighted the differences between the inputs of the two model runs. Similar to the gross demand, the trend in China was very similar between the two models, albeit with higher values in the updated model. In the Netherlands, higher values were again predicted, although the trend showed a slight decrease over time, contrary to the initial model which simulated an increase. The same diversion was present in the trend analysis for the United States, which in fact showed that the modelled abstractions not only had opposite trends, but also that the values crossed. The modelled decreases in industrial water supply and demand are attributed to the technological improvements applied in the conceptual model. A further analysis of industrial water abstractions in the United States showed that this decreasing trend over time does in fact correlate with the observed values from the USGS at the national scale. At the state and county scales, however, the updated model data had worse correlations and slopes than the initial model data. A comparison of the thermoelectric demand and withdrawals showed discrepancies between the input and observed datasets, contributing to the poor overall local model performance in the United States.

Analyses of the modelled discharge showed regional changes as well. Data from the Mississippi River and the Rhine showed an increase in modelled discharge from the initial to updated model, while data from the Yellow River generally showed a decrease (albeit with significantly smaller variations than seen along the Mississippi River and the Rhine). These changes are due to the difference in local demand, and therefore abstractions, affecting the streamflow of natural systems. It can be concluded from these analyses that the implementation of thermoelectric water use at the source, and downscaling of the manufacturing water demand by population density, decreased the demand and abstractions at the stations used to measure discharge along the Mississippi River and the Rhine. This caused the abstractions to increase over time, relative to the initial model.

In conclusion, this study succeeded at developing a conceptual model to estimate manufacturing water withdrawals at the national scale, and upon integration with manufacturing recycling ratios and thermoelectric water use, an updated industrial water demand file was created for integration into PCR-GLOBWB. Validation of the model output showed that it proved effective at simulating industrial water use trends in the United States at the national scale, but that further analyses are necessary to assess its efficacy in other regions. The analysis in the United States also showed that the integration of the thermoelectric dataset and subsequent downscaling of the manufacturing water demand by population density adversely affected the local output of industrial water use. In that regard, future testing is necessary to continue improving the local attributes of the industrial water demand data and the input parameters of PCR-GLOBWB. This will ultimately lead to model outputs that are more indicative of hydrologic trends, and allow for improved future projections of water availability and sectoral water use through the application of RCPs and their corresponding SSPs.

References

- Australian Bureau of Statistics (2020). *Water Account, Australia 2018-19*.
- Bao, C., & Fang, C. L. (2012). Water resources flows related to urbanization in China: challenges and perspectives for water management and urban development. *Water Resources Management, 26*(2), 531-552.
- Bernhard, J., Reynaud, A., De Roo, A., Karsenberg, D., & Jong, S. D. (2018). Mapping industrial water use and water productivity levels in Europe at high sectoral and spatial detail. *Under review*.
- Bijl, D. L., Biemans, H., Bogaart, P. W., Dekker, S. C., Doelman, J. C., Stehfest, E., & van Vuuren, D. P. (2018). A global analysis of future water deficit based on different allocation mechanisms. *Water Resources Research, 54*(8), 5803-5824.
- Bijl, D. L., Bogaart, P. W., Kram, T., de Vries, B. J., & van Vuuren, D. P. (2016). Long-term water demand for electricity, industry and households. *Environmental Science & Policy, 55*, 75-86.
- British Petroleum. (2013). *Water in the Energy Industry: An Introduction*.
- Byers, L., Friedrich, J., Hennig, R., Kressig, A., Li, X., McCormick, C., & Valeri, L. M. (2018). A global database of power plants. *World Resources Institute, 18*.
- Dieter, C.A., Linsey, K.S., Caldwell, R.R., Harris, M.A., Ivahnenko, T.I., Lovelace, J.K., Maupin, M.A., and Barber, N.L. (2018a). *Estimated Use of Water in the United States County-Level Data for 2015*. [United States Geological Survey].
- Dieter, C. A., Maupin, M. A., Caldwell, R. R., Harris, M. A., Ivahnenko, T. I., Lovelace, J. K., ... & Linsey, K. S. (2018b). *Estimated use of water in the United States in 2015* (No. 1441). US Geological Survey.
- Dupont, D. P., & Renzetti, S. (2001). The role of water in manufacturing. *Environmental and resource economics, 18*(4), 411-432.
- Earth Observatory (2017). *Earth at Night: Flat Maps*. NASA.
- Edmonds, J., Wise, M., Pitcher, H., Richels, R., Wigley, T., & MacCracken, C. (1997). An integrated assessment of climate change and the accelerated introduction of advanced energy technologies-an application of MiniCAM 1.0. *Mitigation and adaptation strategies for global change, 1*(4), 311-339.

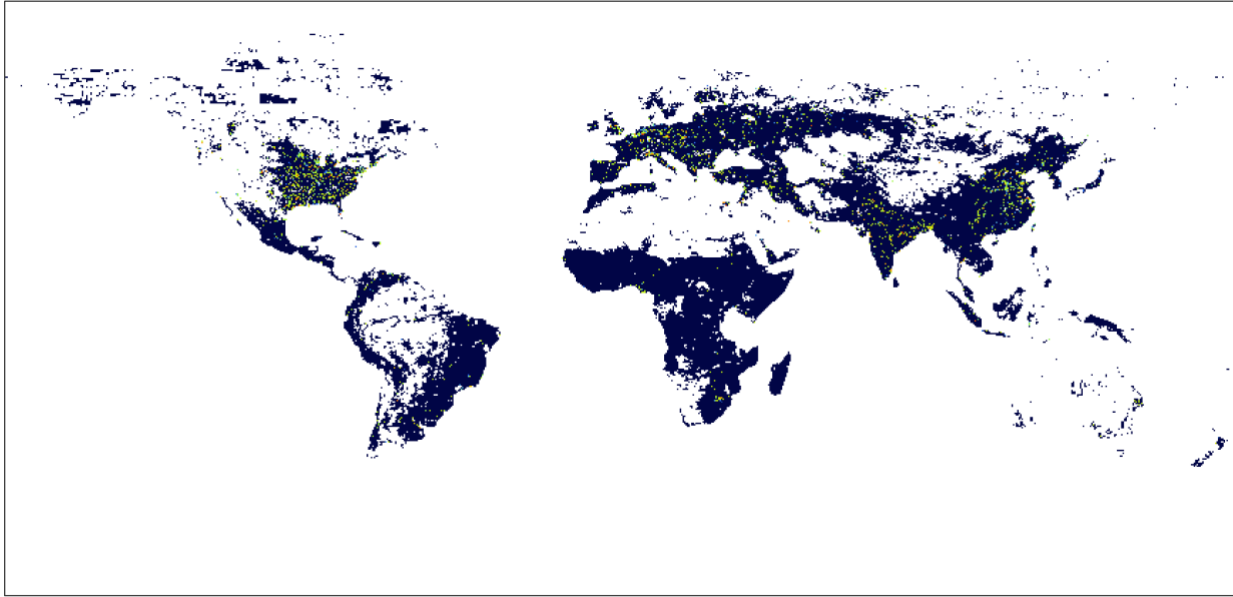
- Eurostat (2021). *Water use in the manufacturing industry by activity and supply category*.
- Food and Agriculture Organization of the United Nations (2021). *AQUASTAT Database*.
- Flörke, M., Kynast, E., Bärlund, I., Eisner, S., Wimmer, F., & Alcamo, J. (2013). Domestic and industrial water uses of the past 60 years as a mirror of socio-economic development: A global simulation study. *Global Environmental Change*, 23(1), 144-156.
- Frost, K., & Hua, I. (2019). Quantifying spatiotemporal impacts of the interaction of water scarcity and water use by the global semiconductor manufacturing industry. *Water Resources and Industry*, 22, 100115.
- Huang, Z., Hejazi, M., Li, X., Tang, Q., Vernon, C., Leng, G., ... & Wada, Y. (2018a). Global gridded monthly sectoral water use dataset for 1971-2010: v2 (Version V2.0).
- Huang, Z., Hejazi, M., Li, X., Tang, Q., Vernon, C., Leng, G., ... & Wada, Y. (2018b). Reconstruction of global gridded monthly sectoral water withdrawals for 1971–2010 and analysis of their spatiotemporal patterns. *Hydrology and Earth System Sciences*, 22(4), 2117-2133.
- International Institute for Applied Systems Analysis (2012). *IIASA-POP World Regions*.
- Jia, S., Yang, H., Zhang, S., Wang, L., & Xia, J. (2006). Industrial water use Kuznets curve: evidence from industrialized countries and implications for developing countries. *Journal of Water Resources Planning and Management*, 132(3), 183-191.
- Kim, S. H., Edmonds, J., Lurz, J., Smith, S. J., & Wise, M. (2006). The ObjECTS framework for integrated assessment: hybrid modeling of transportation. *The Energy Journal*, (Special Issue# 2).
- King, C. W., Holman, A. S., & Webber, M. E. (2008). Thirst for energy. *Nature geoscience*, 1(5), 283-286.
- Lange, S., Menz, C., Gleixner, M. C., Weedon, G. P., Amici, A., Bellouin, N., ... & Cagnazzo, C. (2021). *WFDE5 over land merged with ERA5 over the ocean (W5E5 v2.0)*. ISIMIP Repository.
- Lips, S. E. (2020). Towards a global high resolution water demand dataset: Effect of data quality and downscaling techniques-the case for Europe (Master's thesis).
- Liu, Y., Hejazi, M., Kyle, P., Kim, S. H., Davies, E., Miralles, D. G., ... & Niyogi, D. (2016). Global and regional evaluation of energy for water. *Environmental science & technology*, 50(17), 9736-9745.

- Lohrmann, A., Farfan, J., Caldera, U., Lohrmann, C., & Breyer, C. (2019). Global scenarios for significant water use reduction in thermal power plants based on cooling water demand estimation using satellite imagery. *Nature Energy*, *4*(12), 1040-1048.
- Long, J., & Robertson, C. (2018). Comparing spatial patterns. *Geography Compass*, *12*(2), e12356.
- Luo, T., Krishnaswami, A., & Li, X. (2018). A Methodology to Estimate Water Demand for Thermal Power Plants in Data-Scarce Regions Using Satellite Images.
- Mekonnen, M. M., & Hoekstra, A. Y. (2011). National water footprint accounts: The green, blue and grey water footprint of production and consumption. Volume 1: Main Report.
- Mekonnen, M. M., & Hoekstra, A. Y. (2011). National water footprint accounts: The green, blue and grey water footprint of production and consumption. Volume 2: appendices.
- Munasinghe, M. (1999). Is environmental degradation an inevitable consequence of economic growth: Tunneling through the environmental Kuznets curve. *Ecological Economics*, *29*(1), 89-109.
- Murray, C. (2014). *Water use parameters in manufacturing industries, 2011 – Provinces and territories*. [Statistics Canada].
- Planbureau voor de Leefomgeving (2018). *IMAGE regions and countries (ISO)*. PBL Netherlands Environmental Assessment Agency.
- Renzetti, S. (1992). Estimating the structure of industrial water demands: the case of Canadian manufacturing. *Land Economics*, 396-404.
- Reynaud, A. (2003). An econometric estimation of industrial water demand in France. *Environmental and Resource Economics*, *25*(2), 213-232.
- Rübelke, D., & Vögele, S. (2011). Impacts of climate change on European critical infrastructures: the case of the power sector. *Environmental science & policy*, *14*(1), 53-63.
- Schillinger, J. (2016). Global modelling of domestic and manufacturing water uses. (Master's thesis).
- Schornagel, J., Niele, F., Worrell, E., & Böggemann, M. (2012). Water accounting for (agro)industrial operations and its application to energy pathways. *Resources, Conservation and Recycling*, *61*, 1-15.

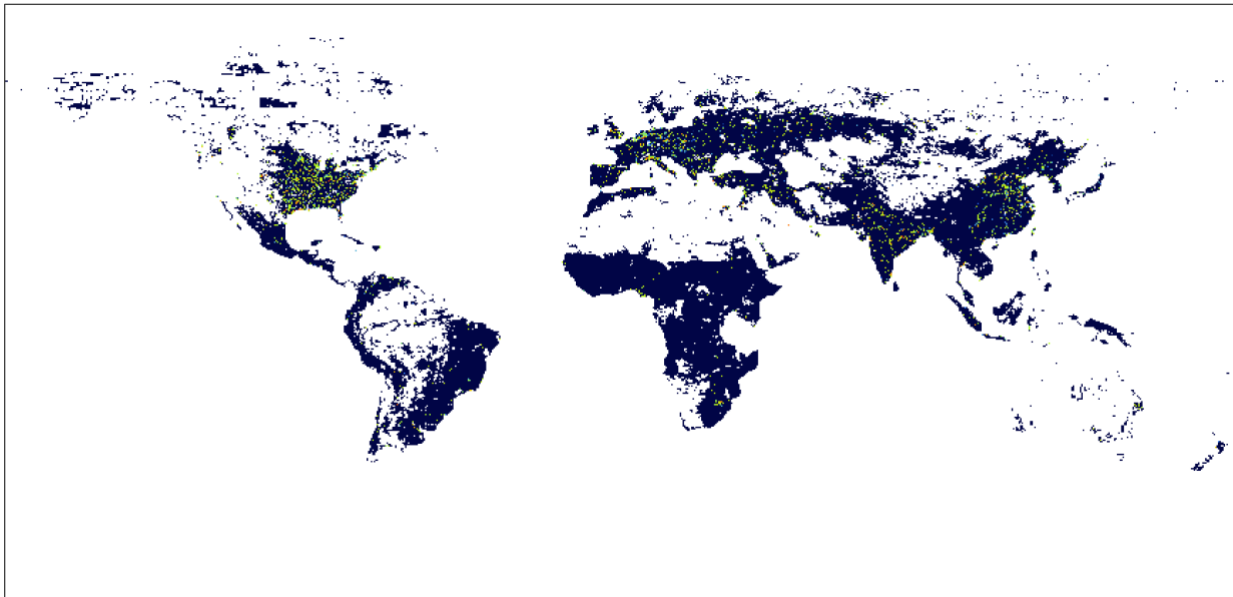
- Shang, Y., Lu, S., Li, X., Sun, G., Shang, L., Shi, H., ... & Wang, H. (2017). Drivers of industrial water use during 2003–2012 in Tianjin, China: A structural decomposition analysis. *Journal of Cleaner Production*, 140, 1136-1147.
- Sutanudjaja, E. H., Beek, R. V., Wanders, N., Wada, Y., Bosmans, J. H., Drost, N., ... & Bierkens, M. F. (2018). PCR-GLOBWB 2: a 5 arc minute global hydrological and water resources model. *Geoscientific Model Development*, 11(6), 2429-2453.
- Tate, D. M. (1986). Structural change implications for industrial water use. *Water Resources Research*, 22(11), 1526-1530.
- The World Bank (2021a). *Chemicals (% of value added in manufacturing)*.
- The World Bank (2021b). *Food, beverages and tobacco (% of value added in manufacturing)*.
- The World Bank (2021c). *GDP (constant 2010 US\$)*.
- The World Bank (2021d). *GDP per capita (constant 2010 US\$)*.
- The World Bank (2021e). *Gross value added at basic prices (GVA) (constant 2010 US\$)*.
- The World Bank (2021f). *Machinery and transport (% of value added in manufacturing)*.
- The World Bank (2021g). *Manufacturing, value added (constant 2010 US\$)*.
- The World Bank (2021h). *Other manufacturing (% of value added in manufacturing)*.
- The World Bank (2021i). *Textiles and clothing (% of value added in manufacturing)*.
- The World Bank (2021j). *Urban population (% of total population)*.
- The World Bank (2021k). *World Bank Country and Lending Groups*.
- Thiede, S., Kurle, D., & Herrmann, C. (2017). The water–energy nexus in manufacturing systems: Framework and systematic improvement approach. *CIRP Annals*, 66(1), 49-52.
- Thiede, S., Schönemann, M., Kurle, D., & Herrmann, C. (2016). Multi-level simulation in manufacturing companies: The water-energy nexus case. *Journal of Cleaner Production*, 139, 1118-1127.
- United Nations Statistics Division (2021). *GDP by Type of Expenditure at constant (2015) prices – US dollars*.

- U.S. Energy Information Administration (2020). *Thermoelectric cooling water data*.
- USGS (2018c). *Water Use in the United States*.
- van Beek, L. P. H., Wada, Y., & Bierkens, M. F. (2011). Global monthly water stress: 1. Water balance and water availability. *Water Resources Research*, 47(7).
- van Vliet, M. T., Flörke, M., & Wada, Y. (2017). Quality matters for water scarcity. *Nature Geoscience*, 10(11), 800-802.
- van Vliet, M. T., Jones, E. R., Flörke, M., Franssen, W. H., Hanasaki, N., Wada, Y., & Yearsley, J. R. (2021). Global water scarcity including surface water quality and expansions of clean water technologies. *Environmental Research Letters*, 16(2), 024020.
- van Vliet, M. T., Wiberg, D., Leduc, S., & Riahi, K. (2016). Power-generation system vulnerability and adaptation to changes in climate and water resources. *Nature Climate Change*, 6(4), 375-380.
- van Vliet, M. T., Yearsley, J. R., Ludwig, F., Vögele, S., Lettenmaier, D. P., & Kabat, P. (2012). Vulnerability of US and European electricity supply to climate change. *Nature Climate Change*, 2(9), 676-681.
- Vassolo, S., & Döll, P. (2005). Global-scale gridded estimates of thermoelectric power and manufacturing water use. *Water Resources Research*, 41(4).
- Wada, Y., Wisser, D., & Bierkens, M. F. (2014). Global modeling of withdrawal, allocation and consumptive use of surface water and groundwater resources. *Earth System Dynamics*, 5(1), 15-40.
- World Resources Institute (2018). *Global Power Plant Database*.
- Yu, J. Q., Chen, Y., Shao, S., Zhang, Y., Liu, S. L., & Zhang, S. S. (2014). A study on establishing an optimal water network in a dyeing and finishing industrial park. *Clean Technologies and Environmental Policy*, 16(1), 45-57.

Appendix



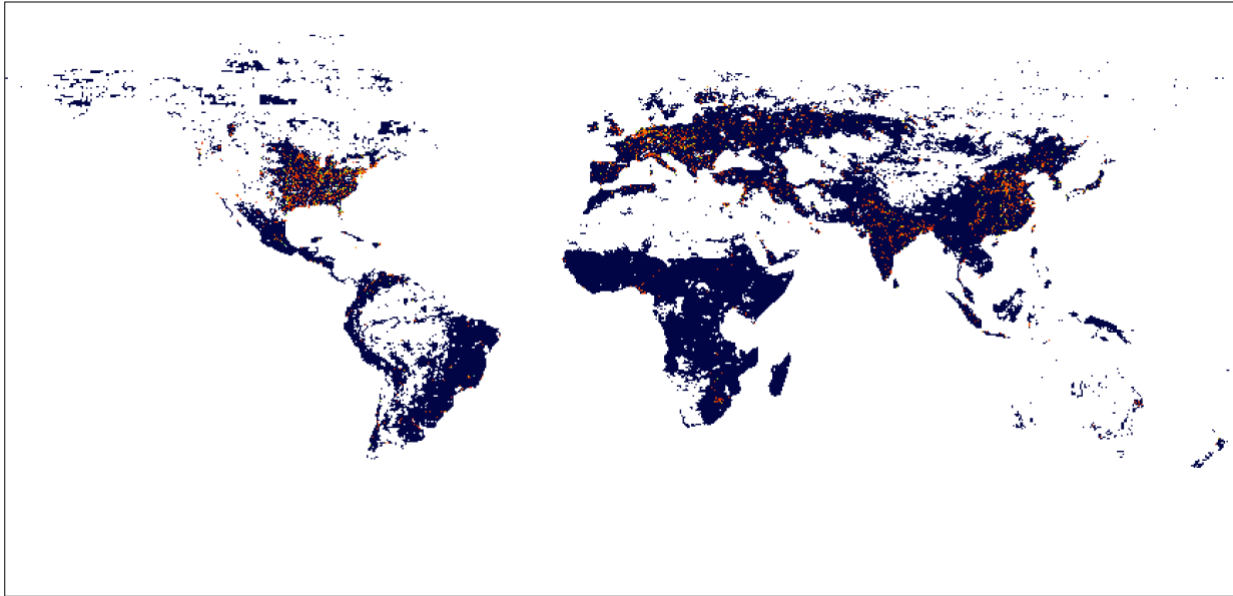
a



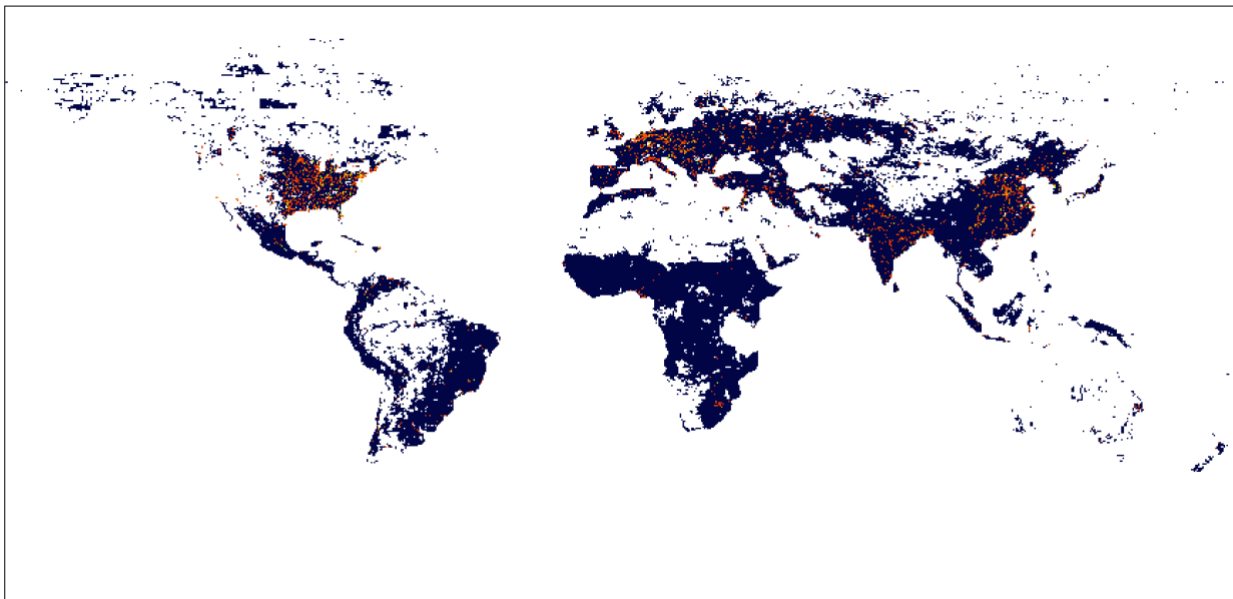
b



Figure A1 Percent contribution of gross (a) and net (b) manufacturing water demand to total net industrial water demand in 2015, where any empty cells (white) have no estimated net industrial water demand or missing values.



a



b



Figure A2 Percent contribution of gross (a) and net (b) thermoelectric water demand to total net industrial water demand in 2015, where any empty cells (white) have no net industrial water demand or missing values.

Table A1 Water consumption, withdrawals, and recycling ratios for the cooling of thermoelectric power plants in 2015 by nation (Lohrmann et al., 2019).

Nation	Consumption [m³]	Withdrawals [m³]	Ratio
Afghanistan	2.65E+02	2.65E+02	0.00%
Albania	9.33E+03	1.06E+06	99.12%
Algeria	6.69E+06	8.28E+06	19.18%
Angola	2.22E+06	7.05E+07	96.85%
Argentina	1.29E+08	2.87E+09	95.50%
Armenia	1.32E+07	2.01E+07	34.27%
Australia	3.71E+08	2.48E+09	85.03%
Austria	2.22E+07	9.22E+08	97.59%
Azerbaijan	6.57E+06	6.25E+08	98.95%
Bahamas	1.38E+06	9.73E+07	98.58%
Bahrain	1.82E+07	5.53E+08	96.70%
Bangladesh	7.03E+07	1.52E+09	95.37%
Barbados	2.84E+06	4.13E+06	31.34%
Belarus	5.72E+07	1.70E+09	96.64%
Belgium	1.11E+08	2.39E+08	53.54%
Bolivia	2.62E+06	3.26E+06	19.57%
Bosnia and Herzegovina	1.93E+07	2.37E+07	18.40%
Botswana	7.90E+06	9.71E+06	18.61%
Brazil	1.26E+08	3.71E+09	96.60%
Brunei	9.71E+06	1.39E+07	30.04%
Bulgaria	4.91E+07	2.83E+09	98.27%
Cambodia	3.56E+05	8.53E+07	99.58%
Cameroon	1.72E+04	1.72E+04	0.00%
Canada	1.82E+08	2.28E+10	99.20%
Cayman Islands	1.52E+05	2.22E+07	99.31%
Chile	2.42E+07	2.80E+09	99.13%
China	4.68E+09	5.43E+10	91.38%
Colombia	2.20E+07	9.42E+08	97.67%

Nation	Consumption [m³]	Withdrawals [m³]	Ratio
Congo	2.53E+06	3.16E+06	20.00%
Costa Rica	4.12E+05	5.94E+07	99.31%
Croatia	1.43E+06	2.51E+08	99.43%
Cuba	1.26E+07	1.78E+09	99.29%
Cyprus	1.03E+06	1.26E+08	99.18%
Czech Republic	1.36E+08	2.36E+08	42.59%
Denmark	4.60E+06	1.07E+09	99.57%
Djibouti	1.77E+06	2.58E+06	31.34%
Dominican Republic	2.29E+07	5.22E+08	95.61%
Ecuador	8.99E+06	4.27E+08	97.89%
Egypt	1.10E+08	1.13E+10	99.03%
El Salvador	1.77E+04	1.77E+04	0.00%
Eritrea	1.20E+05	1.75E+07	99.31%
Estonia	9.14E+06	1.33E+09	99.31%
Finland	3.50E+07	6.33E+09	99.45%
France	1.07E+09	1.19E+10	91.00%
Gabon	1.91E+05	2.79E+07	99.31%
Georgia	7.00E+06	1.02E+07	31.34%
Germany	7.22E+08	3.04E+09	76.24%
Ghana	1.50E+07	2.16E+07	30.26%
Greece	4.56E+07	5.80E+08	92.14%
Guam	1.80E+06	2.63E+08	99.31%
Guatemala	7.79E+06	1.06E+07	26.72%
Haiti	1.20E+03	1.20E+03	0.00%
Honduras	7.31E+06	1.06E+07	31.34%
Hong Kong	2.23E+07	4.52E+09	99.51%
Hungary	2.07E+07	2.94E+08	92.94%
India	1.97E+09	8.30E+09	76.20%
Indonesia	1.25E+08	1.30E+10	99.04%
Iran	3.89E+08	1.29E+09	69.99%

Nation	Consumption [m³]	Withdrawals [m³]	Ratio
Iraq	3.04E+07	2.53E+09	98.80%
Ireland	2.77E+06	4.65E+08	99.40%
Isle of Man	1.75E+05	2.17E+05	19.61%
Israel	1.86E+07	3.13E+09	99.40%
Italy	5.48E+07	3.52E+09	98.44%
Ivory Coast	1.63E+06	2.02E+06	19.71%
Jamaica	4.20E+06	1.39E+08	96.97%
Japan	1.17E+09	3.21E+10	96.35%
Jordan	1.24E+06	1.52E+06	18.34%
Kazakhstan	1.21E+08	1.20E+09	89.99%
Kenya	1.20E+05	1.48E+05	19.07%
Kuwait	4.49E+07	5.22E+09	99.14%
Kyrgyzstan	1.22E+06	1.52E+08	99.20%
Latvia	4.14E+06	5.82E+06	28.83%
Lebanon	1.71E+07	2.14E+07	20.00%
Liberia	4.47E+05	5.58E+05	20.00%
Libya	2.92E+05	2.92E+05	0.00%
Lithuania	1.37E+07	7.98E+08	98.28%
Luxembourg	9.69E+03	9.69E+03	0.00%
Madagascar	2.04E+06	2.50E+06	18.40%
Malaysia	4.02E+07	5.38E+09	99.25%
Malta	3.49E+05	4.96E+07	99.30%
Mauritania	2.68E+05	3.91E+07	99.31%
Mauritius	5.35E+06	7.10E+06	24.60%
Mexico	4.08E+08	3.61E+09	88.70%
Moldova	3.15E+06	4.77E+08	99.34%
Mongolia	9.63E+06	1.18E+07	18.40%
Montenegro	2.39E+06	2.93E+06	18.40%
Morocco	4.01E+07	2.97E+08	86.47%
Mozambique	1.87E+04	1.87E+04	0.00%

Nation	Consumption [m³]	Withdrawals [m³]	Ratio
Myanmar	1.10E+06	1.47E+06	25.46%
Namibia	7.56E+03	7.56E+03	0.00%
Netherlands	5.57E+07	6.09E+09	99.09%
New Zealand	2.20E+07	2.91E+07	24.36%
Nicaragua	1.85E+06	2.70E+06	31.34%
Nigeria	2.81E+07	1.32E+09	97.88%
North Korea	8.91E+06	1.62E+09	99.45%
Norway	4.40E+06	5.91E+08	99.26%
Oman	3.04E+06	3.79E+06	20.01%
Pakistan	1.89E+08	2.71E+08	30.29%
Panama	1.94E+06	2.24E+08	99.13%
Peru	1.46E+07	6.98E+07	79.00%
Philippines	2.84E+07	5.41E+09	99.48%
Poland	2.04E+08	3.55E+09	94.26%
Portugal	3.13E+07	3.86E+07	19.07%
Puerto Rico	4.52E+07	6.25E+07	27.65%
Qatar	3.74E+07	1.07E+09	96.52%
Republic of North Macedonia	9.00E+06	1.80E+07	50.12%
Romania	7.88E+07	2.03E+09	96.12%
Russia	1.13E+09	3.88E+10	97.08%
Saint Lucia	7.68E+05	1.12E+06	31.34%
Saudi Arabia	7.53E+07	3.60E+08	79.07%
Senegal	1.25E+05	1.22E+07	98.97%
Serbia	1.30E+07	2.53E+09	99.49%
Singapore	2.34E+07	2.35E+09	99.00%
Sint Maarten	1.73E+05	2.53E+07	99.31%
Slovakia	4.73E+07	1.25E+08	62.18%
Slovenia	2.25E+07	1.43E+08	84.29%
South Africa	3.27E+08	2.16E+09	84.85%
South Korea	3.36E+08	2.86E+10	98.83%

Nation	Consumption [m³]	Withdrawals [m³]	Ratio
Spain	3.20E+08	4.04E+09	92.08%
Sri Lanka	1.49E+06	3.50E+08	99.57%
Sudan	9.50E+06	1.34E+07	29.20%
Sweden	6.81E+07	1.13E+10	99.40%
Switzerland	5.70E+07	1.66E+09	96.56%
Syria	5.49E+07	7.71E+07	28.75%
Taiwan	1.13E+08	1.13E+10	99.00%
Tanzania	3.45E+06	4.31E+06	19.96%
Thailand	2.27E+08	2.95E+08	23.07%
Timor-Leste	1.07E+04	1.07E+04	0.00%
Togo	4.68E+03	4.68E+03	0.00%
Trinidad and Tobago	1.38E+07	1.42E+09	99.03%
Tunisia	3.95E+06	1.25E+08	96.85%
Turkey	2.26E+08	7.18E+08	68.51%
Turkmenistan	8.14E+06	8.38E+08	99.03%
Uganda	2.88E+03	2.88E+03	0.00%
Ukraine	2.52E+08	9.53E+09	97.36%
United Arab Emirates	1.31E+06	1.44E+06	8.50%
United Kingdom	3.34E+08	1.11E+10	96.97%
United States	5.25E+09	1.04E+11	94.96%
Uruguay	4.58E+06	4.84E+08	99.05%
Uzbekistan	8.54E+07	2.31E+09	96.30%
Venezuela	8.63E+07	1.73E+09	95.02%
Vietnam	5.37E+07	2.61E+09	97.94%
Yemen	2.75E+04	2.75E+04	0.00%
Zambia	8.19E+03	8.19E+03	0.00%
Zimbabwe	1.71E+07	2.09E+07	18.40%

Table A2 Water consumption, withdrawals, and recycling ratios for the cooling of thermoelectric power plants in 2015 by region (Lohrmann et al., 2019; The World Bank, 2021k).

Region	Consumption [m³]	Withdrawals [m³]	Ratio
East Asia & Pacific	7.25E+09	1.64E+11	95.59%
Eastern Europe & Central Asia	2.54E+09	7.07E+10	96.40%
Latin America & Caribbean	9.50E+08	2.10E+10	95.48%
Middle East & North Africa	8.55E+08	2.61E+10	96.72%
North America	5.43E+09	1.27E+11	95.72%
Southern Asia	2.24E+09	1.04E+10	78.58%
Sub-Saharan Africa	4.23E+08	3.73E+09	88.67%
Western Europe	2.94E+09	6.28E+10	95.32%

Table A3 Water consumption, withdrawals, and recycling ratios for the cooling of thermoelectric power plants in 2015 by economic classification (Lohrmann et al., 2019; The World Bank, 2021k).

Economic Classification	Consumption [m³]	Withdrawals [m³]	Ratio
Low income	3.47E+07	1.68E+09	97.93%
Lower middle income	3.10E+09	5.74E+10	94.59%
Upper middle income	8.29E+09	1.34E+11	93.80%
High income	1.12E+10	2.93E+11	96.18%

Table A4 Water consumption, withdrawals, and recycling ratios for the cooling of thermoelectric power plants in 2015 by primary fuel type (Lohrmann et al., 2019).

Primary Fuel	Consumption [m³]	Withdrawals [m³]	Ratio
Coal	1.19E+10	1.88E+11	93.65%
Gas	4.81E+09	9.69E+10	95.04%
Nuclear	4.84E+09	1.74E+11	97.23%
Oil	1.06E+09	2.71E+10	96.08%

Table A5 Water consumption, withdrawals, and recycling ratios for the cooling of thermoelectric power plants in 2015 by technology (Lohrmann et al., 2019).

Technology	Cons. [m³]	With. [m³]	Ratio
BWR	8.99E+08	2.70E+10	97%
CCGT with Cogen	2.84E+08	4.32E+09	93%
CCGT with Cogen (Subcritical Boiler)	2.49E+05	5.98E+07	100%
Combined Cycle Gas Turbine (CCGT)	1.34E+09	2.42E+10	94%
Combined Cycle Gas Turbine (CCGT) (Subcritical Boiler)	7.73E+06	2.90E+08	97%
Combined Cycle Internal Combustion Plant (CCICP)	1.39E+06	1.73E+06	20%
FBR	4.25E+06	7.00E+08	99%
Gas Turbine	1.20E+09	1.20E+10	90%
Gas Turbine with Cogen	2.56E+08	4.39E+09	94%
GCR	5.65E+07	9.32E+09	99%
IGCC with Cogen	3.11E+07	2.80E+08	89%
Integrated Gasification Combined Cycle (IGCC)	2.63E+07	2.70E+08	90%
Internal Combustion	7.20E+07	1.69E+09	96%
Internal combustion with Cogen	2.91E+06	7.15E+07	96%
LWGR	1.48E+08	4.94E+09	97%
PHWR	2.06E+08	2.46E+10	99%
PWR	3.52E+09	1.08E+11	97%
Steam Turbine	1.89E+09	5.50E+10	97%
Steam Turbine (Subcritical Boiler)	7.48E+09	1.36E+11	94%
Steam Turbine (Supercritical Boiler)	2.96E+09	2.55E+10	88%
Steam Turbine with Cogen	6.38E+08	1.69E+10	96%
Steam Turbine with Cogen (Subcritical Boiler)	1.16E+09	2.41E+10	95%
Steam Turbine with Cogen (Supercritical Boiler)	2.33E+08	1.53E+09	85%
Thermal	1.81E+08	5.14E+09	96%
Thermal (Subcritical Boiler)	2.08E+07	5.07E+08	96%

Table A6 Water consumption, withdrawals, and recycling ratios for the cooling of thermoelectric power plants in 2015 by cooling system (Lohrmann et al., 2019).

Cooling System	Consumption [m³]	Withdrawals [m³]	Ratio
Dry	2.77E+07	3.18E+07	12.86%
Dry and Once-through	5.60E+06	8.16E+06	31.34%
Inlet	3.47E+08	4.34E+08	20.00%
Inlet and Dry	5.64E+06	7.05E+06	20.00%
Once-through	3.49E+09	4.26E+11	99.18%
Once-through and Dry	8.15E+06	1.37E+09	99.40%
Once-through and Pond	1.01E+07	8.92E+08	98.86%
Once-through with Dry	3.61E+07	5.19E+07	30.39%
Once-through with Pond	2.94E+07	3.95E+07	25.68%
Pond	9.04E+08	3.12E+10	97.10%
Pond and Dry	9.17E+05	2.43E+08	99.62%
Pond with Tower	1.45E+05	3.48E+07	99.58%
Tower	1.70E+10	2.47E+10	31.10%
Tower and Dry	4.59E+08	5.85E+08	21.46%
Tower and Once-through	1.42E+08	2.05E+08	31.01%
Tower and Pond	1.24E+08	1.77E+08	29.88%

Table A7 Water consumption, withdrawals, and recycling ratios for the cooling of thermoelectric power plants in 2015 by whether or not seawater is used (Lohrmann et al., 2019).

Seawater	Consumption [m³]	Withdrawals [m³]	Ratio
TRUE	6.60E+09	2.12E+11	96.88%
FALSE	1.60E+10	2.74E+11	94.16%

Table A8 2015 raw data used for developing the conceptual model, including industrial water withdrawals (FAO AQUASTAT, 2021), thermoelectric water withdrawals (Lohrmann et al., 2019), MVA in US dollars with constant value from 2010 (The World Bank, 2021g), and GDP in US dollars with constant value from 2010 (The World Bank, 2021c). Blank cells indicate that there was no raw data value provided.

Nation	IWW [m³]	TWW [m³]	MVA [\$]	GDP [\$]
Afghanistan	1.70E+08	2.65E+02	2.19E+09	1.98E+10
Albania	1.30E+08	1.06E+06	7.64E+08	1.30E+10
Algeria	1.22E+08	8.28E+06	5.67E+10	1.90E+11
American Samoa		0.00E+00		5.50E+08
Andorra		0.00E+00		3.29E+09
Angola	2.40E+08	7.05E+07	4.94E+09	1.05E+11
Antigua and Barbuda	2.50E+06	0.00E+00	2.68E+07	1.25E+09
Argentina	4.00E+09	2.87E+09	6.81E+10	4.56E+11
Armenia	1.09E+08	2.01E+07		1.15E+10
Aruba		0.00E+00		2.69E+09
Australia	2.77E+09	2.48E+09	8.68E+10	1.31E+12
Austria	2.70E+09	9.22E+08	7.30E+10	4.13E+11
Azerbaijan	2.97E+09	6.25E+08	3.12E+09	5.85E+10
Bahamas		9.73E+07	2.02E+08	1.03E+10
Bahrain	1.43E+07	5.53E+08	4.51E+09	3.07E+10
Bangladesh	7.70E+08	1.52E+09	2.98E+10	1.57E+11
Barbados	6.20E+06	4.13E+06		4.52E+09
Belarus	3.07E+08	1.70E+09	1.35E+10	6.06E+10
Belgium	3.21E+09	2.39E+08	6.77E+10	5.13E+11
Belize	2.12E+07	0.00E+00	9.78E+07	1.55E+09
Benin	3.00E+07	0.00E+00	1.36E+09	1.19E+10
Bermuda	1.10E+06	0.00E+00	2.79E+07	5.85E+09
Bhutan	3.00E+06	0.00E+00	1.71E+08	2.02E+09
Bolivia	3.20E+07	3.26E+06	2.78E+09	2.57E+10
Bosnia and Herzegovina	5.99E+07	2.37E+07	2.16E+09	1.84E+10

Nation	IWW [m³]	TWW [m³]	MVA [\$]	GDP [\$]
Botswana	3.11E+07	9.71E+06	1.04E+09	1.61E+10
Brazil	1.29E+10	3.71E+09	2.52E+11	2.34E+12
British Virgin Islands		0.00E+00		1.08E+09
Brunei		1.39E+07	2.01E+09	1.36E+10
Bulgaria	3.90E+09	2.83E+09		5.50E+10
Burkina Faso	2.17E+07	0.00E+00	1.64E+09	1.32E+10
Burundi	1.50E+07	0.00E+00	2.01E+08	2.32E+09
Cambodia	3.30E+07	8.53E+07	2.62E+09	1.59E+10
Cameroon	1.05E+08	1.72E+04	4.76E+09	3.36E+10
Canada	2.81E+10	2.28E+10	1.81E+11	1.79E+12
Cape Verde	4.00E+05	0.00E+00	1.11E+08	1.79E+09
Cayman Islands		2.22E+07	3.47E+07	4.55E+09
Central African Republic	1.20E+07	0.00E+00	2.87E+08	1.56E+09
Chad	1.04E+08	0.00E+00	1.81E+08	1.35E+10
Chile	1.97E+09	2.80E+09	2.66E+10	2.65E+11
China	1.34E+11	5.43E+10		8.91E+12
Colombia	3.78E+09	9.42E+08	4.54E+10	3.60E+11
Comoros	5.00E+05	0.00E+00		1.05E+09
Congo	2.40E+07	0.00E+00	6.55E+08	1.50E+10
Costa Rica	2.40E+08	5.94E+07	5.49E+09	4.47E+10
Croatia	1.89E+08	2.51E+08	7.87E+09	5.93E+10
Cuba	7.40E+08	1.78E+09	1.12E+10	7.39E+10
Curaçao		0.00E+00		2.90E+09
Cyprus	6.00E+06	1.26E+08	9.81E+08	2.36E+10
Czech Republic	9.36E+08	2.36E+08	5.14E+10	2.27E+11
Democratic Republic of the Congo	1.47E+08	3.16E+06	5.16E+09	3.13E+10
Denmark	3.49E+07	1.07E+09	4.03E+10	3.43E+11
Djibouti	0.00E+00	2.58E+06		2.25E+09

Nation	IWW [m³]	TWW [m³]	MVA [\$]	GDP [\$]
Dominica	0.00E+00	0.00E+00	1.01E+07	4.91E+08
Dominican Republic	6.60E+08	5.22E+08	9.71E+09	6.85E+10
Ecuador	5.49E+08	4.27E+08	1.05E+10	8.64E+10
Egypt	1.20E+09	1.13E+10	3.89E+10	2.50E+11
El Salvador	2.13E+08	1.77E+04	3.35E+09	2.10E+10
Equatorial Guinea	3.00E+06	0.00E+00	3.37E+09	1.65E+10
Eritrea	1.00E+06	1.75E+07		1.85E+09
Estonia	1.52E+09	1.33E+09	3.48E+09	2.32E+10
Ethiopia	5.11E+07	0.00E+00	2.34E+09	4.87E+10
Faroe Islands		0.00E+00		2.32E+09
Federated States of Micronesia		0.00E+00	1.17E+06	2.96E+08
Fiji	9.60E+06	0.00E+00	4.40E+08	3.78E+09
Finland	1.36E+09	6.33E+09	3.75E+10	2.50E+11
France	1.97E+10	1.19E+10	2.89E+11	2.78E+12
French Polynesia		0.00E+00		4.90E+09
Gabon	1.41E+07	2.79E+07	2.94E+09	1.85E+10
Gambia	2.12E+07	0.00E+00	8.18E+07	1.57E+09
Georgia	2.68E+08	1.02E+07	1.41E+09	1.56E+10
Germany	1.81E+10	3.04E+09	7.55E+11	3.69E+12
Ghana	9.50E+07	2.16E+07	2.47E+09	4.53E+10
Gibraltar		0.00E+00		2.56E+09
Greece	1.26E+08	5.80E+08	1.76E+10	2.45E+11
Greenland		0.00E+00	1.98E+08	2.54E+09
Grenada	0.00E+00	0.00E+00	2.73E+07	8.98E+08
Guadeloupe	9.31E+05	0.00E+00		
Guam		2.63E+08		5.20E+09
Guatemala	6.03E+08	1.06E+07	9.09E+09	5.00E+10
Guinea	5.91E+07	0.00E+00	9.65E+08	8.58E+09

Nation	IWW [m³]	TWW [m³]	MVA [\$]	GDP [\$]
Guinea-Bissau	1.19E+07	0.00E+00	1.16E+08	9.99E+08
Guyana	2.04E+07	0.00E+00	2.46E+08	4.03E+09
Haiti	5.10E+07	1.20E+03	2.27E+09	1.35E+10
Honduras	1.14E+08	1.06E+07	3.08E+09	1.88E+10
Hong Kong		4.52E+09	3.84E+09	2.64E+11
Hungary	3.16E+09	2.94E+08	2.70E+10	1.46E+11
Iceland	1.98E+08	0.00E+00	2.24E+09	1.57E+10
India	1.70E+10	8.30E+09	3.97E+11	2.29E+12
Indonesia	1.05E+10	1.30E+10	2.13E+11	9.88E+11
Iran	1.10E+09	1.29E+09	6.15E+10	4.76E+11
Iraq	1.86E+09	2.53E+09	1.68E+09	1.88E+11
Ireland	3.92E+08	4.65E+08	9.00E+10	3.08E+11
Isle of Man		2.17E+05		7.07E+09
Israel	1.13E+08	3.13E+09	3.44E+10	2.77E+11
Italy	7.70E+09	3.52E+09	3.00E+11	2.06E+12
Ivory Coast	2.42E+08	2.02E+06	4.04E+09	3.40E+10
Jamaica	4.80E+08	1.39E+08	1.05E+09	1.37E+10
Japan	1.12E+10	3.21E+10	1.27E+12	5.99E+12
Jordan	3.72E+07	1.52E+06	5.74E+09	3.10E+10
Kazakhstan	6.12E+09	1.20E+09	1.94E+10	1.86E+11
Kenya	1.25E+08	1.48E+05	5.38E+09	5.23E+10
Kiribati		0.00E+00	8.13E+06	1.90E+08
Kosovo		0.00E+00	7.75E+08	6.83E+09
Kuwait	2.33E+07	5.22E+09	7.84E+09	1.38E+11
Kyrgyzstan	3.36E+08	1.52E+08	8.30E+08	6.08E+09
Laos	1.70E+08	0.00E+00	1.14E+09	1.04E+10
Latvia	3.50E+07	5.82E+06	3.11E+09	2.85E+10
Lebanon	9.00E+08	2.14E+07	2.93E+09	4.24E+10

Nation	IWW [m³]	TWW [m³]	MVA [\$]	GDP [\$]
Lesotho	2.00E+07	0.00E+00	2.67E+08	2.81E+09
Liberia	5.34E+07	5.58E+05	5.72E+07	2.56E+09
Libya	2.80E+08	2.92E+05		3.79E+10
Liechtenstein		0.00E+00		5.77E+09
Lithuania	1.89E+08	7.98E+08	8.17E+09	4.47E+10
Luxembourg	2.00E+06	9.69E+03	3.02E+09	6.13E+10
Macau		0.00E+00	1.63E+08	3.22E+10
Madagascar	1.62E+08	2.50E+06		1.14E+10
Malawi	4.77E+07	0.00E+00	7.73E+08	8.50E+09
Malaysia	1.64E+09	5.38E+09	7.57E+10	3.30E+11
Maldives	3.00E+05	0.00E+00	7.62E+07	3.41E+09
Mali	4.00E+06	0.00E+00	9.19E+08	1.27E+10
Malta	1.00E+06	4.96E+07	9.82E+08	1.18E+10
Marshall Islands		0.00E+00	3.17E+06	1.64E+08
Martinique	1.70E+06	0.00E+00		
Mauritania	3.18E+07	3.91E+07	5.29E+08	7.01E+09
Mauritius	1.40E+07	7.10E+06	1.55E+09	1.20E+10
Mexico	7.83E+09	3.61E+09	1.90E+11	1.22E+12
Moldova	6.49E+08	4.77E+08	9.82E+08	8.37E+09
Monaco	0.00E+00	0.00E+00		7.15E+09
Mongolia	9.00E+07	1.18E+07	6.77E+08	1.17E+10
Montenegro	6.28E+07	2.93E+06	2.01E+08	4.53E+09
Morocco	2.12E+08	2.97E+08	1.67E+10	1.13E+11
Mozambique	2.50E+07	1.87E+04	1.32E+09	1.57E+10
Myanmar	4.98E+08	1.47E+06	1.56E+10	7.03E+10
Namibia	1.40E+07	7.56E+03	1.44E+09	1.45E+10
Nauru		0.00E+00		9.99E+07
Nepal	2.95E+07	0.00E+00	1.14E+09	1.98E+10

Nation	IWW [m³]	TWW [m³]	MVA [\$]	GDP [\$]
Netherlands	1.48E+10	6.09E+09	9.37E+10	8.79E+11
New Caledonia		0.00E+00		8.09E+09
New Zealand	1.18E+09	2.91E+07	1.69E+10	1.69E+11
Nicaragua	7.36E+07	2.70E+06	1.78E+09	1.14E+10
Niger	3.34E+07	0.00E+00	8.12E+08	1.04E+10
Nigeria	1.97E+09	1.32E+09	4.36E+10	4.62E+11
North Korea	1.15E+09	1.62E+09		1.50E+10
Northern Mariana Islands		0.00E+00		8.16E+08
Norway	1.07E+09	5.91E+08	3.25E+10	4.67E+11
Oman	1.87E+08	3.79E+06	6.65E+09	7.11E+10
Pakistan	1.40E+09	2.71E+08	2.79E+10	2.16E+11
Palau		0.00E+00	2.34E+06	2.23E+08
Palestinian National Authority	2.53E+07	0.00E+00		
Panama	6.40E+06	2.24E+08	2.66E+09	4.27E+10
Papua New Guinea	1.68E+08	0.00E+00	3.18E+08	1.89E+10
Paraguay	1.54E+08	0.00E+00	6.57E+09	3.31E+10
Peru	2.17E+08	6.98E+07	2.60E+10	1.86E+11
Philippines	9.93E+09	5.41E+09	5.93E+10	2.79E+11
Poland	7.46E+09	3.55E+09	9.53E+10	5.55E+11
Portugal	1.79E+09	3.86E+07	2.85E+10	2.28E+11
Puerto Rico	2.37E+09	6.25E+07		9.56E+10
Qatar	1.15E+08	1.07E+09	2.11E+10	1.73E+11
Republic of North Macedonia	1.86E+08	1.80E+07	1.44E+09	1.06E+10
Réunion	8.87E+07	0.00E+00		
Romania	4.17E+09	2.03E+09	4.16E+10	1.91E+11
Russia	2.86E+10	3.88E+10	2.26E+11	1.66E+12
Rwanda	2.05E+07	0.00E+00	5.77E+08	8.69E+09
Saint Kitts and Nevis	0.00E+00	0.00E+00	5.57E+07	8.56E+08

Nation	IWW [m³]	TWW [m³]	MVA [\$]	GDP [\$]
Saint Lucia	0.00E+00	1.12E+06	5.92E+07	1.52E+09
Saint Vincent and the Grenadines	2.00E+03	0.00E+00	3.42E+07	7.18E+08
Samoa		0.00E+00	5.28E+07	6.89E+08
San Marino		0.00E+00		1.62E+09
São Tomé and Príncipe		0.00E+00	1.86E+07	2.46E+08
Saudi Arabia	9.77E+08	3.60E+08	7.96E+10	6.79E+11
Senegal	5.80E+07	1.22E+07	3.21E+09	2.02E+10
Serbia	3.31E+09	2.53E+09	6.83E+09	4.37E+10
Seychelles	3.80E+06	0.00E+00	9.06E+07	1.23E+09
Sierra Leone	5.55E+07	0.00E+00	6.41E+07	3.16E+09
Singapore	3.39E+08	2.35E+09	5.34E+10	2.99E+11
Sint Maarten		2.53E+07		9.81E+08
Slovakia	2.34E+08	1.25E+08	2.27E+10	1.02E+11
Slovenia	7.29E+08	1.43E+08	9.00E+09	4.92E+10
Solomon Islands		0.00E+00		9.99E+08
Somalia	2.00E+06	0.00E+00		1.34E+09
South Africa	3.59E+09	2.16E+09	5.20E+10	4.19E+11
South Korea	4.45E+09	2.86E+10	3.62E+11	1.33E+12
South Sudan	2.25E+08	0.00E+00	2.98E+08	7.83E+09
Spain	6.06E+09	4.04E+09	1.59E+11	1.42E+12
Sri Lanka	8.31E+08	3.50E+08	1.20E+10	7.65E+10
Sudan	7.50E+07	1.34E+07		6.45E+10
Suriname	1.36E+08	0.00E+00	7.71E+08	4.73E+09
Swaziland	2.07E+07	0.00E+00	1.64E+09	5.12E+09
Sweden	1.35E+09	1.13E+10	7.23E+10	5.52E+11
Switzerland	6.43E+08	1.66E+09	1.20E+11	6.34E+11
Syria	6.15E+08	7.71E+07		1.76E+10
Taiwan		1.13E+10		4.92E+11

Nation	IWW [m³]	TWW [m³]	MVA [\$]	GDP [\$]
Tajikistan	9.72E+08	0.00E+00		7.91E+09
Tanzania	2.50E+07	4.31E+06	3.77E+09	4.36E+10
Thailand	2.78E+09	2.95E+08	1.11E+11	3.95E+11
Timor-Leste	2.00E+06	1.07E+04	1.16E+07	1.09E+09
Togo	6.30E+06	4.68E+03	5.89E+08	4.62E+09
Tonga		0.00E+00	2.44E+07	4.09E+08
Trinidad and Tobago	1.29E+08	1.42E+09		2.31E+10
Tunisia	6.98E+08	1.25E+08	7.42E+09	4.82E+10
Turkey	2.33E+09	7.18E+08	1.76E+11	1.09E+12
Turkmenistan	8.39E+08	8.38E+08		3.73E+10
Turks and Caicos Islands		0.00E+00		8.67E+08
Tuvalu		0.00E+00		3.81E+07
Uganda	5.00E+07	2.88E+03	5.79E+09	3.45E+10
Ukraine	4.16E+09	9.53E+09	1.27E+10	1.21E+11
United Arab Emirates	9.59E+07	1.44E+06	2.95E+10	3.73E+11
United Kingdom	9.39E+08	1.11E+10	2.43E+11	2.74E+12
United States	2.10E+11	1.04E+11	1.89E+12	1.67E+13
United States Virgin Islands	1.65E+08	0.00E+00		3.17E+09
Uruguay	8.00E+07	4.84E+08	5.90E+09	4.76E+10
Uzbekistan	1.96E+09	2.31E+09	7.48E+09	6.69E+10
Vanuatu		0.00E+00		7.54E+08
Venezuela	7.93E+08	1.73E+09		3.17E+11
Vietnam	3.07E+09	2.61E+09	2.38E+10	1.55E+11
Yemen	6.50E+07	2.75E+04		2.08E+10
Zambia	1.30E+08	8.19E+03	2.12E+09	2.61E+10
Zimbabwe	8.14E+07	2.09E+07	1.26E+09	1.70E+10

Table A9 Nations included in the offline conceptual model with their corresponding geographic and economic regions (Bijl et al., 2018; The World Bank, 2021k).

Nation	The World Bank (2021k)	Bijl et al. (2018)
Afghanistan	South Asia Low	Rest of South Asia
Albania	East Europe & Central Asia High	Central Europe
Algeria	Middle East & North Africa High	North Africa
American Samoa	East Asia & Pacific High	Oceania
Andorra	West Europe High	West Europe
Angola	Sub-Saharan Africa Low	Rest of Southern Africa
Antigua and Barbuda	Latin America & Caribbean High	Rest of Central America
Argentina	Latin America & Caribbean High	Rest of South America
Armenia	East Europe & Central Asia Low	Russia
Aruba	Latin America & Caribbean High	Rest of Central America
Australia	East Asia & Pacific High	Oceania
Austria	West Europe High	West Europe
Azerbaijan	East Europe & Central Asia High	Russia
Bahamas	Latin America & Caribbean High	Rest of Central America
Bahrain	Middle East & North Africa High	Middle East
Bangladesh	South Asia Low	Rest of South Asia
Barbados	Latin America & Caribbean High	Rest of Central America
Belarus	East Europe & Central Asia High	Ukraine Region
Belgium	West Europe High	West Europe
Belize	Latin America & Caribbean High	Rest of Central America
Benin	Sub-Saharan Africa Low	West Africa
Bermuda	North America High	Rest of Central America
Bhutan	South Asia Low	Rest of South Asia
Bolivia	Latin America & Caribbean Low	Rest of South America
Bosnia and Herzegovina	East Europe & Central Asia High	Central Europe
Botswana	Sub-Saharan Africa High	Rest of Southern Africa

Nation	The World Bank (2021k)	Bijl et al. (2018)
Brazil	Latin America & Caribbean High	Brazil
British Virgin Islands	Latin America & Caribbean High	Rest of Central America
Brunei	East Asia & Pacific High	Oceania
Bulgaria	East Europe & Central Asia High	Central Europe
Burkina Faso	Sub-Saharan Africa Low	West Africa
Burundi	Sub-Saharan Africa Low	East Africa
Cambodia	East Asia & Pacific Low	Southeast Asia
Cameroon	Sub-Saharan Africa Low	West Africa
Canada	North America High	Canada
Cape Verde	Sub-Saharan Africa Low	West Africa
Cayman Islands	Latin America & Caribbean High	Rest of Central America
Central African Republic	Sub-Saharan Africa Low	West Africa
Chad	Sub-Saharan Africa Low	West Africa
Chile	Latin America & Caribbean High	Rest of South America
China	East Asia & Pacific High	China
Colombia	Latin America & Caribbean High	Rest of South America
Comoros	Sub-Saharan Africa Low	Rest of Southern Africa
Congo	Sub-Saharan Africa Low	West Africa
Costa Rica	Latin America & Caribbean High	Rest of Central America
Croatia	East Europe & Central Asia High	Central Europe
Cuba	Latin America & Caribbean High	Rest of Central America
Curaçao	Latin America & Caribbean High	Rest of Central America
Cyprus	East Europe & Central Asia High	West Europe
Czech Republic	East Europe & Central Asia High	Central Europe
Democratic Republic of the Congo	Sub-Saharan Africa Low	West Africa
Denmark	West Europe High	West Europe
Djibouti	Middle East & North Africa Low	East Africa
Dominica	Latin America & Caribbean High	Rest of Central America

Nation	The World Bank (2021k)	Bijl et al. (2018)
Dominican Republic	Latin America & Caribbean High	Rest of Central America
Ecuador	Latin America & Caribbean High	Rest of South America
Egypt	Middle East & North Africa Low	North Africa
El Salvador	Latin America & Caribbean Low	Rest of Central America
Equatorial Guinea	Sub-Saharan Africa High	West Africa
Eritrea	Sub-Saharan Africa Low	East Africa
Estonia	East Europe & Central Asia High	Central Europe
Ethiopia	Sub-Saharan Africa Low	East Africa
Faroe Islands	West Europe High	West Europe
Federated States of Micronesia	East Asia & Pacific Low	Oceania
Fiji	East Asia & Pacific High	Oceania
Finland	West Europe High	West Europe
France	West Europe High	West Europe
French Polynesia	East Asia & Pacific High	Oceania
Gabon	Sub-Saharan Africa High	West Africa
Gambia	Sub-Saharan Africa Low	West Africa
Georgia	East Europe & Central Asia Low	Russia
Germany	West Europe High	West Europe
Ghana	Sub-Saharan Africa Low	West Africa
Gibraltar	West Europe High	West Europe
Greece	West Europe High	West Europe
Greenland	West Europe High	West Europe
Grenada	Latin America & Caribbean High	Rest of Central America
Guadeloupe	Latin America & Caribbean High	Rest of Central America
Guam	East Asia & Pacific High	Oceania
Guatemala	Latin America & Caribbean Low	Rest of Central America
Guinea	Sub-Saharan Africa Low	West Africa
Guinea-Bissau	Sub-Saharan Africa Low	West Africa

Nation	The World Bank (2021k)	Bijl et al. (2018)
Guyana	Latin America & Caribbean High	Rest of South America
Haiti	Latin America & Caribbean Low	Rest of Central America
Honduras	Latin America & Caribbean Low	Rest of Central America
Hong Kong	East Asia & Pacific High	China
Hungary	East Europe & Central Asia High	Central Europe
Iceland	West Europe High	West Europe
India	South Asia Low	India
Indonesia	East Asia & Pacific Low	Indonesia
Iran	Middle East & North Africa High	Middle East
Iraq	Middle East & North Africa High	Middle East
Ireland	West Europe High	West Europe
Isle of Man	West Europe High	West Europe
Israel	Middle East & North Africa High	Middle East
Italy	West Europe High	West Europe
Ivory Coast	Sub-Saharan Africa Low	West Africa
Jamaica	Latin America & Caribbean High	Rest of Central America
Japan	East Asia & Pacific High	Japan
Jordan	Middle East & North Africa Low	Middle East
Kazakhstan	East Europe & Central Asia High	Central Asia
Kenya	Sub-Saharan Africa Low	East Africa
Kiribati	East Asia & Pacific Low	Oceania
Kosovo	East Europe & Central Asia High	Central Europe
Kuwait	Middle East & North Africa High	Middle East
Kyrgyzstan	East Europe & Central Asia Low	Central Asia
Laos	East Asia & Pacific Low	Southeast Asia
Latvia	East Europe & Central Asia High	Central Europe
Lebanon	Middle East & North Africa High	Middle East
Lesotho	Sub-Saharan Africa Low	Rest of Southern Africa

Nation	The World Bank (2021k)	Bijl et al. (2018)
Liberia	Sub-Saharan Africa Low	West Africa
Libya	Middle East & North Africa High	Middle East
Liechtenstein	West Europe High	West Europe
Lithuania	East Europe & Central Asia High	Central Europe
Luxembourg	West Europe High	West Europe
Macau	East Asia & Pacific High	China
Madagascar	Sub-Saharan Africa Low	East Africa
Malawi	Sub-Saharan Africa Low	Rest of Southern Africa
Malaysia	East Asia & Pacific High	Southeast Asia
Maldives	South Asia High	Rest of South Asia
Mali	Sub-Saharan Africa Low	West Africa
Malta	Middle East & North Africa High	West Europe
Marshall Islands	East Asia & Pacific High	Oceania
Martinique	Latin America & Caribbean High	Rest of Central America
Mauritania	Sub-Saharan Africa Low	West Africa
Mauritius	Sub-Saharan Africa High	Rest of Southern Africa
Mexico	Latin America & Caribbean High	Mexico
Moldova	East Europe & Central Asia Low	Central Europe
Monaco	West Europe High	West Europe
Mongolia	East Asia & Pacific Low	China
Montenegro	East Europe & Central Asia High	Central Europe
Morocco	Middle East & North Africa Low	North Africa
Mozambique	Sub-Saharan Africa Low	Rest of Southern Africa
Myanmar	East Asia & Pacific Low	Southeast Asia
Namibia	Sub-Saharan Africa High	Rest of Southern Africa
Nauru	East Asia & Pacific High	Oceania
Nepal	South Asia Low	Rest of South Asia
Netherlands	West Europe High	West Europe

Nation	The World Bank (2021k)	Bijl et al. (2018)
New Caledonia	East Asia & Pacific High	Oceania
New Zealand	East Asia & Pacific High	Oceania
Nicaragua	Latin America & Caribbean Low	Rest of Central America
Niger	Sub-Saharan Africa Low	West Africa
Nigeria	Sub-Saharan Africa Low	West Africa
North Korea	East Asia & Pacific Low	Korea Region
Northern Mariana Islands	East Asia & Pacific High	Oceania
Norway	West Europe High	West Europe
Oman	Middle East & North Africa High	Middle East
Pakistan	South Asia Low	Rest of South Asia
Palau	East Asia & Pacific High	Oceania
Palestinian National Authority	Middle East & North Africa Low	Middle East
Panama	Latin America & Caribbean High	Rest of Central America
Papua New Guinea	East Asia & Pacific Low	Indonesia
Paraguay	Latin America & Caribbean High	Rest of South America
Peru	Latin America & Caribbean High	Rest of South America
Philippines	East Asia & Pacific Low	Southeast Asia
Poland	East Europe & Central Asia High	Central Europe
Portugal	West Europe High	West Europe
Puerto Rico	Latin America & Caribbean High	Rest of Central America
Qatar	Middle East & North Africa High	Middle East
Republic of North Macedonia	East Europe & Central Asia High	Central Europe
Réunion	Sub-Saharan Africa High	Rest of Southern Africa
Romania	East Europe & Central Asia High	Central Europe
Russia	East Europe & Central Asia High	Russia
Rwanda	Sub-Saharan Africa Low	East Africa
Saint Kitts and Nevis	Latin America & Caribbean High	Rest of Central America
Saint Lucia	Latin America & Caribbean High	Rest of Central America

Nation	The World Bank (2021k)	Bijl et al. (2018)
Saint Vincent and the Grenadines	Latin America & Caribbean High	Rest of Central America
Samoa	East Asia & Pacific High	Oceania
San Marino	West Europe High	West Europe
São Tomé and Príncipe	Sub-Saharan Africa Low	West Africa
Saudi Arabia	Middle East & North Africa High	Middle East
Senegal	Sub-Saharan Africa Low	West Africa
Serbia	East Europe & Central Asia High	Central Europe
Seychelles	Sub-Saharan Africa High	Rest of Southern Africa
Sierra Leone	Sub-Saharan Africa Low	West Africa
Singapore	East Asia & Pacific High	Southeast Asia
Sint Maarten	Latin America & Caribbean High	Rest of Central America
Slovakia	East Europe & Central Asia High	Central Europe
Slovenia	East Europe & Central Asia High	Central Europe
Solomon Islands	East Asia & Pacific Low	Oceania
Somalia	Sub-Saharan Africa Low	East Africa
South Africa	Sub-Saharan Africa High	South Africa
South Korea	East Asia & Pacific High	Korea Region
South Sudan	Sub-Saharan Africa Low	East Africa
Spain	West Europe High	West Europe
Sri Lanka	South Asia Low	Rest of South Asia
Sudan	Sub-Saharan Africa Low	East Africa
Suriname	Latin America & Caribbean High	Rest of South America
Swaziland	Sub-Saharan Africa Low	Rest of Southern Africa
Sweden	West Europe High	West Europe
Switzerland	West Europe High	West Europe
Syria	Middle East & North Africa Low	Middle East
Taiwan	East Asia & Pacific High	China
Tajikistan	East Europe & Central Asia Low	Central Asia

Nation	The World Bank (2021k)	Bijl et al. (2018)
Tanzania	Sub-Saharan Africa Low	Rest of Southern Africa
Thailand	East Asia & Pacific High	Southeast Asia
Timor-Leste	East Asia & Pacific Low	Oceania
Togo	Sub-Saharan Africa Low	West Africa
Tonga	East Asia & Pacific High	Oceania
Trinidad and Tobago	Latin America & Caribbean High	Rest of Central America
Tunisia	Middle East & North Africa Low	North Africa
Turkey	East Europe & Central Asia High	Turkey
Turkmenistan	East Europe & Central Asia High	Central Asia
Turks and Caicos Islands	Latin America & Caribbean High	Rest of Central America
Tuvalu	East Asia & Pacific High	Oceania
Uganda	Sub-Saharan Africa Low	East Africa
Ukraine	East Europe & Central Asia Low	Ukraine Region
United Arab Emirates	Middle East & North Africa High	Middle East
United Kingdom	West Europe High	West Europe
United States	North America High	USA
United States Virgin Islands	Latin America & Caribbean High	Rest of Central America
Uruguay	Latin America & Caribbean High	Rest of South America
Uzbekistan	East Europe & Central Asia Low	Central Asia
Vanuatu	East Asia & Pacific Low	Oceania
Venezuela	Latin America & Caribbean High	Rest of South America
Vietnam	East Asia & Pacific Low	Southeast Asia
Yemen	Middle East & North Africa Low	Middle East
Zambia	Sub-Saharan Africa Low	Rest of Southern Africa
Zimbabwe	Sub-Saharan Africa Low	Rest of Southern Africa

Table A10 Output table of manufacturing water withdrawal estimates for the reference year 2015, including the updated industrial water withdrawals and percentage contributions of industrial water withdrawals coming from the manufacturing (M) and thermoelectric (TE) sub-sectors.

Nation	MWW [m³]	Updated IWW [m³]	M %	TE %
Afghanistan	1.69E+08	1.70E+08	100%	0%
Albania	1.29E+08	1.30E+08	99%	1%
Algeria	1.14E+08	1.22E+08	93%	7%
American Samoa	3.35E+06	3.35E+06	100%	0%
Andorra	1.79E+07	1.79E+07	100%	0%
Angola	1.69E+08	2.40E+08	71%	29%
Antigua and Barbuda	2.50E+06	2.50E+06	100%	0%
Argentina	1.13E+09	4.00E+09	28%	72%
Armenia	8.93E+07	1.09E+08	82%	18%
Aruba	2.37E+07	2.37E+07	100%	0%
Australia	2.91E+08	2.77E+09	11%	89%
Austria	1.77E+09	2.70E+09	66%	34%
Azerbaijan	2.35E+09	2.97E+09	79%	21%
Bahamas	1.51E+07	1.12E+08	13%	87%
Bahrain	3.07E+08	8.59E+08	36%	64%
Bangladesh	1.11E+09	2.62E+09	42%	58%
Barbados	2.07E+06	6.20E+06	33%	67%
Belarus	1.75E+09	3.45E+09	51%	49%
Belgium	2.97E+09	3.21E+09	93%	7%
Belize	2.12E+07	2.12E+07	100%	0%
Benin	3.00E+07	3.00E+07	100%	0%
Bermuda	1.10E+06	1.10E+06	100%	0%
Bhutan	3.00E+06	3.00E+06	100%	0%
Bolivia	2.87E+07	3.20E+07	90%	10%
Bosnia and Herzegovina	3.62E+07	5.99E+07	60%	40%
Botswana	2.14E+07	3.11E+07	69%	31%

Nation	MWW [m³]	Updated IWW [m³]	M %	TE %
Brazil	9.18E+09	1.29E+10	71%	29%
British Virgin Islands	9.50E+06	9.50E+06	100%	0%
Brunei	5.80E+07	7.19E+07	81%	19%
Bulgaria	1.07E+09	3.90E+09	27%	73%
Burkina Faso	2.17E+07	2.17E+07	100%	0%
Burundi	1.50E+07	1.50E+07	100%	0%
Cambodia	4.09E+08	4.94E+08	83%	17%
Cameroon	1.05E+08	1.05E+08	100%	0%
Canada	5.29E+09	2.81E+10	19%	81%
Cape Verde	4.00E+05	4.00E+05	100%	0%
Cayman Islands	2.59E+06	2.48E+07	10%	90%
Central African Republic	1.20E+07	1.20E+07	100%	0%
Chad	1.04E+08	1.04E+08	100%	0%
Chile	1.99E+09	4.79E+09	42%	58%
China	7.92E+10	1.34E+11	59%	41%
Colombia	2.84E+09	3.78E+09	75%	25%
Comoros	5.00E+05	5.00E+05	100%	0%
Congo	2.40E+07	2.40E+07	100%	0%
Costa Rica	1.81E+08	2.40E+08	75%	25%
Croatia	1.02E+09	1.27E+09	80%	20%
Cuba	8.34E+08	2.61E+09	32%	68%
Curaçao	2.55E+07	2.55E+07	100%	0%
Cyprus	1.27E+08	2.53E+08	50%	50%
Czech Republic	7.00E+08	9.36E+08	75%	25%
Democratic Republic of the Congo	1.44E+08	1.47E+08	98%	2%
Denmark	1.47E+09	2.53E+09	58%	42%
Djibouti	1.44E+07	1.69E+07	85%	15%
Dominica	7.54E+05	7.54E+05	100%	0%

Nation	MWW [m³]	Updated IWW [m³]	M %	TE %
Dominican Republic	1.38E+08	6.60E+08	21%	79%
Ecuador	1.22E+08	5.49E+08	22%	78%
Egypt	1.62E+09	1.30E+10	13%	87%
El Salvador	2.13E+08	2.13E+08	100%	0%
Equatorial Guinea	3.00E+06	3.00E+06	100%	0%
Eritrea	2.20E+07	3.94E+07	56%	44%
Estonia	1.86E+08	1.52E+09	12%	88%
Ethiopia	5.11E+07	5.11E+07	100%	0%
Faroe Islands	1.26E+07	1.26E+07	100%	0%
Federated States of Micronesia	1.83E+05	1.83E+05	100%	0%
Fiji	9.60E+06	9.60E+06	100%	0%
Finland	1.36E+09	7.69E+09	18%	82%
France	7.82E+09	1.97E+10	40%	60%
French Polynesia	2.98E+07	2.98E+07	100%	0%
Gabon	5.15E+07	7.95E+07	65%	35%
Gambia	2.12E+07	2.12E+07	100%	0%
Georgia	2.58E+08	2.68E+08	96%	4%
Germany	1.50E+10	1.81E+10	83%	17%
Ghana	7.34E+07	9.50E+07	77%	23%
Gibraltar	1.39E+07	1.39E+07	100%	0%
Greece	6.38E+08	1.22E+09	52%	48%
Greenland	7.21E+06	7.21E+06	100%	0%
Grenada	2.04E+06	2.04E+06	100%	0%
Guadeloupe	9.31E+05	9.31E+05	100%	0%
Guam	3.17E+07	2.95E+08	11%	89%
Guatemala	5.92E+08	6.03E+08	98%	2%
Guinea	5.91E+07	5.91E+07	100%	0%
Guinea-Bissau	1.19E+07	1.19E+07	100%	0%

Nation	MWW [m³]	Updated IWW [m³]	M %	TE %
Guyana	2.04E+07	2.04E+07	100%	0%
Haiti	5.10E+07	5.10E+07	100%	0%
Honduras	1.03E+08	1.14E+08	91%	9%
Hong Kong	1.11E+08	4.63E+09	2%	98%
Hungary	2.86E+09	3.16E+09	91%	9%
Iceland	1.98E+08	1.98E+08	100%	0%
India	8.70E+09	1.70E+10	51%	49%
Indonesia	3.32E+10	4.62E+10	72%	28%
Iran	4.19E+09	5.48E+09	76%	24%
Iraq	1.15E+08	2.65E+09	4%	96%
Ireland	3.27E+09	3.73E+09	88%	12%
Isle of Man	3.84E+07	3.87E+07	99%	1%
Israel	2.34E+09	5.47E+09	43%	57%
Italy	4.18E+09	7.70E+09	54%	46%
Ivory Coast	2.40E+08	2.42E+08	99%	1%
Jamaica	3.41E+08	4.80E+08	71%	29%
Japan	3.67E+10	6.88E+10	53%	47%
Jordan	3.57E+07	3.72E+07	96%	4%
Kazakhstan	4.92E+09	6.12E+09	80%	20%
Kenya	1.25E+08	1.25E+08	100%	0%
Kiribati	1.27E+06	1.27E+06	100%	0%
Kosovo	1.00E+08	1.00E+08	100%	0%
Kuwait	5.34E+08	5.76E+09	9%	91%
Kyrgyzstan	1.84E+08	3.36E+08	55%	45%
Laos	1.70E+08	1.70E+08	100%	0%
Latvia	2.92E+07	3.50E+07	83%	17%
Lebanon	8.79E+08	9.00E+08	98%	2%
Lesotho	2.00E+07	2.00E+07	100%	0%

Nation	MWW [m³]	Updated IWW [m³]	M %	TE %
Liberia	5.28E+07	5.34E+07	99%	1%
Libya	2.80E+08	2.80E+08	100%	0%
Liechtenstein	3.14E+07	3.14E+07	100%	0%
Lithuania	1.06E+09	1.86E+09	57%	43%
Luxembourg	1.99E+06	2.00E+06	100%	0%
Macau	4.71E+06	4.71E+06	100%	0%
Madagascar	1.59E+08	1.62E+08	98%	2%
Malawi	4.77E+07	4.77E+07	100%	0%
Malaysia	2.19E+09	7.57E+09	29%	71%
Maldives	3.00E+05	3.00E+05	100%	0%
Mali	4.00E+06	4.00E+06	100%	0%
Malta	6.68E+07	1.16E+08	57%	43%
Marshall Islands	9.16E+04	9.16E+04	100%	0%
Martinique	1.70E+06	1.70E+06	100%	0%
Mauritania	6.79E+07	1.07E+08	63%	37%
Mauritius	6.90E+06	1.40E+07	49%	51%
Mexico	4.21E+09	7.83E+09	54%	46%
Moldova	1.72E+08	6.49E+08	27%	73%
Monaco	3.89E+07	3.89E+07	100%	0%
Mongolia	7.82E+07	9.00E+07	87%	13%
Montenegro	5.99E+07	6.28E+07	95%	5%
Morocco	6.97E+08	9.94E+08	70%	30%
Mozambique	2.50E+07	2.50E+07	100%	0%
Myanmar	4.97E+08	4.98E+08	100%	0%
Namibia	1.40E+07	1.40E+07	100%	0%
Nauru	6.08E+05	6.08E+05	100%	0%
Nepal	2.95E+07	2.95E+07	100%	0%
Netherlands	8.67E+09	1.48E+10	59%	41%

Nation	MWW [m³]	Updated IWW [m³]	M %	TE %
New Caledonia	4.93E+07	4.93E+07	100%	0%
New Zealand	1.15E+09	1.18E+09	98%	2%
Nicaragua	7.09E+07	7.36E+07	96%	4%
Niger	3.34E+07	3.34E+07	100%	0%
Nigeria	6.43E+08	1.97E+09	33%	67%
North Korea	5.05E+08	2.12E+09	24%	76%
Northern Mariana Islands	4.97E+06	4.97E+06	100%	0%
Norway	4.80E+08	1.07E+09	45%	55%
Oman	1.83E+08	1.87E+08	98%	2%
Pakistan	1.13E+09	1.40E+09	81%	19%
Palau	6.76E+04	6.76E+04	100%	0%
Palestinian National Authority	2.53E+07	2.53E+07	100%	0%
Panama	1.98E+08	4.22E+08	47%	53%
Papua New Guinea	1.68E+08	1.68E+08	100%	0%
Paraguay	1.54E+08	1.54E+08	100%	0%
Peru	1.47E+08	2.17E+08	68%	32%
Philippines	4.52E+09	9.93E+09	45%	55%
Poland	3.92E+09	7.46E+09	52%	48%
Portugal	1.76E+09	1.79E+09	98%	2%
Puerto Rico	2.30E+09	2.37E+09	97%	3%
Qatar	1.44E+09	2.51E+09	57%	43%
Republic of North Macedonia	1.68E+08	1.86E+08	90%	10%
Réunion	8.87E+07	8.87E+07	100%	0%
Romania	2.14E+09	4.17E+09	51%	49%
Russia	2.93E+10	6.81E+10	43%	57%
Rwanda	2.05E+07	2.05E+07	100%	0%
Saint Kitts and Nevis	4.16E+06	4.16E+06	100%	0%
Saint Lucia	4.42E+06	5.54E+06	80%	20%

Nation	MWW [m³]	Updated IWW [m³]	M %	TE %
Saint Vincent and the Grenadines	2.00E+03	2.00E+03	100%	0%
Samoa	1.53E+06	1.53E+06	100%	0%
San Marino	8.80E+06	8.80E+06	100%	0%
São Tomé and Príncipe	2.38E+06	2.38E+06	100%	0%
Saudi Arabia	6.17E+08	9.77E+08	63%	37%
Senegal	4.58E+07	5.80E+07	79%	21%
Serbia	7.76E+08	3.31E+09	23%	77%
Seychelles	3.80E+06	3.80E+06	100%	0%
Sierra Leone	5.55E+07	5.55E+07	100%	0%
Singapore	1.54E+09	3.89E+09	40%	60%
Sint Maarten	8.63E+06	3.39E+07	25%	75%
Slovakia	1.08E+08	2.34E+08	46%	54%
Slovenia	5.86E+08	7.29E+08	80%	20%
Solomon Islands	3.37E+07	3.37E+07	100%	0%
Somalia	2.00E+06	2.00E+06	100%	0%
South Africa	1.43E+09	3.59E+09	40%	60%
South Korea	1.05E+10	3.91E+10	27%	73%
South Sudan	2.25E+08	2.25E+08	100%	0%
Spain	2.02E+09	6.06E+09	33%	67%
Sri Lanka	4.81E+08	8.31E+08	58%	42%
Sudan	6.16E+07	7.50E+07	82%	18%
Suriname	1.36E+08	1.36E+08	100%	0%
Swaziland	2.07E+07	2.07E+07	100%	0%
Sweden	2.62E+09	1.39E+10	19%	81%
Switzerland	4.38E+09	6.03E+09	73%	27%
Syria	5.38E+08	6.15E+08	87%	13%
Taiwan	3.00E+09	1.43E+10	21%	79%
Tajikistan	9.72E+08	9.72E+08	100%	0%

Nation	MWW [m³]	Updated IWW [m³]	M %	TE %
Tanzania	2.07E+07	2.50E+07	83%	17%
Thailand	2.48E+09	2.78E+09	89%	11%
Timor-Leste	1.99E+06	2.00E+06	99%	1%
Togo	6.30E+06	6.30E+06	100%	0%
Tonga	7.05E+05	7.05E+05	100%	0%
Trinidad and Tobago	2.03E+08	1.62E+09	13%	87%
Tunisia	5.73E+08	6.98E+08	82%	18%
Turkey	1.61E+09	2.33E+09	69%	31%
Turkmenistan	6.20E+05	8.39E+08	0%	100%
Turks and Caicos Islands	7.63E+06	7.63E+06	100%	0%
Tuvalu	2.32E+05	2.32E+05	100%	0%
Uganda	5.00E+07	5.00E+07	100%	0%
Ukraine	2.45E+09	1.20E+10	20%	80%
United Arab Emirates	9.45E+07	9.59E+07	99%	1%
United Kingdom	8.83E+09	1.99E+10	44%	56%
United States	1.06E+11	2.10E+11	50%	50%
United States Virgin Islands	1.65E+08	1.65E+08	100%	0%
Uruguay	4.41E+08	9.25E+08	48%	52%
Uzbekistan	1.45E+09	3.75E+09	39%	61%
Vanuatu	2.54E+07	2.54E+07	100%	0%
Venezuela	2.79E+09	4.52E+09	62%	38%
Vietnam	4.65E+08	3.07E+09	15%	85%
Yemen	6.50E+07	6.50E+07	100%	0%
Zambia	1.30E+08	1.30E+08	100%	0%
Zimbabwe	6.05E+07	8.14E+07	74%	26%

Table A11 Comparison of the observed and modelled manufacturing water withdrawals between 2009 and 2018 for several nations in Europe (Eurostat, 2021).

Nation	Year	Observed MWW [m³]	Modelled MWW [m³]	Percent estimated
Albania	2017	6.20E+06	1.30E+08	2092%
Albania	2018	5.24E+06	1.30E+08	2480%
Belgium	2009	1.22E+09	3.02E+09	248%
Belgium	2012	1.26E+09	2.99E+09	237%
Belgium	2013	1.16E+09	2.99E+09	257%
Belgium	2014	1.17E+09	2.98E+09	255%
Belgium	2015	1.09E+09	2.97E+09	274%
Bulgaria	2009	2.39E+08	1.06E+09	441%
Bulgaria	2010	2.20E+08	1.06E+09	481%
Bulgaria	2011	2.10E+08	1.06E+09	504%
Bulgaria	2012	2.10E+08	1.06E+09	505%
Bulgaria	2013	1.94E+08	1.06E+09	548%
Bulgaria	2014	1.99E+08	1.07E+09	536%
Bulgaria	2015	2.18E+08	1.07E+09	490%
Bulgaria	2016	2.14E+08	1.07E+09	499%
Bulgaria	2017	2.43E+08	1.07E+09	441%
Bulgaria	2018	2.25E+08	1.07E+09	477%
Croatia	2009	1.78E+08	1.01E+09	567%
Croatia	2010	1.72E+08	1.01E+09	588%
Croatia	2011	1.84E+08	1.01E+09	550%
Croatia	2012	1.81E+08	1.01E+09	561%
Croatia	2013	1.78E+08	1.02E+09	570%
Croatia	2014	1.79E+08	1.02E+09	569%
Croatia	2015	1.77E+08	1.02E+09	577%
Croatia	2016	1.72E+08	1.02E+09	593%
Croatia	2017	1.70E+08	1.02E+09	602%

Nation	Year	Observed MWW [m³]	Modelled MWW [m³]	Percent estimated
Croatia	2018	1.72E+08	1.03E+09	595%
Cyprus	2009	5.60E+06	1.29E+08	2304%
Cyprus	2010	5.30E+06	1.29E+08	2428%
Cyprus	2011	4.70E+06	1.28E+08	2732%
Cyprus	2012	3.50E+06	1.28E+08	3659%
Cyprus	2013	3.25E+06	1.28E+08	3930%
Cyprus	2014	3.06E+06	1.27E+08	4164%
Cyprus	2015	3.16E+06	1.27E+08	4023%
Cyprus	2016	2.60E+06	1.27E+08	4869%
Cyprus	2017	3.43E+06	1.26E+08	3687%
Denmark	2010	6.05E+07	1.48E+09	2453%
Denmark	2011	5.84E+07	1.48E+09	2533%
Denmark	2012	5.62E+07	1.48E+09	2626%
Denmark	2013	5.48E+07	1.47E+09	2689%
Denmark	2014	6.10E+07	1.47E+09	2407%
Denmark	2015	6.07E+07	1.47E+09	2413%
Denmark	2016	6.28E+07	1.46E+09	2327%
Denmark	2017	5.87E+07	1.46E+09	2483%
Denmark	2018	6.45E+07	1.45E+09	2256%
Estonia	2010	2.80E+07	1.84E+08	659%
Estonia	2011	2.88E+07	1.85E+08	642%
Estonia	2012	3.41E+07	1.85E+08	543%
Estonia	2013	2.78E+07	1.85E+08	667%
Estonia	2014	2.58E+07	1.86E+08	719%
Estonia	2015	3.59E+07	1.86E+08	519%
Estonia	2016	2.75E+07	1.86E+08	679%
Estonia	2017	2.89E+07	1.87E+08	646%
Germany	2010	4.66E+09	1.52E+10	327%

Nation	Year	Observed MWW [m³]	Modelled MWW [m³]	Percent estimated
Germany	2011	4.94E+09	1.52E+10	307%
Germany	2012	4.70E+09	1.51E+10	322%
Germany	2013	4.36E+09	1.51E+10	346%
Germany	2014	4.43E+09	1.51E+10	340%
Germany	2015	4.42E+09	1.50E+10	340%
Germany	2016	4.43E+09	1.50E+10	338%
Greece	2011	1.89E+08	6.45E+08	340%
Greece	2012	1.89E+08	6.43E+08	339%
Greece	2013	1.89E+08	6.42E+08	339%
Greece	2014	1.89E+08	6.40E+08	338%
Greece	2015	1.89E+08	6.38E+08	337%
Greece	2016	1.85E+08	6.37E+08	343%
Greece	2017	1.85E+08	6.35E+08	343%
Greece	2018	1.85E+08	6.34E+08	342%
Italy	2012	5.25E+09	4.21E+09	80%
Italy	2015	3.74E+09	4.18E+09	112%
Latvia	2009	1.95E+07	2.89E+07	148%
Latvia	2010	1.95E+07	2.89E+07	148%
Latvia	2011	1.93E+07	2.90E+07	150%
Latvia	2012	1.89E+07	2.90E+07	153%
Latvia	2013	1.84E+07	2.91E+07	158%
Latvia	2014	1.54E+07	2.91E+07	190%
Latvia	2015	1.44E+07	2.92E+07	203%
Latvia	2016	1.45E+07	2.92E+07	201%
Latvia	2017	1.40E+07	2.93E+07	209%
Latvia	2018	1.02E+07	2.93E+07	288%
Lithuania	2009	3.36E+07	1.05E+09	3118%
Lithuania	2010	3.43E+07	1.05E+09	3062%

Nation	Year	Observed MWW [m³]	Modelled MWW [m³]	Percent estimated
Lithuania	2011	3.85E+07	1.05E+09	2728%
Lithuania	2012	4.22E+07	1.05E+09	2499%
Lithuania	2013	4.12E+07	1.06E+09	2565%
Lithuania	2014	3.98E+07	1.06E+09	2655%
Lithuania	2015	4.03E+07	1.06E+09	2627%
Lithuania	2016	3.97E+07	1.06E+09	2675%
Lithuania	2017	4.19E+07	1.06E+09	2539%
Lithuania	2018	4.17E+07	1.07E+09	2552%
Luxembourg	2015	1.90E+06	1.99E+06	105%
Malta	2009	2.88E+06	6.78E+07	2354%
Malta	2010	2.86E+06	6.76E+07	2365%
Malta	2011	2.88E+06	6.75E+07	2342%
Malta	2012	2.83E+06	6.73E+07	2378%
Malta	2013	2.73E+06	6.71E+07	2459%
Malta	2014	2.96E+06	6.70E+07	2262%
Malta	2015	3.01E+06	6.68E+07	2219%
Malta	2016	3.26E+06	6.66E+07	2044%
Malta	2017	3.58E+06	6.65E+07	1856%
Malta	2018	3.52E+06	6.63E+07	1883%
Netherlands	2009	4.05E+09	8.80E+09	217%
Netherlands	2010	3.71E+09	8.78E+09	237%
Netherlands	2011	3.75E+09	8.76E+09	234%
Netherlands	2012	3.78E+09	8.73E+09	231%
Netherlands	2013	3.66E+09	8.71E+09	238%
Netherlands	2014	3.35E+09	8.69E+09	259%
Netherlands	2015	3.04E+09	8.67E+09	285%
Netherlands	2016	3.35E+09	8.65E+09	258%
Netherlands	2017	3.35E+09	8.63E+09	258%

Nation	Year	Observed MWW [m³]	Modelled MWW [m³]	Percent estimated
Netherlands	2018	3.31E+09	8.60E+09	260%
Norway	2009	1.03E+09	4.88E+08	47%
Poland	2009	5.86E+08	3.87E+09	662%
Poland	2010	6.28E+08	3.88E+09	618%
Poland	2011	6.65E+08	3.89E+09	584%
Poland	2012	6.52E+08	3.90E+09	597%
Poland	2013	6.40E+08	3.90E+09	610%
Poland	2014	6.56E+08	3.91E+09	596%
Poland	2015	6.59E+08	3.92E+09	594%
Poland	2016	6.72E+08	3.92E+09	584%
Poland	2017	6.82E+08	3.93E+09	577%
Poland	2018	6.66E+08	3.94E+09	591%
Portugal	2009	2.98E+08	1.78E+09	599%
North Macedonia	2017	2.48E+06	1.69E+08	6800%
Serbia	2009	1.38E+08	7.67E+08	556%
Serbia	2010	1.32E+08	7.68E+08	581%
Serbia	2011	1.44E+08	7.70E+08	535%
Serbia	2012	1.23E+08	7.71E+08	630%
Serbia	2013	1.12E+08	7.73E+08	691%
Serbia	2014	1.08E+08	7.74E+08	718%
Serbia	2015	1.21E+08	7.76E+08	641%
Serbia	2016	1.19E+08	7.77E+08	656%
Serbia	2017	1.43E+08	7.78E+08	544%
Serbia	2018	9.15E+07	7.80E+08	852%
Slovenia	2012	4.90E+07	5.83E+08	1189%
Slovenia	2013	5.20E+07	5.84E+08	1122%
Slovenia	2014	5.21E+07	5.85E+08	1122%
Slovenia	2015	5.01E+07	5.86E+08	1169%

Nation	Year	Observed MWW [m³]	Modelled MWW [m³]	Percent estimated
Slovenia	2016	4.97E+07	5.87E+08	1181%
Slovenia	2017	5.13E+07	5.88E+08	1146%
Slovenia	2018	5.01E+07	5.89E+08	1177%
Spain	2009	1.04E+09	2.05E+09	196%
Spain	2010	1.07E+09	2.04E+09	190%
Spain	2011	1.03E+09	2.04E+09	197%
Spain	2012	1.03E+09	2.03E+09	197%
Spain	2013	1.01E+09	2.03E+09	200%
Spain	2014	1.03E+09	2.02E+09	196%
Spain	2015	9.42E+08	2.02E+09	214%
Spain	2016	9.49E+08	2.01E+09	212%
Sweden	2010	2.18E+09	2.66E+09	122%
Sweden	2015	1.78E+09	2.62E+09	147%
Switzerland	2012	6.69E+08	4.41E+09	659%
Turkey	2010	1.69E+09	1.53E+09	90%
Turkey	2012	1.86E+09	1.56E+09	84%
Turkey	2014	2.40E+09	1.59E+09	66%
Turkey	2016	2.52E+09	1.63E+09	65%
Turkey	2018	3.11E+09	1.66E+09	53%

Table A12 Percent change between the observed (FAO AQUASTAT, 2021) and estimated national industrial water withdrawals from the conceptual model.

Nation	1982	1987	1992	1997	2002	2007	2012
Afghanistan			329%	108%	30%	40%	30%
Albania			-27%	-51%	-60%	-60%	-60%
Algeria	1098%	265%	45%	51%	63%	106%	136%
Angola		475%	183%	92%	47%	32%	38%
Antigua and Barbuda			69%	44%	27%	8%	-10%
Argentina				80%	43%	43%	90%
Armenia				202%	291%	126%	24%
Australia					499%	528%	574%
Austria	7%	7%	3%	3%	4%	7%	4%
Azerbaijan			-27%	6%	5%	-2%	-4%
Bangladesh		327%	147%	89%	51%	31%	30%
Barbados				201%	203%	198%	243%
Belarus				490%	598%	653%	679%
Belgium	-66%	-65%	-65%	-62%	-56%	-45%	-31%
Belize			102%	5%	-16%	-13%	-10%
Benin		-22%	-32%	-38%	-40%	-33%	-25%
Bhutan		-49%	-48%	-47%	-46%	-43%	-37%
Bolivia		-35%	-25%	-13%	3%	25%	38%
Bosnia and Herzegovina					98%	4%	-43%
Botswana			658%	473%	379%	377%	384%
Brazil				96%	97%	79%	55%
Bulgaria			-77%	-74%	-77%	-76%	-70%
Burkina Faso				132%	-33%	-46%	-47%
Burundi			-21%	-54%	-56%	-44%	-35%
Cambodia		3585%	1499%	951%	703%	590%	622%
Cameroon		-24%	-17%	-2%	-8%	-21%	-14%

Nation	1982	1987	1992	1997	2002	2007	2012
Canada			-63%	-62%	-65%	-69%	-67%
CAR		11103%	6605%	4688%	3848%	3748%	3756%
Chad		945%	28%	-25%	-39%	-38%	-31%
Chile	27%	2%	-10%	-12%	-33%	-55%	-54%
China	23%	22%	-33%	-48%	-53%	-59%	-58%
Colombia					738%	252%	140%
Comoros					-43%	-36%	-27%
Congo		1143%	1184%	1228%	1278%	481%	490%
Costa Rica							162%
Croatia					1929%	949%	767%
Cuba	33%	-2%	-12%	-20%	-19%	-18%	-11%
Cyprus		137573%	55619%	45900%	30547%	25313%	48465%
Czech Republic				92%	129%	176%	223%
DRC			-1%	-24%	-34%	-34%	-27%
Denmark	586%	235%	429%	698%	1568%	2319%	690%
Dominican Republic					168%	19%	-21%
Ecuador					-40%	-50%	-49%
Egypt				-75%	-69%	-56%	-1%
El Salvador			11%	-16%	-23%	-13%	-10%
Equatorial Guinea		-4%	-23%	-33%	-38%	-37%	-30%
Eritrea					-54%	1499%	1672%
Estonia			-93%	-87%	-88%	-89%	-89%
Ethiopia					11%	-46%	-37%
Fiji		-92%	-95%	-5%	-21%	-25%	-8%
Finland			16%	13%	124%	148%	180%
France		-59%	-56%	-39%	-40%	-38%	-32%
Gabon		72%	101%	138%	151%	147%	176%
Gambia	1991%	82%	6%	-20%	-32%	-32%	-25%

Nation	1982	1987	1992	1997	2002	2007	2012
Georgia			-59%	-31%	-14%	-42%	-42%
Germany				-47%	-40%	-28%	-8%
Ghana	-14%	-20%	-25%	-28%	692%	697%	706%
Greece	890%	568%	454%	493%	492%	427%	1342%
Guatemala			118%	31%	-5%	-17%	-15%
Guinea		18%	-14%	-29%	-33%	-29%	-21%
Guinea-Bissau			179%	-19%	-25%	-33%	-25%
Guyana			117%	77%	15%	-17%	-14%
Haiti			345%	114%	-10%	-42%	-47%
Honduras			11%	-7%	-18%	-18%	-15%
Hungary	-9%	-27%	-44%	-36%	-27%	-31%	-22%
Iceland	2079%	1705%	2030%	1580%	1386%	114%	1%
India	-4%	-8%	-17%	3%	4%	-15%	-22%
Indonesia			963%	289%	56%	13%	86%
Iran				229%	204%	191%	180%
Iraq	64%	-57%	-89%	-94%	-95%	-92%	-85%
Ireland	528%	515%	527%	669%	1372%	6505%	6790%
Israel	561%	696%	1114%	530%	594%	454%	556%
Italy	-39%	-20%	-18%	-29%	-30%	-17%	20%
Ivory Coast		36%	-40%	-52%	-49%	-45%	-29%
Jamaica				396%	488%	60%	-51%
Japan	198%	201%	199%	211%	263%	242%	270%
Jordan	12%	-14%	-21%	-29%	-33%	-50%	-27%
Kazakhstan				-37%	-26%	-39%	-45%
Kenya			-26%	-23%	-17%	-20%	-16%
Kyrgyzstan				-68%	-69%	-70%	-69%
Laos		5%	-9%	-18%	-24%	-22%	-17%
Latvia						-35%	-50%

Nation	1982	1987	1992	1997	2002	2007	2012
Lebanon	881%	1255%	1504%	613%	368%	46%	-13%
Lesotho		-40%	-48%	-53%	-52%	-46%	-39%
Liberia		39%	-9%	-28%	-35%	-32%	-25%
Libya			1139%	796%	614%	426%	238%
Lithuania				-71%	-56%	-27%	99%
Luxembourg				-63%	-53%	-12%	41%
Madagascar		111%	-9%	-35%	-44%	-42%	-33%
Malawi		-34%	-32%	-34%	-38%	-37%	-29%
Malaysia			75%	38%	43%	49%	96%
Mali		-92%	-88%	-83%	-73%	-54%	-49%
Malta				8130%	584%	323%	113%
Mauritania	-87%	-85%	-83%	-80%	-79%	-80%	-77%
Mexico					-35%	-27%	-28%
Moldova			-84%	-85%	-84%	-81%	-78%
Mongolia				-86%	-89%	-87%	-82%
Montenegro						-8%	0%
Morocco			16%	18%	-44%	6%	129%
Mozambique			432%	282%	190%	153%	209%
Myanmar		75%	9%	-12%	-34%	-45%	-42%
Namibia			-80%	-84%	-84%	-82%	-80%
Nepal				-53%	-63%	-49%	-44%
Netherlands			0%	12%	-22%	-34%	-34%
New Zealand		541%	430%	351%	198%	33%	13%
Nicaragua					87%	54%	57%
Niger			-46%	-59%	-64%	-56%	-10%
Nigeria		79%	8%	-21%	-37%	-42%	-40%
North Korea		-84%	-80%	-72%	-65%	-66%	-65%
Norway				-42%	-47%	-59%	-54%

Nation	1982	1987	1992	1997	2002	2007	2012
Oman			24%	-9%	3%	-66%	-83%
Pakistan	-95%	-95%	-95%	-96%	-94%	-89%	-85%
Palestine					-8%	-37%	-31%
Panama					10110%	10949%	18530%
Papua New Guinea		252%	47%	1%	-23%	-31%	-23%
Paraguay		285%	256%	231%	89%	-4%	-10%
Peru							-50%
Philippines				16%	-28%	-53%	-60%
Poland			19%	27%	43%	47%	104%
Portugal			48%	236%	224%	222%	203%
Puerto Rico			-87%	-86%	-88%	-82%	-79%
Qatar				-53%	-56%	-55%	-74%
North Macedonia				-17%	38%	4%	70%
Romania	-74%	-73%	-71%	-46%	-37%	-6%	-7%
Russia				17%	34%	43%	47%
Rwanda		-50%	-41%	-31%	-37%	-44%	-34%
Saudi Arabia			-88%	-91%	-95%	-97%	-98%
Senegal		-34%	-40%	-44%	-39%	-25%	-20%
Sierra Leone		62%	-2%	-25%	-34%	-32%	-25%
Singapore	-18%	-42%	-54%	-61%	-66%	-63%	-31%
Slovakia				-88%	-85%	-66%	-67%
Slovenia					-4%	-11%	-11%
Somalia					-61%	-69%	-64%
South Africa			8%	45%	54%	26%	13%
South Korea			343%	225%	146%	150%	155%
South Sudan							-35%
Spain		-57%	-9%	-9%	-6%	12%	16%
Sri Lanka			46%	-4%	-33%	-44%	-40%

Nation	1982	1987	1992	1997	2002	2007	2012
Sudan							-24%
Suriname		361%	395%	433%	93%	-14%	-11%
Swaziland	-64%	-57%	-48%	-37%	-42%	-51%	-44%
Sweden	11%	49%	62%	89%	90%	87%	91%
Switzerland							591%
Syria				-29%	-5%	-11%	5%
Tajikistan				-6%	1%	30%	33%
Thailand	5%	1%	57%	107%	78%	56%	90%
Timor-Leste					-39%	-3%	-2%
Togo		-77%	-67%	-48%	-4%	-32%	-6%
Trinidad and Tobago				367%	261%	176%	425%
Tunisia			1302%	1140%	1038%	1042%	473%
Turkey			-19%	33%	-10%	218%	211%
Turkmenistan				-88%	-91%	-97%	-97%
Uganda	-32%	-39%	-43%	-45%	-28%	-21%	-13%
Ukraine			-80%	-75%	-66%	-57%	-33%
UAE	-98%	-99%	-99%	-99%	-98%	-98%	-98%
United Kingdom					71%	932%	1134%
United States			-39%	-39%	-40%	-37%	-22%
Uruguay	267%	223%	191%	167%	159%	168%	182%
Uzbekistan				-75%	-80%	-74%	-77%
Venezuela	307%	343%	330%	383%	355%	361%	400%
Vietnam	-91%	-92%	-92%	-92%	-91%	-90%	-90%
Yemen			-75%	-84%	-87%	-87%	-88%
Zambia			-47%	-47%	-43%	-35%	-27%
Zimbabwe		-76%	-86%	-88%	-90%	-85%	-72%

Table A13 Percent change between thermoelectric withdrawals (USGS, 2018c) and gross thermoelectric demand (Lohrmann et al., 2019) for states in the contiguous United States.

State	1985	1990	1995	2000	2005	2010
AL	-100%	-100%	-99%	-98%	-96%	-95%
AZ	66%	-14%	50%	16%	155%	156%
AR	270%	156%	138%	143%	353%	489%
CA	-6%	117%	447%	250%	4925%	7064%
CO	154%	145%	146%	110%	164%	383%
CT	-53%	-28%	-47%	117%	101%	111%
DE	-99%	-100%	-100%	-96%	-94%	208%
DC	-100%	-100%	-100%	-100%	-100%	
FL	102%	82%	179%	289%	473%	603%
GA	-94%	-93%	-93%	-76%	-65%	-46%
ID		-63%			2194%	4123%
IL	-97%	-96%	-96%	-94%	-94%	-79%
IN	-91%	-93%	-92%	-90%	-87%	-85%
IA	-69%	-71%	-70%	-38%	-21%	-9%
KS	-16%	-67%	-58%	-68%	98%	200%
KY	-63%	-63%	-58%	-53%	-55%	-54%
LA	-85%	-83%	-82%	-82%	-84%	-76%
ME	-78%	55%	318%	14%	31%	389%
MD	-66%	-46%	138%	375%	312%	525%
MA	-77%	31%	698%	1368%	1479%	1286%
MI	-97%	-97%	-94%	-89%	-87%	-82%
MN	-88%	-32%	-5%	-12%	-15%	-2%
MS	2%	52%	132%	69%	88%	-22%
MO	-88%	-86%	-89%	-85%	-81%	-71%
MT	-45%	13%	1369%	363%	467%	239%
NE	-100%	-99%	-97%	-97%	-97%	-93%

State	1985	1990	1995	2000	2005	2010
NV	175%	104%	210%	155%	279%	642%
NH	-99%	-99%	-98%	-98%	-98%	-98%
NJ	-62%	-18%	-2%	205%	318%	456%
NM	-4%	290%	279%	363%	1105%	1560%
NY	-89%	-92%	-91%	-84%	-90%	-64%
NC	-96%	-92%	-68%	-76%	-78%	-68%
ND	-99%	-99%	-99%	-99%	-99%	-98%
OH	-96%	-95%	-94%	-92%	-91%	-86%
OK	217%	565%	462%	441%	606%	261%
OR	-37%	-35%	15%	85%	247%	132%
PA	-95%	-90%	-89%	-91%	-90%	-88%
RI				18618%	31097%	31242%
SC	-85%	-79%	-78%	-81%	-77%	-60%
SD	61%	7226%	17066%	25733%	32371%	16369%
TN	-96%	-97%	-97%	-98%	-98%	-96%
TX	-20%	-8%	-27%	-27%	-23%	-24%
UT	6886%	1792%	3326%	2562%	2762%	2306%
VT	-100%	-100%	-100%	-100%	-100%	-100%
VA	-82%	-80%	-83%	-79%	-82%	-63%
WA	-38%	-16%	25%	-10%	4%	1815%
WV	-86%	-76%	-71%	-77%	-75%	-64%
WI	-96%	-96%	-96%	-95%	-96%	-92%
WY	-98%	-97%	-96%	-90%	-88%	-52%